An Evaluation of Char Reactivity and Ash Properties in Biomass Gasification

Fundamental Processes in Biomass Gasification

Lasse Holst Sørensen, Jan Fjellerup, Ulrik Henriksen
Antero Moilanen, Esa Kurkela, Erik Winther

ReaTech, September 2000

Prepared for Elkraft A.m.b.A. and Energistyrelsen

EFP-98 1383/98-0003

English Abstract

This work focus on the connection between char reactivity, ash agglomeration and sintering and the gas composition in the turbid environment in a circulating fluidised bed gasification process, where biomass is gasified, with focus on straw gasification. The model approach intends to combine equilibrium calculation programming of complex multicomponent-multiphase systems involving gas, solid and liquid solutions of salts and silicates with the concept of catalytic effects in fuel reactivity. Char gasification reactivity and ash characteristics have been tested experimentally in a bench scale fluidised bed, in different thermal balances and in high-temperature light-microscope equipment. Ten different Danish straw samples and some artificial samples and catalysts were tested. It was found that the most important difference between the straw behaviour, that seems to determine the reactivity and the sintering tendency, were the calculated solid bed mol-ratio, $\gamma_K=SiO_2/K_2O$. We suggest that a fuel has high agglomeration tendency if $2<\gamma_K<15$ and very high agglomeration tendency if $3<\gamma_K<5$. It has also been found that a number of additives if properly added are effective for the prevention of agglomeration and sintering of straw ash. A literature survey study on tar cracking from biomass gasification has been performed.

Danish Abstract

Denne rapport fokuserer på sammenhængen mellem koksreaktivitet, askeagglomerering og sintring samt gas sammensætningen under de komplekse omgivelser der eksisterer i en cirkulerende fluid bed forgasser, hvor der forgasses biomasse (strå). Model forståelsen bygger på en kombination af ligevægtsberegninger af komplekse multicomponent-multifase systemer samt katalytisk brændselsreaktivitet. I systemet indgår gas, faste stoffer og smeltede opløsninger af salte og silikater. Koksforgasningsreaktivitet og askeegenskaber er blevet undersøgt eksperimentelt i en 'bench scale fluidised bed' samt ved anvendelse af termisk udstyr og et højtemperatur lysmikroskop. Ti forskellige Danske strå samt kunstigt producerede prøver og katalysatorer er undersøgt. Den vigtigste forskel mellem halmstrå, der synes at bestemme reaktiviteten og sintringstendensen er det beregnede bed-molforhold, $\gamma_K=SiO_2/K_2O$ for faste stoffer. Vi foreslår at brændslet har høj agglomereringstendens hvis $2<\gamma_K<15$ - og særdeles høj agglomererings og sintringstendens for $3<\gamma_K<5$. Det er desuden blevet fundet, at en del undersøgte additiver effektivt forhindrer agglomering og sintring. En litteraturundersøgelse er blevet udført på emnet tjærekrakning fra biomasse forgasning.

ISBN 87-988105-0-2

Content

Acknowledgement

Jimmy Bak (Risø), Poul Norby (Oslo University), Charlotte C. Appel (GEUS) and Klaus Hjuler (dk-TEKNIK) are thanked for several good discussions and for having performed specific analysis during the project. Maria Bario (NTNU, Norway) is thanked for her thorough assistance during the experiments with catalyst addition to synthetic carbon and ash samples. Håvar Risnes is thanked for his great interoperability and constant motivation during reactivity and equilibrium calculation work. Johan Hustad (NTNU) is thanked for his creative participation in the present work. Benny Gøbel (DTU) is thanked for doing a great work on reactivity measurements. Torben Lyngbech (DTU) is thanked for performing great care doing macro-TGA measurements. Per Stoltze (Esbjerg University Ålborg) is acknowledged for good discussions on fundamental catalysis and Dorthe Posselt (Roskilde University) is thanked for inspiring discussions about fundamental topics related to the physical structure of biological materials. We acknowledge Ms. Jaana Korhonen (VTT-Energy) who carried out the thermobalance tests and Ms. Jaana Laatikainen-Luntama (VTT-Energy) who carried out the bench-scale fluidised-bed tests. The ribbe-harvested straws were provided by Torsten Reffstrup (KONCEPTOR) and the other straws were collected in co-operation with Flemming Klogborg (Bjerringbro Gymnasium), Morten Lillevang Nielsen (Risø) and Torben Dietrich Pedersen (Risø).

ELKRAFT A.m.b.A. and The Danish Ministry of Environment and Energy have supported the research work through the Energy Research Programme (EFP). The work made by VTT-Energy was mainly financed by Technology Development Centre Finland (Tekes) and also co-sponsored by Carbona Oy (Finland), ELKRAFT (Denmark), Foster Wheeler Energia (Finland), Imatran Voima Oy and VTT Energy.

Lasse Holst Sørensen, Jan Fjellerup, Ulrik Henriksen, Antero Moilanen, Esa Kurkela,

Erik Winther

ReaTech, Roskilde, Denmark, August 2000

Symbols

X	fractional conversion, daf-char basis	
P, p	pressure	[bar]
E	activation energy	[kJ/mol]
R	gas constant	[J/mol K]
R	reactivity	[s^{-1}],[min^{-1}],[% min^{-1}]
k	frequency factor or reaction rate constant	[s^{-1}] or [bar^{-1} s^{-1}]
T	temperature	[K or °C]
Y	gas	[bar]
r_c	reaction rate	[s^{-1}]
f	structural function	[-]
Z	composition range	
A	area/g carbon	[m^2/g carbon]
σ_1	number of catalyst sites/number of reactive carbon sites	[-]
σ_2	number of reactive carbon sites /m^2 pore area	[mol m^{-2}]
p_1	the likelihood that a catalytic site is activated	[-]
Mw:	molecular weight	[g/mol]
(O)	chemisorped oxygen	
γ	theoretical agglomeration and sintering index	
k_1 & k_{-1}	reaction rate coefficients	[$s^{-1}bar^{-1}$]
k_3	reaction rate coefficients	[s^{-1}]
η	effective conversion factor	[-]

Indices

c	char
i	number
f	forward reaction or reactive site
b	backward
w	water reaction
v	volume or void
a	area
tot	total
ash	ash
add	additive
bed	bed
d.b.	dry basis

Abbreviations

TGA: Thermal Gravimetric Analysis
DTA: Differential Thermal Analysis
SDT: Simultaneous DTA & TGA
SEM: Scanning Electron Microscopy
EDX: Energy Dispersive X-ray spectroscopy
HTLM: High Temperature Light Microscopy
SAI: Sintering and Agglomeration Index
PDU: Process Development Unit (CFBG)
CFBG: Circulating Fluidised Bed Gasifier

1 Introduction

This work relates to the pyrolysis and gasification of carbonaceous materials such as biomass, (straw). The intention is to contribute to the improvement of gasification or pyrolysis processes carried out in the presence of alkali metals and alkali metal compounds. In particular the process under consideration focuses on the circulating fluidised bed gasification process. However this work may be of interest for gasification processes in the following reactors: the bubbling fluidised bed reactor, the fixed bed reactor (also called moving bed reactor) or processes with one or more preparation steps of the type, washing, drying or devolatilization utilised in separate or combined steps before the gasification process. Three major topics are considered: catalysis, ash agglomeration/ash sintering and tar cracking, with emphasis on the first two. Tar is unwanted since heavy tar products can cause deposits in downstream equipment's such as i.e. filters and cyclones, therefore also the topic tar cracking is considered in appendix 2.

2 Background

In the circulating fluidised bed gasifier (CFBG) the fuel particles are fed into a hot bed of particles suspended by up flowing gases. The bed is composed of particles that are small enough to be entrained from the bed, separated by a cyclone and returned to the bed. In gasification of high-volatile straw and wood bed material, such as sand or dolomite or calcium, is required for maintaining a stable bed content since the amount of residual char is relative low and the char reactivity is relatively high compared to coal char and the low-density char particles are easily elutriated from the bed (Kurkela 1996). In particular due to the high content of potassium, sodium and silicium in straw, gasification of straw may easily cause bed sintering. Alkali silicates with low melting temperatures are formed. Additionally volatile alkali salts may condense on particle surface and produce salt melts (Hallgren and Oscarsson 1998) that acts as a glue between particles in agglomerates (Steenari and Lindquist 1998). A sticky layer on the particles is formed, particles starting to agglomerate and eventually giving rise to agglomeration or in the worst case alkali induced defluidisation due to partial sintering (Hallgren 1994 & 1996). Operational measures to

decrease the tendency of agglomeration and sintering in a fluidised bed is (Hallgren and Oscarsson 1998): 1) avoiding hot spots, 2) decreasing process temperatures, 3) fuel refinement (extraction of Na, K), 4) co-firing with fuels with less problematic ashes, 5) modifying the bed material; additives, size distributions, intelligent choice of bed material for prevailing conditions. The viewpoint in the present work focuses on 2) and primarily 5). Rapid carbonaceous char gasification may be obtained at low temperatures through the utilisation of various char gasification catalysts (K, Na or Ca) at temperatures below the relevant eutectica. Rapid char conversion may also be obtained by using additives to absorb products of the inorganic catalysts that in the form of salt melts or alkali silicates causes sintering and agglomeration at moderate temperatures and thereby allow the necessary elevation of gasification temperature in order to obtain proper carbon conversion.

The two-stage gasifier (Henriksen 1997) has separate pyrolysis- and char gasification reactors. After the pyrolysis reactor, the char and volatiles product enters the gasification reactor. At the bottom of the gasification reactor a char bed is formed. Above the char bed, air and superheated steam are added to the volatile pyrolysis products hereby raising the temperature through partial gas combustion and decomposing the tar components. Dragging the gas and added steam through the char bed gasifies the char particles and cracks the tar components at temperatures between 950 and 750°C. One of the advantages of this combined concept is production of a gas with extremely low tar content. However, at low bed temperatures, steam and CO_2 gasification reactions with carbonaceous material are slow with appropriate gasification atmospheres. Therefore the parameters which controls the reactivity of wood and straw chars must be determined especially for utilisation of reactivity estimates for scale-up purposes.

The effect of dispersion and mass transport processes of potassium and sodium is evaluated in order to investigate if catalyst properties can be utilised in the gasification processes. The catalyst state, form and vapour pressure is important for their function during the gasification process. In straw sodium and potassium may be present as water-soluble salts as e.g. K_2SO_4, KCl, NaCl, and K_3PO_4 (Kiørboe and Lilleng 1990)/ K_2CO_3, Na_2CO_3 and hydroxides or associated with the organic matrix of the fuel. A major part of the inorganic-rich particles are located close to the grain boundary as small spherical particles, phytates, arranged in clusters. The phytates serves as a main storage-location of K, P and N typically present in the approximate mole ratios 1:1:3, in the grains (Marchner 1995). Na, K, Ca and Mg may also to some extent occur as silicates in biomass

fuels (Hansen 1997).

Si and Ca are typically abundant in the fuel and additionally often used as bed materials in fluidised-bed systems in the form of silica and calcium carbonate. Under relevant biomass gasification conditions the active catalysts may react with each other to salt melts or with silica and small amounts of calcium to produce eutectic mixtures with low-temperature melting points. Molten potassium-silicates and potassium (or alkaline) salts are likely causes of agglomeration, fouling and corrosion. High-silica potassium silicates like $K_2O*4SiO_2$ have low liquidus temperatures, T_m=765°C and, $K_2O*4SiO_2$ mixed with small amounts of $CaO*SiO_2$ produces an eutectica below 750°C. With addition of sodium, liquidus temperature at a ternary eutectic may decrease to 540°C (Kracek 1932). Other constituents can lower the liquidus temperatures even further (Blander and Pelton 1997) and cause severe agglomeration and sintering in combustion, gasification and pyrolysis reactors. For one straw composition, Blander found from the calculations using the chemsage equilibrium program that it was likely that a liquid would persist down to at least 500°C at combustion conditions. Low-silica potassium silicates have higher liquidus temperatures, for $K_2O*2SiO_2$, T_m= 1045°C and for K_2O*SiO_2, T_m= 976°C, however, beside the crystalline phases, abundant amounts of melts are observed. In these melts the K_2O/SiO_2 ratio varies and is fractal. The melting of inorganic compounds into sintering particles causes bed defluidization and diminishes the carbon-catalyst contact. Additional $CaCO_3$ have been shown in laboratory scale to cause significant neck growth between the particles (Skrifvars 1994, 1997) that may lead to agglomeration in the bed. Information about melting temperatures for several inorganic mixtures including oxides of Si, Mg, Ca, K and Na can be found in (Levin 1985). See the diagrams: Fig. 391 (K_2O-CaO-SiO_2), Fig. 395($K_2O*4SiO_2$-$CaO*SiO_2$), Fig. 401 (K_2O-MgO-SiO_2), Fig. 485 ($Na_2O*2SiO_2$-$Na_2O*2CaO*3SiO_2$), Fig. 1263 ($CaCl_2$-KCl), Fig. 1410 (KCl-NaCl-$CaCl_2$), Fig. 1877 (KCl-NaCl-K_2CO_3-Na_2CO_3) etc.

When considering such equilibrium systems, however, it is of great importance to know which compounds are actually available and stable in the solid phase taken into account the mass balance for all elements, the temperature and the pressure. In complex multicomponent-multiphase systems including solid and liquid solutions of salts and silicates, practical experience supported by available diagrams (Levin 1985) gains greatly from the use of equilibrium programs like HSC-Chemistry and FACT that provides algorithms for free energy minimisation. These programs represent the combination of computer power with the accumulation of data and the scientific and

technical knowledge from a great number of scientists over decades. The results from the programs must be evaluated carefully, since the databases are still incomplete and since equilibrium programs do not include kinetics. Kinetics must be taken care of through proper input relations and finally the results must be critically compared to experiments.

Additives are materials added to the process in preferentially small amount in order to improve the gasification process. The addition of anti-agglomeration additives is a way to avoid agglomeration and sintering during the combustion, gasification or pyrolysis process. Such additives typically dilute or bind the inorganic catalysts and thus the wanted catalytic effects are also removed. Some additives, however, also have weekly catalysing effects. The aim is, to maintain as much catalytic effect as possible at as high a temperature as necessary to obtain complete carbon conversion and at the same time avoid severe agglomeration and sintering during the combustion, gasification or pyrolysis process.

A number of possible additives are known. Such additives should be abundant and cost effective and preferentially the product should be useful e.g. as a fertiliser. Additives are typically relatively expensive and their utilisation should be minimised during optimisation of the process. Therefore additives preferentially are reactive, so that they are rapidly and completely converted into the desired compounds. Kaolinite is well known as a reactive additive (Ivarsson 1988, Steenari 1998). Kaolinite is, however, relatively expensive (1500-3000 kr/ton dependent of the quality). The straw price is around 500 kr/ton. A typical amount of 100% clean kaolinite used for a 100 MW gasifier (180000 ton straw) will be around 5000-10000 ton/year if the effective conversion of kaolinite is 50-100%. Other typical additives are $CaMg(CO_3)_2$, $CaCO_3$, CaO, $Ca(OH)_2$, Al_2O_3, $MgCO_3$, MgO, $Mg(OH)_2$, TiO_2, $Al_2SiO_5(OH)_4$, Kaolinite and dolomite has recently been investigated thoroughly by (Steenari 1998). Additives such as alumina or calcium typically raise the liquidus temperature (Blander et al. 1997). The precise amount of additive required depends on the precise process conditions, the fuel composition as well as the amount and composition of other additives or bed materials and the specification of the quality of the residual product. Normally the amount of additive is minimised due to economic reasons. Sufficient amounts are however such amounts that introduces enough additive to react with most alkali components in the process. Simple stoichiometric relations can also be utilised in combination with the valuable operational experience that is obtained from running full-scale reactors. It is one of the aims of the present work to contribute to the development of a valid method to quantify the needed

amounts of varying catalysts and anti-agglomeration additives to specific or mixtures of straw samples. I.e. the goal is to manufacture the fuel and the residue. This should be done in such a way that for a broad range of straw the amount of additive addition should not vary with straw composition.

An estimate of the needed amount of additive can be calculated using an equilibrium program like HSC, (Roine 1999). HSC calculates equilibrium compositions using a minimisation method for Gibbs free energy and use a database based on thermochemical data like (Barin 1995) and (Knacke 1991). Other equilibrium programs are Chemsage and FACT. These programs can together with process knowledge be used to estimate the needed amount of additive to the process. Also an estimate of char reactivity may be done with the aid of using equilibrium programs like HSC-Chemistry and FACT as will be presented later.

3. Theoretical

In the following some theoretical evaluations will be made on catalysis, char reactivity and multiphase equilibrium. A connection between the two formulations will be drawn. Also a sintering and agglomeration index (SAI) and a visual corrosion index (CI) will be introduced.

3.1 Char Reactivity

The mechanisms of catalytic char gasification are not completely understood and seem not to be the same for all catalyst systems and reactions. The ranking of catalytic activity of various potassium compounds has been estimated as KOH ≈ K_2CO_3 > $KHCO_3$, > KNO_3 > K_2SO_4 >> KCl. (Yuh and Wolf (1983)). (Meier 1991) suggested that the active intermediate is in the form of K_nC or K-OH clusters with varying sizes (depending on the K/C ratio) anchored by phenolate groups to the carbon surface. In the case where the reaction is strongly catalysed by e.g. potassium, (McKee 1983) proposed the following reactions:

$$2\,K + 2\,H_2O \Leftrightarrow 2\,KOH + H_2,\quad 2\,KOH + CO \Leftrightarrow H_2 + K_2CO_3,\quad K_2CO_3 + 2\,C \Leftrightarrow 2\,K + 3\,CO,$$

thus suggesting that elemental potassium is an intermediate. (Cerfontain and Moulijn 1983) show that the decomposition of K_2CO_3 at the carbon surface can be followed *in situ* using FTIR-transmission spectroscopy combined with temperature programmed desorption. Carbon samples were prepared by milling a pre-oxidised activated carbon containing 30 wt.%. K_2CO_3 , i.e. around 5 mol% potassium. Complete decomposition of K_2CO_3 (and Na_2CO_3) was observed far below the normal decomposition temperature and CO_2 originating from K_2CO_3 (Yokoyama et al. 1980), ^{13}C-labelled $K_2{}^{13}CO_3$ was used, desorption occured already below 900K, while above 800K desorption of CO took place. The following two reactions were suggested:

a) $K_2CO_3 \rightarrow K_2O + CO_2$ (T < 900 K, i.e. 627°C)

b) $K_2O + C \rightarrow 2\,K + CO$ (T > 800K, i.e. 527°C)

According to (Mims and Pabst 1981) decomposition of K_2CO_3 is caused by the reaction of alkali

carbonate with oxygen containing groups at the carbon surface and under production of C-O-K complexes

c) $K_2CO_3 + 2C\text{-}OH \rightarrow 2C\text{-}O\text{-}K + H_2O + CO_2$

(Cerfontain and Moulijn 1983) find evidence that during heating at 773 K (i.e. 500°C) the ionic carboxyl group have disappeared, so that the K_2CO_3 on the carbon surface and the COOK groups have decomposed and that CO_2 is desorbed as proposed in c). Also a small increase in H_2O background was noted. From this work it is proposed that the active intermediate for potassium catalyst include K-O-C. In other work the carbon surface act as a "getter" for potassium. Also metallic K, K_2O, K_2O_2, K_2CO_3 and clusters which are nonstoichimetric compounds with excess metal have been proposed (Chen 1997). When the catalyst loading is high, (Chen and Yang 1997) suggest that most of the catalyst exist in the form of clusters or particles. They found that the single C-O-K group has only little catalytic activity as compared to KOH particles or O-K clusters. It is known that the active sites for the carbon-CO_2 and carbon-H_2O reactions are the edge sites (Yang 1984). The basal plane carbon atoms are usually not gasified by CO_2 and H_2O. (Chen and Yang 1997) suggest that the catalytic effect can only be attributed to an increase in the active intermediate (clusters) and not the number of active sites denoted C_f. If the gasification temperature is around 700°C and the cluster size is small, the atoms (or ions) in these clusters will gain great mobility. The oxygen atoms collected in the clusters can migrate from one active site to another with a much smaller energy barrier than in the uncatalysed reactions.

In the turbid environment where gasification takes place it may be important that as the presence of carbon destabilises K_2CO_3 already at 500°C and the intermediates become mobile. Through their movement the intermediates may form catalytic clusters at carbon edges and also react with other inorganic components and form e.g. silicates and thus ash compositions with low temperature eutectica may form in competition to the more preferred catalytic clusters. In particular this is the case when the carbon is gasified, the number of available active carbon sites for catalysts are diminished and the ash to carbon ratio is increased. Therefore it may be realistic already at relatively low temperatures to utilise a multi-phase equilibrium program to estimate composition of the ash residue. Beside being the agent to be converted, the carbon acts itself as a "catalyst" for the generation of catalytic clusters on active sites and also for the generation of more stable ash

components that may following lead to inorganic mixtures. From the following work the reactivity and the agglomeration tendency of the char is dependent of the silicium, the potassium and the calcium content of the ash. Significant amount of silicium in the ash reacts with potassium which leads to agglomeration and sintering and a reduction of the catalytic O-K clusters which leads to a reduction of the reactivity. This is in particular the case when reactive inorganic components as K_2CO_3 or KOH are the added catalysts. K_3PO_4 is seldom discussed as a gasification catalyst. This is partly because K_3PO_4 is much less catalytic than K_2CO_3 during gasification of ash-free carbon. In an environment, however, where straw ash and thus silica and calcium oxides are abundant, K_3PO_4 may have advantages to K_2CO_3 since it is much more stable and more resistant to agglomeration and sintering than K_2CO_3 in gasification environment.

Since the water soluble potassium fraction of the fuel, except KCl, typically reacts to potassium silicate melts at high temperatures, it may be attractive to utilise specific additives in order to bind potassium in chemical compounds with high melting points. In this way, however, the catalytic effect of potassium is removed.

Therefore the addition of other catalysts may be preferable. Calcium based additives are typical gasification catalyst that may be relevant for gasification of straw. In the present study only a few experiments with calcium have been made. In a co-operation between ReaTech and the University of Roskilde (Larsen and Nielsen 2000 and Posselt 1999 & 2000) found that no significant increase in reactivity was obtained when 5 wt % Faxe limestone (85%<45µm) or when a 5 wt % mikrovit limestone (85%<45µm) was added to straw samples using the impregnation method of (Henriksen 1996). (Ohtsuka 1996) reports that the use of $Ca(OH)_2$ - and $CaCO_3$ - kneaded with water significantly increases the char reactivity of a petroleum coke in an CO_2 atmosphere. (Leboda 1998) found that impregnation (calcium acetate) as well as ion exchange of calcium ions (nitric acid + calcium acetate) significantly increased the reactivity of an active carbon made from plum stone. Very small 0.1µm calcite grains co-slurried with a demineralized Pittsburgh#8 was shown to increase the volatiles yield from a Pittsburgh#8 Seam bituminous coal (Franklin 1981). With respect to addition of calcium based catalysts we will conclude that as it is the case with tar cracking, see Appendix 2, the activity of calcium depends on the method by which it is added to the fuel. The finely dispersed natural calcium or calcium added as very small grains or impregnated as water soluble calcium Ca^{2+} seem to be very effective catalysts. Clearly calcium ions like it is the case with potassium ions will be very reactive – also towards other inorganic

elements. Therefore the evaluation of how the reactivity changes as a function of anti-agglomeration additives and added catalysts becomes complicated and related.

In order to get a better fundamental understanding of ash and catalyst behaviour, agglomeration and char reactivity in the turbid environment where gasification takes place, e.g. for fluid bed facilities and two-stage gasifiers, an equilibrium model approach is described in the following.

3.2 Equilibrium calculation work

Several commercial equilibrium programs are available. In the present work HSC Chemistry and FACT are used to evaluate the biomass gasification process. An equilibrium calculation may provide valuable knowledge about which chemical products and phases and their possible elemental composition ranges, Z_i (i=ash, additive, bed), which can be obtained under specified process conditions.

Equilibrium is often not obtained due to e.g. kinetic limitations. Therefore the calculation results currently have to be held up against experimental data. Phases that are inert on relevant time scales should be left out from the calculations. In the present work, a pseudo kinetic factor or effective conversion factor, $\eta \in [0,1]$, is introduced in order to represent the reactivity of specific elements or compounds. The value of η depends on the process conditions and must be evaluated carefully before any calculation. For straw and wood a thermodynamic gasification study includes the most abundant elements CHNOS-Cl K-Na-Ca-Mg-Si-P and Al and the trace metals like Cr, Ni, Cu, Zn, Pb and Cd, see Table 3.2.1. The inorganic elements inherent in the straws is in the following considered reactive, i.e., $\eta_i = 1$. The input to the equilibrium programs is given as mole elements per ton dry fuel. It is of great importance that the mass balance well represents the relevant chemical processes. When the data are considered sufficiently reliable for the relevant process conditions and the results are evaluated and compared to binary or ternary phase diagram, the model can be used to provide quantitative estimates of how unwanted phases may be removed with the use of additives.

Calculations have been made for a number of different biomass fuels. In the present report, however, only the Danish wheat straw, ‘DW95’, has been used for the examples.

Bed materials

Among possible bedmaterials and additives the following was originally suggested to be tested by simulations (Sørensen and Kurkela 1998): SiO_2 (quartz sand), Al_2O_3 (alumina), $CaCO_3$ and CaO (calcium carbonate and calcium oxide), $MgCO_3$ and MgO (magnesium carbonate and magnesium oxide), $CaMg(CO_3)_2$ (dolomite), $Al_2Si_2O_5(OH)_4$ (kaolinite). The idea was to add realistic amounts of the bedmaterials and assume varying degree of conversion, i.e. to vary η. The advantageous of these materials may partly be to dilute the gasified material and partly to act as a catalyst for specific reactions, e.g. as a cracking agent for tars.

At modest temperatures several of the bed materials may have very low η, e.g.: $\eta < 0.1$. This is the case for alumina and quartz particles. Oppositely, as it is well known, kaolinite being composed of the same elements are much more reactive and thus the relevant range for η is typically the range: $0.1<\eta<1$ dependent on the temperature and process conditions. The reactivity of calcium and magnesium carbonates or dolomite strongly depends on the process conditions and the type of the material as well as the temperatures. Also the interaction between bed materials and additives may influence the response to each other. In Table 3.2.1 an input calculation scheme for Danish wheat straw, DW95, is shown.

Steam addition and total pressure

The effect of steam addition was theoretically tested using HSC [Sørensen and Kurkela 1998] for wheat straw DW95. 0 kg steam, 0.05 kg steam and 1.0 kg steam per kg fuel were tested. Only *very small* effects on major mineral and trace element behaviour were observed with steam addition.

Also the total pressure is an input parameter to the program. A few calculations were performed in order to test pressure effects. With the air ratio maintained constant, a great effect of pressure was observed. At high pressures, e.g. 20 bar, the amount of the solid phase increases, i.e. gaseous phases $\rightarrow$ solid phases. In particular we observed that at specific high temperatures an increase in the pressure increased the amount of solid or melted KCl. Additionally if the CO_2 partial pressure is increased, carbonates are favoured relative to their oxides. The pressure effects are however not the topic of the present work.

Gasifier 95	**Straw 95, ds**		dry feed fuel	**Normalised**	Gasif. temp [C]		850	
Moisture (%)	**12**		sample	**to**	Comb. Temp [C]		850	
Ash %, d.r.	**4.8**		kmol/kg dry	**186.99**	feed [kg/h]		**23376.62**	
Daf feed	Mw	**Straw**	[kmol /kg,d.r]	**[kmlol/t**	dry feed [kg/h]		**20571.43**	
C	12.011	47.5	3.95E-02	**3.95E+01**	steam [kg/h]		**20571.43**	
H	1.0079	5.9	5.85E-02	**5.85E+01**	air [kg/h]		**29602.28**	
N	14.007	0.7	5.00E-04	**5.00E-01**	kg dry air/kg dry feed		**1.439**	
S	32.06	0.1	3.12E-05	**3.12E-02**	steam/dry feed		**1**	
O	15.999	41	2.56E-02	**2.56E+01**	Bed material feed		**1028.57**	
Major elem.d.r. (SUM)		**95.2**	1.24E-01	1.24E+02	Bed mat. F./dry feed		0.050	
					Purge N2		**0**	
Si	28.086	16.00	2.73E-04	**2.73E-01**	Purge N2/kg dry feed		0.0000	
Al	26.982	0.16	2.82E-06	**2.82E-03**	Ash (kg/h)		**987.43**	
Fe	55.847	0.14	1.20E-06	**1.20E-03**				
Ca	40.08	6.00	7.19E-05	**7.19E-02**	HHV, [MJ/kg]			
Mg	24.305	1.30	2.57E-05	**2.57E-02**	LHV, [MJ/kg]		17.5	
K	39.098	25.00	3.07E-04	**3.07E-01**	Air, 15°C and 60% humidity			
Na	22.99	0.40	8.36E-06	**8.36E-03**	Humidity		0.6	
Ti	47.867	0.01	1.20E-07	**1.20E-04**	Air, dry	**mole %**		**Mw**
S	32.06	1.28	1.92E-05	**1.92E-02**	N2 (%)		78.97	**28.014**
P	30.974	1.70	2.64E-05	**2.64E-02**	CO2(%)		0.03	**44.108**
C, carbonate	12.011	0.00	0.00E+00	**0.00E+00**	H2O(%)		0	**18.0148**
O, oxygen in ash	15.999	31.06	9.32E-04	**9.32E-01**	O2(%)		21	**31.998**
Ash-form.(dry ash%),SUM		**83.07**	1.67E-03	1.67E+00	Air, dry	**Weight%**		
					N2 (%)		76.667	
Cu	63.546	46	7.24E-07	**7.24E-04**	CO2(%)		0.046	
Zn	65.38	110	1.68E-06	**1.68E-03**	H2O(%)		0.000	
Pb	207.2	86	4.15E-07	**4.15E-04**	O2(%)		23.287	
Cd	112.41	0.02	1.78E-10	**1.78E-07**	Sum		100.000	
Hg	200.59	0.01	4.99E-11	**4.99E-08**	H2O(%), with dry air		1	18.0148
Cl	35.456	5970	1.68E-04	**1.68E-01**	H2O wt% with dry air		0.624	
Trace el,ppm.(dry fuel)SUM		6212	1.71E-04	1.71E-01	bedmaterial/ash			
					0.05 in gasifier, 0.2-0.4 in FB and PDU			
Steam (added)	18.015	0.05	2.78E-03	**2.78E+00**	**bed materials:**	kg/kg dryfuel		efficiency
Moisture (Fuel)	18.015	0.1364	7.57E-03	**7.57E+00**	Al2O3		**0**	0
Moisture(Air)	18.015	0.009	4.99E-04	**4.99E-01**	TiO2		**0**	0
Moisture, kg (SUM)		0.1953	1.08E-02	1.08E+01	CaCO3		**0**	0
					MgCO3		**0**	0
SUM N2	28.014	1.1032	3.94E-02	**3.94E+01**	CaMg(CO3)2		**0**	0
Purge N2	28.014	0	0.00E+00	**0.00E+00**	SiO2		**0**	0
N2 (air)	28.014	1.1032	3.94E-02	**3.94E+01**	Al2Si2O5(OH)4		**0.05**	1
CO2 (air)	44.108	0.0007	1.50E-05	**1.50E-02**	Sum bed (kg/kg dF):		**0.05**	
O2 (air)	31.998	0.3351	1.05E-02	**1.05E+01**				
Air, kg (SUM)		1.439	4.99E-02	4.99E+01	O(daf fuel) + O(ash)		**26.559**	
					C(daf f.)+C(carbonate)		**39.547**	
Al2O3	101.96	0	0.00E+00	**0.00E+00**				
TiO2	79.898	0	0.00E+00	**0.00E+00**				
CaCO3	100.09	0	0.00E+00	**0.00E+00**				
MgCO3	84.313	0	0.00E+00	**0.00E+00**				
CaMg(CO3)2	184.4	0	0.00E+00	**0.00E+00**				
SiO2	28.086	0	0.00E+00	**0.00E+00**				
Al2Si2O5(OH)4	258.16	0.05	1.94E-04	**1.94E-01**				
Bed material, kg (SUM)		0.05	1.94E-04	1.9368E-01				
Total & normalisation			**1.8699E-01**	**186.99**				

Table 3.2.1. Input table to HSC chemistry and FACT programmes. The data are made in a spreadsheet and used to prepare input data for a 100 MW gasifier. The straw data are taken from wheat straw DW95, see Table 4.2 and 4.4.

Air ratio A_r

The equivalence ratio (or air ratio, Ar), used for the simulations of straw gasification is around Ar = 0.25. The equivalence ratio is defined as the ratio of actual air supplied per kg fuel to the stoichiometric quantity of air required for total conversion of one-kg fuel. Ar is in the following calculated on a dry fuel basis as: Ar = $O_{2,air}$[kmole]/$O_{2,støk}$[kmole], where $O_{2,air}$ is the moles of oxygen added with air, and $O_{2,støk}$ is the stoichiometric amount of air to burn the dry fuel.

$$O_{2,støk}\left[kmole/kg_{dry}\right] = C + S + N + 0.25H - 0.5O$$

The air-ratio Ar, is calculated as Ar = $O_{2,air}$[kmole]/$O_{2,støk}$[kmole]. If Ar is known one finds: $O_{2,air}$[kmole] = Ar$O_{2,støk}$[kmole] and the amount of air added is Air[kmole] = $O_{2,air}(N_{air}/N_{O2})$, where N_X is the number of moles X per volume unit air. $N_{O2}/N_{air} \approx 0.21$ is used). Finally Air[kg] = M_w(air) *Air[kmole], where M_w(air) is the mean molecular weight of the air added including moisture. In the present work we calculate M_w(air) = 28.86 kg/kmole.

The necessary air-ratio is determined by the demands of heat to support the endothermic reactions and to attain high carbon conversion efficiency. Thereby the necessary air-ratio is dependent of the char reactivity, the ash content, the ash melting points constraints and also the added steam to the process. The bed expansion and the rate of ellutriation increase with equivalence ratio. While the gas quantity increases continuously with the equivalence ratio, its heating value deteriorates after a certain limit, since the gas is burned rather than gasified and diluted by nitrogen [Natarajan 1998]. Heat losses of the VTT-PDU reactor are 8-15 % of HHV and also the residence time and thus conversion is lower than in a utility scale reactor. Heat losses from utility gasifiers (50-100 MW) are almost negligible and estimated to be around 1 % [Kurkela 1996]. This means that a certain gasification temperature level can be reached with a lower air-to-fuel ratio in utility gasifiers than in small experimental gasifiers. This has a significant positive effect on the gas composition. In reactors with no externally added heat, the relative low residence time must be compensated for by increasing the air and steam to fuel ratios.

3.3 HSC Chemistry

HSC (Roine, 1999) contains twelve calculation modules which can be used for various thermodynamic calculations. The thermochemical database in HSC3 contains enthalpy (H), entropy (S) and heat capacity data for more than 11000 chemical compounds (15000 in HSC4). The equilibrium module assumes that the activity coefficient of condensed species (solid/liquid) is 1. Heat capacity is calculated using the Kelly equation:

$$C_p = A + B10^{-3} + C10^{5}T^{-2} + D10^{-6}T^{2} \quad (1)$$

A,B,C and D are coefficients estimated from experimental data. In the HSC database, the temperature range for the components is divided into several intervals, so that the Kelly equation can fit the data.

Enthalpy(H) and entropy(S) are calculated using the following equations:

$$H(T) = H_f(298.15) + \int_{298.15}^{T} C_p dT + \sum H_{tr} \quad (2)$$

$$S = S^0(298.15) + \int_{298.15}^{T} (C_p / T) dT + \sum H_{tr} / T_{tr} \quad (3)$$

Where

H_f (298.15) is the enthalpy of formation at 298.15 K
S^0(298.15) is the standard entropy of the substance at 298.15 K
H_{tr} is the enthalpy of phase transformation
T_{tr} is the phase transformation temperature

HSC calculates equilibrium using minimisation of Gibbs energy, where the Gibbs energy is calculated using:

$$G = H - TS \quad (4)$$

Calculation using HSC

The program HSC3 has been used. HSC3 is a general equilibrium program capable to calculate multi-component and multi-phase equilibrium compositions in heterogeneous systems. The user needs to specify the reaction system, with its phases and species and to give also the amounts of raw materials. The program calculates the amounts of products at equilibrium in isothermal and isobaric conditions. The user must specify the substances and potentially stable phases to be taken into account in the calculations. If a stable and significant compound or phase is missing in the system definition, the result will be incorrect.

The database includes more than 11000 compounds: gasses, gas-ions, liquids, solids and it includes several organic compounds (>2C). The HSC database can be checked and a personally own database including specific components, e.g. HCN can overrule the main database. In the present project some month was used to check all data relevant for the gasification approach and a ReaTech database with some 150 corrected data has been used during the calculations.

With HSC Chemistry it is possible to simulate chemical equilibria between pure substances and the ideal and also, to some extent, non-ideal solutions using simple user supplied formulas. In this study however, the HSC calculations have been performed using ideal phase solutions. HSC does not take kinetic phenomena into account and therefore in several cases careful preparation of input data for the mass balance is necessary in order to get usable results. Following a thorough experimental evaluation is necessary. Experimental observation of the effective transformation of specific components may be utilised to refine results.

Examples of how to use HSC chemistry is made in Appendix 1, where it is tested how to calculate effects of adding kaolinite as an additive.

3.4 FACT

The FACT program has been tested together with Håvar Risnes, NTNU. The FACT program has been used by ReaTech for a one-month period. In the following the FACT code is described using information given by the FACT group, and an initial simulation of straw gasification using input feed from Table 3.2.1 (a 100 MW fluid bed gasifier) has been performed.

FACT (*Facility for the Analysis of Chemical Thermodynamics*) (Bale 1999) is an equilibrium program using a fully integrated thermochemical database computing system. FACT has been in operation since 1976. FACT was originally developed as a research tool for chemical metallurgist and it has pure component data for more than 5000 compounds. The pure component Gibbs energy is calculated using equations (2-4), where the heat capacity is calculated using the following equation:

$$C_p = a + bT + cT^{-2} + dT^2 + eT^i + fT^j + gT^k \qquad (5)$$

where a,b,c,d,e,f,g are coefficients and i,j,k are powers defined for each component. These parameters may be fitted for several temperature intervals.

FACT can calculate multicomponent multiphase equilibria for non-ideal alloys, slags, glasses, ceramics, mattes, molten salts and aqueous solutions at different temperatures and composition. The FACT solution database has data for more than 100 non-ideal solutions. The Gibbs energy is defined as:

$$G = \sum_{i=1}^{N} X_i G_i + \Delta G \qquad (6)$$

Where

N is the number of components

X_i is the molefraction of i in the solution

G_i is the Gibbs energy of component i

ΔG is the Gibbs energy of mixing which can be calculated using:

$$\Delta G = RT(\sum_{i=1}^{N} X_i \ln X_i + G^E) \quad (7)$$

Where

R is the gas constant

T is the temperature

G^E is the excess Gibbs energy

For an ideal phase, the excess Gibbs energy is zero.

Solution models for excess Gibbs energy

FACT has 8 solution models for calculating excess Gibbs energy, these are (Bale 1999):

1. Polynomial type (Kohler/Toop) (Pelton,1988)
2. Unified Interaction Parameter Type (Pelton and Bale,1986 and 1990)
3. Blander/Pelton Quasichemical Type (Blander,1984+1987), (Pelton,1986)
4. Sublattice Type (Kohler_Toop) (Pelton,1988).
5. Pitzer/Debye Huckel Type (Harvie,1980).
6. Binary Non-Stoichiometric Compound (Pelton,1991).
7. Polynomial Type, Muggianu (Hillert,1980)
8. Sublattice Type (Muggianu), similar to solution type 4

In the solution type 1, the Kohler (or symmetric) equation is appropriate when components 1,2 and 3 are chemically similar, and the Toop (or asymmetric) equation is more appropriate when one of the components is chemically different from the other two. Solution type 2 uses a modification of the Wagner interaction parameter formalism developed by (Pelton and Bale,1986) and (Bale and Pelton,1990). The unified Formalism used in solution type 2 is thermodynamically consistent at finite concentrations. The unified formalism reduces to the original formalism at infinite dilution. Solution type 3, the modified quasichemical model was developed by (Blander, 1984,1987) and (Pelton, 1986). The model is particularly well suited to systems with short range ordering such as molten silicates. Solution type 5 is used for concentrated aqueous solutions. The

solution type 7 is very similar to the solution type 1; the main difference is that the "Muggianu interpolation method" is used for including binary terms in the Gibbs energy expression of higher-order systems in solution type 7. The solution type 8 (Muggianu) is very similar to solution type 4 (sublattice Kohler/Toop) except that the Muggianu method is used in all common-species subsystems.

Binary terms

In G^E, the binary terms may be entered as Redlich-Kister or Legendre polynomials (Bale, 1974) (Pelton,1986). The j'th Redlich-Kister polynomial term in a binary system M-N is defined as:

$$X_M X_N P_J (X_N - X_M)^j \tag{8}$$

Where

X_M is the mole fraction of M
P_J is the polynomial coefficient

Legendre polynomials are defined in a similar way. The j'th Legendre term in a binary system can be expressed as:

$$X_M X_N (X_N - X_M) \tag{9}$$

The first few Legendre polynomials are:

$$P_0 (X_N - X_M) = 1 \tag{10}$$
$$P_1 (X_N - X_M) = (X_N - X_M)$$
$$P_2 (X_N - X_M) = 1/2 (3(X_N - X_M)^2 - 1)$$
$$P_3 (X_N - X_M) = 1/2 (5(X_N - X_M)^3 - 3(X_N - X_M))$$

The Redlich-Kister and Legendre polynomials is discussed in (Bale,1974) and (Pelton,1986). In the following, the solution type 1, 3 and 4 which have been used in this report for calculating gasification of biomass will be described.

Solution type 1 (Kohler/Toop/Muggianu)

In the SOLUTION model in FACT, there are three different models available for including polynomial binary excess terms in the Gibbs energy expression for ternary and higher-order systems. These are the Kohler, Toop and Muggianu models illustrated, for the case of a ternary system, in Figure 3.4.1. The excess molar Gibbs energy at point p in the ternary system is related to the excess molar Gibbs energies in the binary systems at points a, b and c using equations 11,12 and 13 respectively for the Kohler, Toop and Muggianu models. Notice that points a, b and c in Figure 3.4.1 lies at the side of the triangle, there is thus only two variables at each point.

Kohler:

$$g_p^E = (X_1 + X_2)^2 g_a^E + (X_2 + X_3)^2 g_b^E + (X_3 + X_1)^2 g_c^E + (ternary terms) \qquad (11)$$

Toop:

$$g_p^E = \left(\frac{X_2}{X_2 + X_3} \right) g_a^E + \left(\frac{X_3}{X_2 + X_3} \right) g_b^E + (X_2 + X_3)^2 g_c^E + (ternary terms) \qquad (12)$$

Muggianu:

$$g_p^E = \frac{X_1 X_2}{V_{12} V_{21}} g_a^E + \frac{X_2 X_3}{V_{23} V_{32}} g_b^E + \frac{X_1 X_3}{V_{31} V_{13}} g_c^E + (ternary terms) \quad (13)$$

Where $V_{ij} = (1 + x_i - x_j)/2$ (14)

Ternary terms of the form:

(Ternary term) = $X_1^i X_2^j X_3^k \left(A + BT + CT \ln T\right)$ (15)

where i≥1, j≥1 and k≥1 may be added to the expansions in Eqs (11-13). A, B and C are parameters for each mixture. These terms can express the temperature sensitivity of the thermodynamics of the non-ideal mixture. The solution type 1, the Kohler (or symmetric) equation is appropriate when components 1,2 and 3 are chemically similar, and the Toop (or asymmetric) equation is more appropriate when one of the components is chemically different from the other two.

Solution-type 3 - Quasichemical Model

The modified quasichemical model has been developed by (Blander 1984,1987) and (Pelton,1986). The model is particularly well suited to systems with short-range ordering such as molten silicates. The input for this model is very similar to the input for solution-type 1. The entry of components is identical to that for solution-type 1 except that the "charge parameters for equivalent fractions" are now the parameters b_i of the quasichemical model as defined in the references. Equivalent fractions, Y_i, are defined as:

$$Y_i = b_i X_i / \left(b_1 X_1 + b_2 X_2 + ...\right) \quad (16)$$

where the X_i are the mole fractions of actual components.

The polynomial expansions for G^E of solution-type 1 are replaced in the quasichemical model by expansions for $W_{m,n}$, where $W_{m,n}$ is the Gibbs energy change for the nearest-neighbour pair exchange reaction:

$$(M-M)+(N-N)=2(M-N) \tag{17}$$

Where (M - M) indicate a neighbour-neighbour bond of M.

Binary terms can be entered as polynomials:

$$W(M,N)=\sum_{i,j} Y_M^i Y_N^j (A+BT+CT\ln T) \tag{18}$$

as Redlich-Kister series:

$$W(M,N)=\sum_{j} (Y_N-Y_M)^j (A+BT+CT\ln T) \tag{19}$$

or as Legendre series:

$$W(M,N)=\sum_{j} P_j(Y_N-Y_M)(A+BT+CT\ln T) \tag{20}$$

These are very similar to the expansions of G^E for solution-type 1. Note, however, that the leading term in W(M,N) is usually W(M,N) = constant, whereas for solution-type 1 it is usually $G^E = X_M X_N$. Hence, a polynomial expansion of W(M,N) as in Eq (18) usually will start with the term i=j=0, and the Redlich-Kister and Legendre terms in Eqs (19, 20) do not contain the factor $X_M X_N$ found in the polynomial Redlich-Kister and Legendre terms defined previously.

Binary $W_{m,n}$ terms is included in calculations at ternary and multicomponent compositions using a method similar to that of the Kohler/Toop grouping.

Solution-type 4 - Sublattice Model

The sublattice model may be used with **SOLUTION** for a system with two sublattices. An example will first be given for a molten salt system (cationic and anionic sublattices). The model is described in detail in (Pelton,1988).

Molten salt solution

In Table 5, data are given for a molten salt solution with Li, Na and K on the cationic sublattice and F and SO_4 on the anionic sublattice.

Species entry

Using the sublattice model it is necessary to assign the species to different lattice groups. For the present example, each species is assigned to lattice "1" or "2" which, are the cationic and anionic sublattices. A "charge parameter" is assigned to each species. In the present example of a molten salt, this is the absolute charge on the ion. (In the general case, these parameters give the ratios of the numbers of sites on each sublattice. One also must assign a Kohler/Toop grouping for each sublattice. In the present example, since Li, Na and K are chemically similar, they are all assigned to the same group. Since there are fewer than three anions, it does not matter how the anionic grouping is made.

Component entry

Each component must be entered in **F*A*C*T** notation. Each component consists of a cationic and an anionic species. One must also enter how many moles of each species are found in one mole of entered component. For example, one mole of Li_2SO_4 contains two moles of Li species and one mole of SO_4 species.

Gibbs energy expression and entry of excess mixing parameters

The cationic and anionic site fractions, X_i are defined as:

$$X_{Li} = n_{Li} / \left(n_{Li} + n_{Na} + n_K \right) \tag{21}$$

$$X_F = n_F / \left(n_F + n_{SO_4} \right) \tag{22}$$

and similarly for the other species, where n_i is the number of moles of a species.

Equivalent ionic fractions, Y_i, are defined by weighting the mole numbers n_i with the "charge parameters" of the species. In the present example, since the charge parameters for all cations are unity, $Y_i = X_i$ for all cations. For the anions:

$$Y_F = n_F / \left(n_F + 2n_{SO_4} \right) \tag{23}$$

$$Y_{SO_4} = 2n_{SO_4} / \left(n_F + 2n_{SO_4} \right) \tag{24}$$

If b_i is the "charge parameter" of a species, then one mole of that species contains b_i equivalents. A component must have the same number of equivalents of cations and anions. For example, one mole of Li_2SO_4 contains 2 equivalents of Li and 2 equivalents of SO_4. An equivalent of solution contains one equivalent of cations and one equivalent of anions.

All excess property expansions must be in terms of the equivalent fractions. The g^E expressions here are *per equivalent* of solution.

In the LiF-NaF binary, for example, fluorine is common to both components, so that the cationic fraction $Y_1 = Y_{Li}$ is the same as the overall component fraction Y_{LiF}, and similarly $Y_2 = Y_{Na} = Y_{NaF}$. In this system, $Y_i = X_i$, and one equivalent of solution is the same as one mole. In the LiF-Li_2SO_4 system, on the other hand, the number of equivalents per mole is $(X_{LiF} + 2X_{Li_2SO_4})$.

The Gibbs energy expression for the solution is then:

$$\begin{aligned} g(\mathrm{J/equivalent}) = {} & (Y_{Li} Y_F g^0_{LiF} + Y_{Li} Y_{SO_4} g^0_{Li(SO_4)_{1/2}} + Y_{Na} Y_F g^0_{NaF} \\ & + Y_{Na} Y_{SO_4} g^0_{Na(SO_4)_{1/2}} + Y_K Y_F g^0_{KF} + Y_K Y_{SO_4} g^0_{K(SO_4)_{1/2}} \\ & + RT(X_{Li} + X_{Na} + X_K)^{-1}(X_{Li} \ln X_{Li} + X_{Na} \ln X_{Na} \\ & + X_K \ln X_K) + RT(X_F + 2X_{SO_4})^{-1}(X_F \ln X_F + X_{SO_4} \ln X_{SO_4}) \\ & + \sum Y_i g^E (X_i = 1) \\ & + (\mathrm{Reciprocal\ Terms}) \end{aligned} \tag{25}$$

The first term on the right-hand-side of Eq (25) contains the weighted sum of the standard Gibbs energies g^0 per equivalent of all neutral salts. The second and third terms give the ideal Gibbs energy of mixing of the cations and anions, on their respective sublattices, per equivalent. Note the use of mole fractions, X_i, rather than equivalent fractions in this term in accordance with the Temkin model.

The next term in Eq (25) is a weighted sum of equivalent excess Gibbs energies over all common-ion sub-systems (that is, over all sub-systems with only one cation on the cationic sublattice or only one anion on the anionic sublattice). These excess terms are calculated from the entered parameters. For instance, in the Li, Na, K/SO_4 sub-system:

$$\begin{aligned} g^E\left(X_{SO_4}=1\right) = {} & \left(Y_1+Y_2\right)^2\left(\frac{Y_1Y_2}{\left(Y_1+Y_2\right)^2}\right)\left(-4247+\frac{Y_1}{Y_1+Y_2}\left(-1444\right)\right) \\ & +\left(Y_1+Y_3\right)^2(...) \\ & +\left(Y_2+Y_3\right)^2\left(\frac{Y_2Y_3}{\left(Y_2+Y_3\right)^2}\left(-2197\right)\right) \\ & +\left(Y_1Y_2Y_3^{\,2}\right)(400) \end{aligned} \qquad (26)$$

The other terms in the summation are $g^E_{Li,Na,K/F}$, $g^E_{Li/F,SO_4}$, $g^E_{Na/F,SO_4}$ and $g^E_{K/F,SO_4}$. The binary terms in Eq (26) have been combined using the Kohler equation (10) because all 3 cations were assigned to the same Kohler/Toop group.

Finally, in Eq. (26) are found "reciprocal terms" of the general form $Y_m^i Y_n^j Y_p^k Y_q^l$ where m and n are cations, q and r are anions, and i,j,k and l are all greater than zero. The entry of the excess mixing parameters can be found in (Bale,1999).

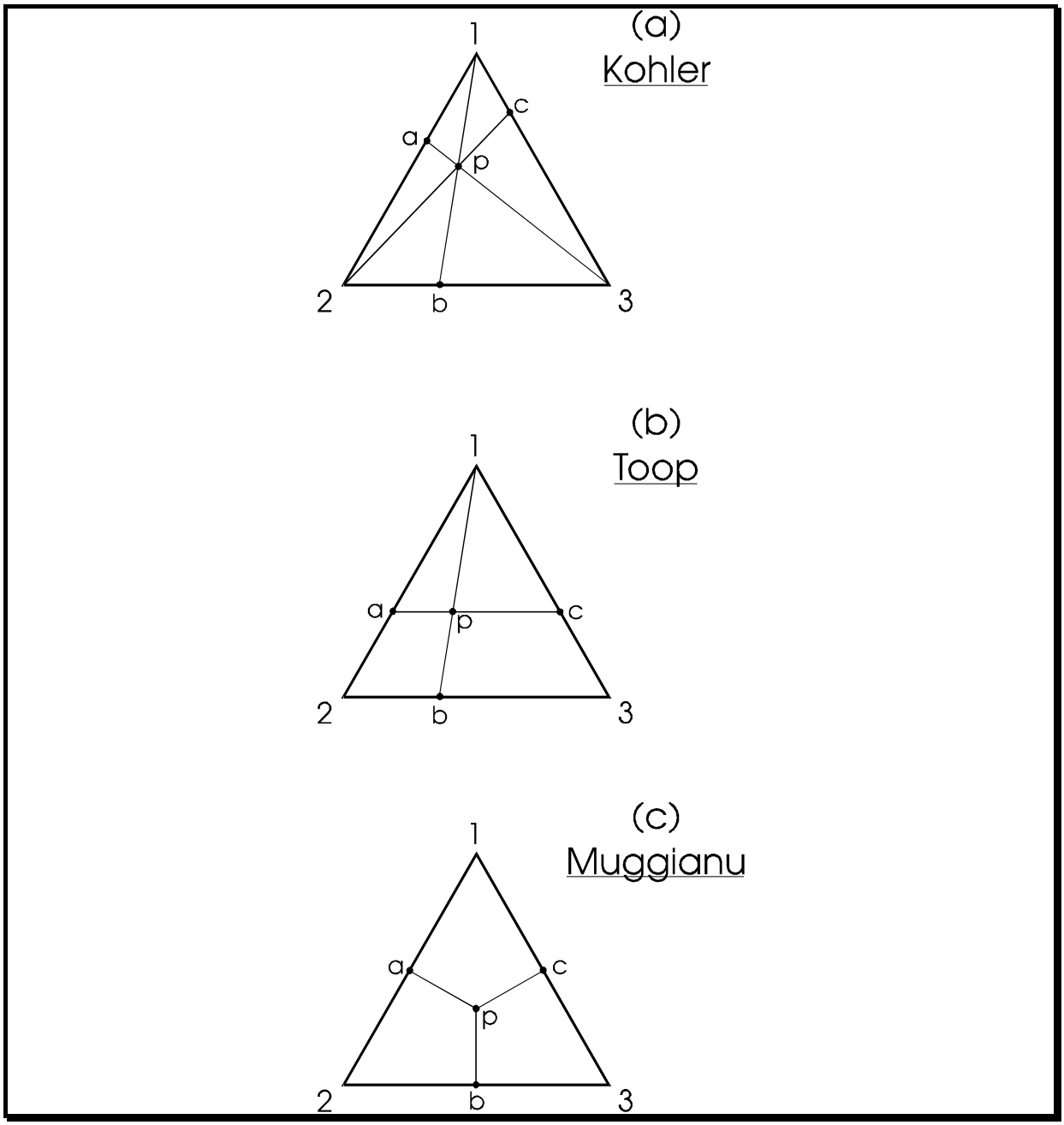

Figure 3.4.1. Kohler, Toop and Muggianu methods of including binary polynomial terms in ternary Gibbs Energy Equations.

3.5 FACT simulation of fluid bed gasification

The FACT program, has been used to simulate the possible chemical compositions in a 100 MW circulating fluid bed gasifier using the input feeds from Table 3.2.1.

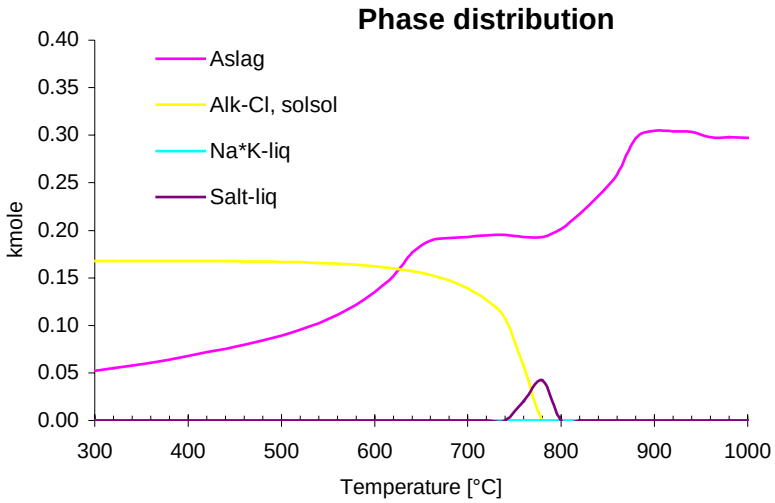

Figure 3.5.1. Solid and liquid solution phases using FACT

FACT predicts that there are four kinds of solid and liquid solutions (mixtures), shown in Figure 3.5.1. "Alk-Cl" is a solid solution consisting of alkali chlorides, KCl+NaCl. The KCl amount in the phase is greater than 98 %. Na*K-liq consists of liquid K_2CO_3 and Na_2CO_3. Salt-liq consists of melted KCl (>95 mole %) and NaCl (< 5 mol %). Aslag is a solid, which primarily consist of SiO_2 and K_2O. The Aslag phase is simulated using the "quasichemical model". Salt phases with KCl and NaCl can be simulated using the solution type 1 (polynomial (Kohler/Toop)) or the solution type 4, "sublattice model". Figure 3.5.1 shows that the amount of "Alk-Cl" (solid) is reduced with temperature, and the amount of that phase is negligible above 780°C. Between 740 and 800°C, the "salt-liq" phase appears, which consist of melted KCl and NaCl. The phase transitions of the two last mentioned phases takes place at temperatures close to the melting point of KCl (771°C), which is the main component of the two phases. This melted salt-liq phase is mobile and may cause problems in a fluid bed gasifier either in the bed as a melted salt or as condensed deposits in the reactor.

The amount of Na*K-liq is negligible at all temperatures. The amount of "Aslag" is increased with temperature, and at temperatures above 800°C, it is the only remaining solid/liquid solution phase. Figure 3.5.2 shows the composition of the Aslag phase, and as can be seen, the major components are SiO_2 and K_2O. The total amount of SiO_2 in the simulation is 0.27 kmol, and the amount of SiO_2 in the Aslag phase is increased with temperature to 0.22 kmol at 940°C. Above 940°C the SiO_2 amount in the Aslag phase is decreased to 0.216 kmol at 1000°C. The molar ratio of SiO_2/K_2O in Aslag is shown in Figure 3.5.3.

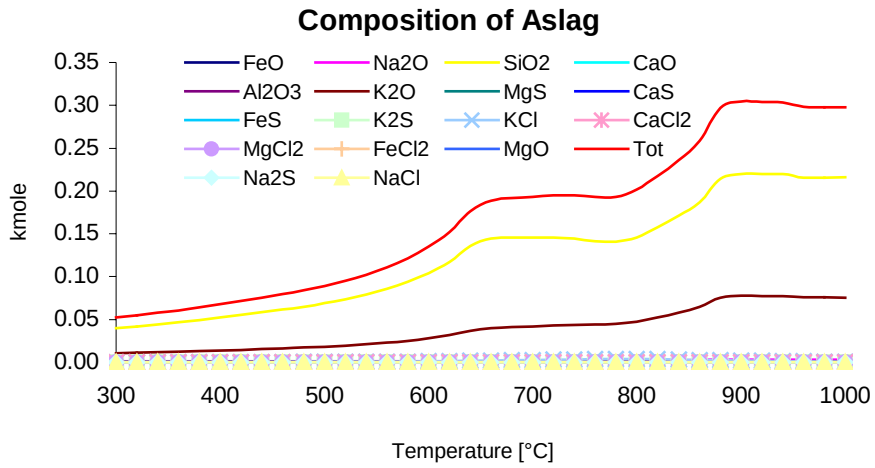

Figure 3.5.2. Composition of Aslag as a function of temperature

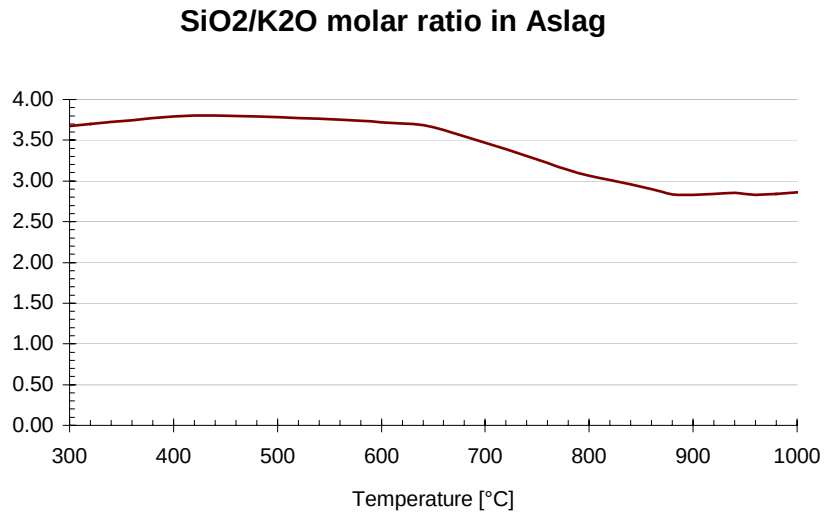

Figure 3.5.3. SiO_2/K_2O molar ratio in Aslag as a function of temperature

Figure 3.5.3 shows that the molar ratio of SiO_2/K_2O in Aslag reaches a maximum value of 3.8 at 420°C, decreases to 3.3 around 750°C, and the minimum value is around 2.8 at 900°C. The melting point of some K_2O/SiO_2 components are shown in Table 3.5.1.

Component	Melting point (°C)
SiO_2	1723
$K_2O*4SiO_2$	770
$K_2O*2SiO_2$	1045
K_2O*SiO_2	976
K_2O	881*
K_2CO_3	901

Table 3.5.1. Melting point of K_2O/SiO_2 compounds
*) Lange's Handbook of Chemistry 1985

In particular, $K_2O*4SiO_2$ has a very low melting point. High silica potassium silicates have low liquidus temperatures. An eutecticum exists around the mole composition $K_2O*3.3SiO_2$ (Kracek 1937 and Figure 167 in Levin 1985). Here the melting temperature is 730-740°C. This is well in accordance with the results from Figure 3.5.3 where it is seen that the calculated SiO_2/K_2O mole-ratio in the Aslag phase approximately equals 3.3 at 730-740°C. As the temperature increases it is observed that the Aslag phase equilibrium composition changes. Additionally with small amounts of sodium, liquidus temperatures at a ternary eutectic are as low as 540°C (Blander 1997). According to our calculations, above 600°C Na_2O and KCl mixes into the Aslag phase in a mole ratio to K_2O of 1-5 % and 1-8 % respectively. Additionally some inhomogeneity is expected in a fluidised bed, therefore local various in SiO_2/K_2O mole ratios and in salt concentrations are likely as observed experimentally. Calculations below 500°C represent a long extrapolation of the high temperature input data (Blander 1997), therefore the Aslag phase for T < 500°C are not certain. Further below 700°C the Aslag formation rate may be very low under typical CFB-gasification conditions.

A more detailed investigation of the theoretical prediction from FACT calculations as well as experimental validation will be the topic for further work. The effect of adding various amounts of different additives will also be tested.

3.6 Theoretical Sintering and Agglomeration Index, γ_K and $\gamma_{K,Na}$.

From the elemental composition of the straw and the knowledge obtained from the complex multicomponent-multiphase systems using the equilibrium programs and comparing to experiments, we introduce a theoretical sintering and agglomeration index, γ_K and $\gamma_{K,Na}$. These index in particular are used for gasification of e.g. straw in the temperature range 800-1000°C and at atmospheric pressure, where most KCl has evaporated. The index describes the molar ratio of SiO_2 to the sum of K_2O and Na_2O. The potassium and sodium that participate in this ratio we chose as the fuel potassium and sodium fractions that is neither bound to Cl as volatile KCl nor bound to phosphor. We hereby estimate the bed content of potassium silicate phase that is known to contribute significantly to bed agglomeration and sintering. We introduce the (theoretical) sintering and agglomeration mole ratio index, $\gamma_K=(SiO_2/K_2O)_{sint}$ and $\gamma_{K,Na}=(SiO_2/(K_2O+Na_2O)_{sint}$. These index are (with a_p being a coefficient) calculated as:

$\gamma_K = 2(Si/28.09)/((K/39.10)-(Cl/35.45)-(a_pP/30.97))$.

$\gamma_{K,Na} = 2(Si/28.09)/((K/39.10) + (Na/22.99)-(Cl/35.45)-(a_pP/30.97))$.

For straw, where typically the mole content of K is much larger than the mole content of Na, γ_K may be sufficient for a proper evaluation of the ash quality. However, if $\gamma_{K,Na}$ is greatly different from γ_K special considerations should be taken. If reactive additives or bed materials are used together with the fuel or fuels, and if the molar amounts of the added elements are significant and effectively reacting with the inherent inorganic ash components, these should be included in the calculations of the index if possible. The precise value of the coefficient a_p depends on the elemental composition of the ash and the gasification conditions. In the present work for simplicity and for small amounts of phosphate we have chosen $a_p=1$ representing products like $KCaPO_4$. If all phosphate is taken up by calcium alone, $a_p=0$, and if the only product is K_3PO_4, $a_p = 3$.

If a fuel is characterised by a very low index, $\gamma_K=1.$, such a ratio typically favours the production of K_2O*SiO_2 with a melting temperature as high as 976°C and only small amounts of melt should be introduced at typical gasification temperatures. If $\gamma_K<1$, and the CO_2 partial pressure is non-vanishing, K_2CO_3 (melting point of 901°C) is much more stable than K_2O (melting point: 881°C). We find at 900°C that ($[K_2CO_3]$/ ($[K_2O]$ [CO2])) = $3.2\cdot10^9$ and thus with $[CO_2]=0.1$ bar, K_2CO_3

strongly dominates K_2O. K_2CO_3 has a melting point of 901°C. Furthermore with $\gamma_K \leq 1.0$, the potassium content is high, and relatively high $K_2O(g)$, $KO(g)$ and $KOH(g)$ partial pressures exist. Therefore the concentration of catalytic clusters at the carbon surface is high and thus the reactivity must be high. The conclusion here assumes that the bed material does not contain SiO_2 and instead is composed of e.g. dolomite or calcium carbonate.

For high values of γ_K, e.g. $\gamma_K>15$ the fuel ash will give little potassium silicate melt formation and thus this phase will contribute only little to agglomeration. Also for high γ_K the reactivity is low since the catalyst is bound to other inorganic species.

The index γ_K and $\gamma_{K,Na}$ here introduced are more suitable for an evaluation of the agglomeration and sintering tendency than absolute parameters as e.g. the Si content being high or low or the potassium content being high or low. The γ-indexes do not vary with the amount of the fuel, however variation of the amount of fuel and thus the amount of ash is important since the mass balance for the reactor of consideration is important. We therefore advocate that besides using the here introduced index equilibrium programs are also used to simulate the actual process whenever new fuels, bed materials or additives are tested.

3.7 Experimental Sintering and Agglomeration Index (SAI)

The sintering and agglomeration index (SAI) as utilised by Moilanen [1999] is in the present work defined in an interval from 0* to 3*, i.e. SAI$\in$[0*,3*]. Normally only integers are used for the classification index or SAI is counted as stars, '*', i.e. *=1* (read: one star), **=2* and ***=3*. The ash residues are characterised after the sample has been gasified until complete conversion of the carbonaceous part of the sample. In case complete conversion can not be obtained the sample is marked unburned as '(u)'.

SAI=0*: The ash is very loose, the structures of the ash particles resemble the structure of the char particles and are easily crumbled by touching. No signs of agglomeration or sintering are observed.
SAI=1*: The ash agglomerates and starts to sinter, the particles contain fused ash.
SAI=2*: The ash agglomerates and includes significantly sintered and fused particles.
SAI=3*: The ash residue has fused to larger blocks.

SAI is visually obtained using a microscope. Steps of 0.5 may be introduced as e.g. (**)=2.5*.

3.8 Corrosion Index (CI)

The simplified corrosion index, CI, is in the present work defined in an interval from 0 to 3, i.e. CI$\in$[0,3]. CI was visually evaluated after each experiment. CI=0 indicates no or very little corrosion of the steel sample holder used for gasification measurements. Higher values indicate that significant corrosion takes place on the scale of hours. CI=3 thus indicates very high corrosion. Since the index is the result of subjective test it is recommended to use only numbers in steps of 1. The steel types tested in the present report are 253 MA and Wst 14841.

3.9 Reactivity

This section shortly outlines how the expression used for determination of gasification reactivity for chars from wood, wheat and barley samples can be derived. After a derivation of a standard Langmuir type kinetics expression, which is often used to describe gasification reactions, we introduce a relation between catalyst partial pressures and the concentration of surface-catalyst on active sites. These values can partly be estimated from equilibrium calculations. In section 3.10 an example is elaborated, where this approach has been taken. Solid fuel char reactivity, R[min^{-1}], towards a reactive gas is defined as

$$R = \frac{1}{1-X}\frac{dX}{dt}$$

R depends on conversion, $X=(M_0-M)/M_0$, where M is the mass of the organic part of the sample, T is the temperature, the total and partial pressure of the gas-mixture $\underline{Y} = (Y_1, Y_2, .. Y_n)$, where Y_i may be N_2, CO_2, CO, H_2O, H_2 and catalyst partial pressures like $K_2O(g)$, KO(g), K(g), KOH(g). Also sample specific properties like internal area/pore and reactive site distribution and the composition of inorganic elements are important. In the following R is split into a chemical kinetics term r_c, and a structural term f found up to a constant, so that $R = r_c f(X)$, where f(X) is a structural profile. Catalytic effects are dependent on catalyst concentration or activity on the carbon surface, their composition and physical behaviour. We consider now a reaction, taking place in a gas mixture composed of H_2O, CO_2, H_2 and CO.

(1)	$C_f + CO_2 \Leftrightarrow C(O) + CO$	k_{1f}, k_{1b}, $K_1 = k_{1f}/k_{1b}$
(1w)	$C_f + H_2O\ (g) \Leftrightarrow C\ (O) + H_2$	k_{1fw}, k_{1bw}, $K_{1W} = k_{1fw}/k_{1bw}$
(3)	$C(O) \rightarrow CO\ (g) + C_f$	k_3

The relevant equations for the (H_2O, H_2) and (CO_2, CO) pairs are

$$r_{c,w} = \frac{k_{1fw} P_{H_2O}}{1 + a_w P_{H_2O} + b_w P_{H_2}}$$

$$r_c = \frac{k_{1f} P_{CO2}}{1 + aP_{CO2} + bP_{CO}}$$

In the following derivation we assume, that the reactions described by $r_{c,w}$ and r_c take place at the same sites but in competition and that k_{1f}, k_{1b}, $k_{1f\,w}$, k_{1bw} and k_3 exist. Let P_i be the partial pressure (bar) of species *i* in the gas phase; C_f: the [mol] number of reactive sites that can possibly be occupied by species *i*, C(O): the surface [mol] number reactive sites actually occupied by species *i*, C_v: the surface [mol] number of void reactive sites to be occupied by species *i*. We get C_f = C(O) + C_v , C_v = C_f - C(O). Finally C_{tot} is the total [mol] number of carbon atoms in the sample. We get, assuming steady state for C(O):

$$\frac{dC(O)}{dt} = k_{1f}(C_f - C(O))P_{CO2} + k_{1fw}(C_f - C(O))P_{H2O} - k_{1bw}C(O)P_{H2} - k_{1b}C(O)P_{CO} - k_3C(O) = 0$$

From which we get

$$(k_{1f}P_{CO2} + k_{1fw}P_{H2O})C_f = (k_3 + k_{1b}P_{CO} + k_{1bw}P_{H2} + k_{1f}P_{CO2} + k_{1fw}P_{H2O})C(O)$$

and

$$C(O) = \frac{k_{1f}P_{CO2} + k_{1fw}P_{H2O}}{k_3 + k_{1b}P_{CO} + k_{1bw}P_{H2} + k_{1f}P_{CO2} + k_{1fw}P_{H2O}} C_f$$

or

$$C(O) = \frac{k_{1f}P_{CO2} + k_{1fw}P_{H2O}}{k_3 + k_{1b}P_{CO} + k_{1bw}P_{H2} + k_{1f}P_{CO2} + k_{1fw}P_{H2O}} \frac{C_f}{C_{tot}} C_{tot}$$

Since $-dC_{tot}/dt = -dC_f/dt$ [(mol s^{-1}] = k_3[s^{-1}] C(O) we get:

$$-\frac{dC_{tot}}{dt} = \frac{k_{1f}P_{CO2} + k_{1fw}P_{H2O}}{1 + bP_{CO} + b_wP_{H2} + aP_{CO2} + a_wP_{H2O}} \frac{C_f}{C_{tot}} C_{tot}$$

By multiplying at both sides of the equation by the molecular weight m_c[g/mol] one obtains:

$$-\frac{dM}{dt}[g/s] = \frac{k_{1f}P_{CO2} + k_{1fw}P_{H2O}}{1 + bP_{CO} + b_wP_{H2} + aP_{CO2} + a_wP_{H2O}} \frac{C_f}{C_{tot}} M[g]$$

Dividing by the mass, we get the reactivity, R [g/g s^{-1}]= -(dM/dt)/M:

$$R = \frac{k_{1f} P_{CO2} + k_{1fw} P_{H2O}}{1 + bP_{CO} + b_w P_{H2} + aP_{CO2} + a_w P_{H2O}} \frac{C_f}{C_{tot}} = r_c f(x)$$

In this case, $f(X) = C_f/C_{tot}$, is the number of reactive carbon sites per carbon atom in the sample. The expression is best understood in the non-catalytic (or constant amount of catalyst) case and may be used for the determination of reactivity of straws that have been pyrolysed at very high temperatures like 1000°C or straw samples that have a very high $\gamma_K = SiO_2/K_2O$. Sørensen et al. (1997) determined kinetic parameters for a wheat straw, a barley (raw and washed). (Gøbel 1999) and (Barrio et al. 1999) report data produced in the present project for a birch and a beech sample.
In the catalytic case we suggest as a first approximation the following relation for the reactivity:

$R = r_c\, g(X, T, A(x), \sigma_1(X), \sigma_2(X), Z_{cat}, Z_{add}, Z_{ash}) = r_c\, A(X)\, \sigma_2(X)\, \sigma_1(X) p_1(T, Y_i)$

This may also be expressed as

$R = r_c\, f(X)\, H(X)\, p_l(T, Y_i)$

0)	R:	Reactivity	[s^{-1}]
1)	r_c:	Reaction rate,	[s^{-1}]
2)	f(X):	No. of reactive carbon sites/No. total carbon atoms, C_f/C_{tot},	[-]
3)	g(X, ..):	Structural function including effects of catalysis	[-]
4)	Z_{ash}:	The elemental composition range for the ash.	
5)	Z_{add}, Z_{bed}:	The elemental composition range for the additives and the bed	
6)	A(X):	Area/mol total carbon	[m^2 /mol]
7)	$\sigma_2(X)$:	Number of reactive carbon sites /m^2 pore area	[mol m^{-2}]
8)	$\sigma_1(X)$:	Number of catalyst sites/number of reactive carbon sites	[-]
9)	$p_1(T,Y_i)$:	The likelihood that a catalytic site is activated	[-]
10)	Y:	Gas partial pressure	[bar]
11)	X:	Conversion	[-]
12)	H(X):	No. of catalytic sites/No. of reactive carbon sites C_{cat}/C_f	[-]

In the present formulation $p_1(T,Y_i)$ is dependent on the concentrations of the various gases, the bed and ash components and the carbon surface and is therefore related to γ_K. If the catalyst is potassium in the form of C-O-K or O-K clusters, p_1 is a strong function of the temperature. We suggest that for a fixed temperature the number and size of these clusters are also related to e.g. the partial pressure of KOH(g), KO(g), K_2O(g) (Sørensen and Stoltze1998). One consequence of this may be that when the partial pressures of these components saturates one may expect no great increase in reactivity as more potassium is added to the sample. $p_l(T,Y_i)$ is dependent of the reactor conditions as well as of the inorganic mass balance and thus complicated to obtain. One approach is to determine p_l using an equilibrium approach. For the potassium catalyst we suggest that p_1 is correlated through equilibrium between the surface active catalytic potassium species at the carbon surface and a multiphase-equilibrium between the inorganic species determining p_1 as well as KOH(g), K_2O(g) and KO(g). The last mentioned may be calculated using the FACT or HSC-chemistry programs. In order to do or illustrate this, it is necessary to find or estimate values for relevant carbon-potassium compounds. In the literature data exists on enthalpy and entropy of formation of graphite and intercalated potassium on graphite compounds, see Table 3.9.1 (Dresselhaus 1981).

Reaction	Graphite – Potassium		
	$-\Delta H_f^0$ cal/mol (Potassium)	$-\Delta S_f^0$ cal/mol K	Molecular weight (g)
$8C(s)+K(g) \rightarrow C_8K(s)$	28500	24.0	135.19
$10C(s)+K(g) \rightarrow C_{10}K(s)$	27000	22.5	159.21
$24C(s)+K(g) \rightarrow C_{24}K(s)$	30400	20.7	327.37
$36C(s)+K(g) \rightarrow C_{36}K(s)$	31700	20.7	471.50
$48C(s)+K(g) \rightarrow C_{48}K(s)$	32300	20.7	615.63
$60C(s)+K(g) \rightarrow C_{60}K(s)$	32800	20.8	759.76

Table 3.9.1 Enthalpies and entropies of formation and molecular weight for graphite-potassium, compounds (Aronson 1968, Dresselhaus 1981).

In order to determine the Gibbs free energy as a function of temperature, the specific heat for the relevant components should be used. The specific heat may be obtained by using the Debye model. The specific heat per atom is found as a function of the Debye temperature θ_D as:

$$c_v = 9R\left(\frac{T}{\Theta_D}\right)^3 \int_0^{\Theta_D/T} \frac{x^4 e^x dx}{(e^x - 1)^2}$$

The Debye-temperature for graphite at higher temperatures is 790 K (Elliott 1998). The data presented by (Dresselhaus 1981) for graphite and intercalated potassium was tested in a few simulations for the $C_{10}K$ compound. The specific heat per mole $C_{10}K$ is simulated as the specific heat for graphite plus an additional term C_{vK} to account for the addition of K to graphitic C_{10}. C_{vZ} was varied between $R < C_{vZ} < 3R$, where R is the gas constant. This was for $C_{10}K$ done to predict the temperature dependent isobar for growth of graphite-K compounds showing experimental intercalant uptake versus temperature difference between graphite and intercalant as shown at page 145 in (Dresselhaus 1981). The presently used simple approach is based on the assumption that the intercalant ions are greatly mobile in two dimensions and except from leaving electron density to graphite do not interact much with the graphite structure.

3.10 Washing straw and returning salts

In the following reactivity and agglomeration is described utilising the equilibrium approach. This is done in order to test which consequences such an approach may have.

The barley straw used by (Henriksen 1996 and 1997) for the reactivity tests had with respect to the major elements an ash composition similar to the wheat DW95. Therefore the very well characterised DW95 is used to consider the possible catalyst behaviour during gasification in a gasifier and during the macro-TGA experiments performed by (Henriksen 1997). Henriksen first washed the straw and thereby obtained a low-salt straw. The salts so removed were arranged in portions and added again to the washed straw fraction in portions.

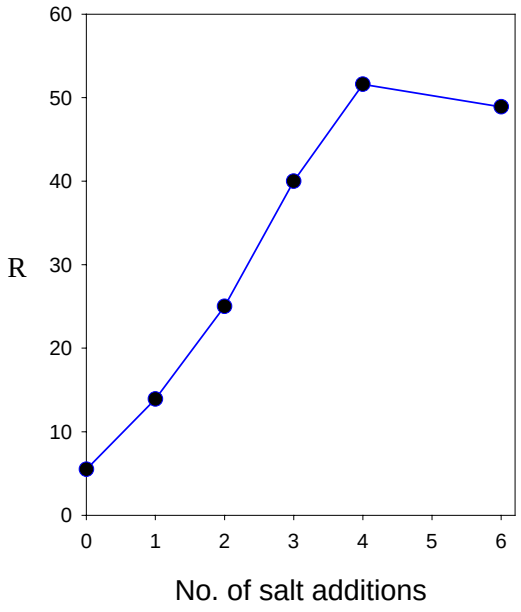

Figure 3.10.1. Reactivity, R (% min^{-1}), of straw char, measured as a function of no. of soluble salt additions (see text)

The reactivity increases with salt addition until four times the original salt concentration have been added and then saturation takes place. Henriksen also demonstrated that roughly the same reactivity was obtained whether the wash was performed at the raw straw or the char. Considering Wheat 95, and the data from Figure 4.2.1 and Table 3.2.1 and using Si as a tracer, i.e. assum-

ing that Si is not removed during a water washing procedure, the total molefraction (%) of the other elements that are washed out is estimated according to the (ash tracer) relation as: $X_{w,ash}=100-100*(A_o/A_1)(100-A_1)/(100-A_o)$. A_0 and A_i are the mole fraction of the inorganic element (disregarding oxygen) in the original ash sample and the washed ash samples, respectively. With elemental silicium as the ash tracer, the total mole fraction, disregarding oxygen, of the other ash components which was washed out according to the ash tracer technique is:

$X_{w,ash} = 100-100(23.14/51.23)(100-51.23)/(100-23.14) \approx 71.34$ %

And the fraction, O_i, of total *mole ash* (disregarding oxygen) which was washed out is then (since Si is not washed out):

$O_i = 0.7134(100-23.14)/100 \approx 0.5483$

From this we find the retained fraction of each of the elements is,

$Y_{w,i}=(1-O_i)A_i/A_{0i}=0.4517A_i/A_0$,

Thus the washed out component mole fraction is

$Z_{w,i}=1-Y_{w,i}$.

It is now possible to express the experiment performed by (Henriksen 1997) so that the number of moles of inorganic components added to the process is: $Q_{w,i} =(Y_{w,i} + nZ_{w,i})N_i$. N_i is the number of moles of the inorganic elements added to the process per ton dry fuel in a 100 MW gasifier. HSC has in the following been used for simulations of the addition of inorganic components according to the above plan.

	O	Na	Mg	Al	Si	P	S	Cl	K	Ca	Ti	Cr	Mn	Fe	Ni	Cu	Zn
Sa	61.1	0.361	1.651	0.173	9.010	1.285	1.404	5.851	13.968	4.694	0.047	0.065	0.067	0.096	0.074	0.130	0.062
		0.93	4.24	0.44	23.14	3.30	3.60	15.03	35.87	12.06	0.12	0.17	0.17	0.25	0.19	0.33	0.16
σ_{sa}	3.9	27.7	7.3	34.7	11.2	7.0	17.1	20.3	9.9	8.9	40.4	9.2	23.9	46.9	27.0	46.2	90.3
Saw	67.8	0.135	2.319	0.112	16.49	1.613	0.182	0.091	2.268	8.378	0.040	0.034	0.068	0.14	0.102	0.116	0.097
		0.42	7.21	0.35	51.23	5.01	0.57	0.28	7.05	26.03	0.12	0.11	0.21	0.43	0.32	0.36	0.30
σ_{sa}	0.5	27.4	11.3	28.6	2.0	7.3	29.7	53.8	3.0	6.0	75.0	58.8	14.7	64.3	29.4	25.9	20.6
A_i/A_{io}		0.452	1.70	0.795	2.21	1.518	0.158	0.019	0.196	2.18	1.	0.65	1.23	1.72	1.68	1.09	1.87
Y_{wi}		0.204	0.768	0.359	1.000	0.686	0.072	0.008	0.089	0.975	0.452	0.292	0.558	0.777	0.761	0.49	0.85
Z_{wi}		0.796	0.232	0.641	0.	0.314	0.929	0.992	0.911	0.025	0.548	0.708	0.442	0.223	0.239	0.51	0.15
DW95																	
$N_I Y_{w,i}$		$1.71\ 10^{-3}$	$1.98\ 10^{-2}$	$1.01\ 10^{-3}$	$2.73\ 10^{-1}$	$1.81\ 10^{-2}$	$1.38\ 10^{-3}$	$1.35\ 10^{-4}$	$2.73\ 10^{-2}$	$7.01\ 10^{-2}$	$5.43\ 10^{-5}$			$9.34\ 10^{-4}$			
$N_I Z_{w,i}$		$6.66\ 10^{-3}$	$5.97\ 10^{-3}$	$1.81\ 10^{-3}$	0	$8.28\ 10^{-3}$	$1.78\ 10^{-2}$	$1.67\ 10^{-1}$	$2.80\ 10^{-1}$	$1.80\ 10^{-3}$	$6.59\ 10^{-5}$			$2.68\ 10^{-4}$			

Table 3.10.1. $Y_{w,i}$ and $Z_{w,i}$ input in kmol (per ton dry fuel) to equilibrium calculations. The procedure used is the method shown in section 3.2.

In the following the moles content in the relevant phases are shown as a function of potassium added [kmol/ton dry fuel]. The amount of potassium in the washed straw is $2.73 \cdot 10^{-2}$ kmol. Each time one portion of solubles is added, $2.80 \cdot 10^{-1}$ kmol K is added. Thus we read the amount of potassium added as: 0X: 0.0273, 1X: 0.3073, 2X: 0.5873, 3X: 0.8673, 4X: 1.1473, 5X: 1.4273, 6X: 1.7073 kmole. In Fig. 3.10.2 the major potassium compounds are shown as a function of added potassium [kmol]. The calculations are made with soluble chloride as taken from Table 3.10.1 (left figures) and with no chloride added (right figures) respectively. Considering the simulations where chloride is not added in the calculations, saturation of KO(g) is observed to take place between 1 and 2 kmol potassium added. Henriksen (1997) observed that the steam gasification kinetics showed saturation phenomena around 4X, which corresponds to 1.15 kmol added K. Consider instead the simulations where the full amount of water-soluble Cl is added together with the additives. In this case KO(g) saturation takes place much later, i.e. after the addition of 5 kmol potassium (or 20 times of salt addition) and this is not in accord with the results shown in Figure 3.10.2.

The amounts of chloride available during the experiments performed by Henriksen are not known completely, since the mass balance during a TGA experiment is not as well defined as desired for the equilibrium calculations to succeed. Also a part of the chloride may during the slow heating period in the TGA leave the sample as HCl(g). Also it must be noticed that the sample may not reach complete equilibrium and so the KO(g) saturation may take place in the TGA before it is

predicted in these simulations. The experiments performed by Henriksen were made using pure steam. Calculations show that the KO(g), KO_2(g) and KOH(g) partial pressures depend on the steam and hydrogen partial pressures. The concentration and chemical form of potassium at the carbon surface therefore also likely depends on the composition and the volume of the gas atmosphere in a more complicated way. Because the relation between the partial pressures and the reactivity seems to be very complex, another effect to be considered is the possible saturation of active sites by O-K bonds or O-K clusters or intercalated potassium as discussed in Chapter 3.1. In order to do this utilising the equilibrium approach, Gibbs free energies is required for the relevant catalyst located at active sites at carbon.

The data presented by (Dresselhaus 1981) for graphite and intercalated potassium was investigated using a few simulations for the $C_{10}K$ compound. The specific heat per mole $C_{10}K$ were simulated as the specific heat for graphite plus an additional term C_{vK} that accounted for the addition of K to graphitic C_{10}. C_{vZ} was varied between $R<C_{vZ}<3R$, where R is the gas constant. This was for $C_{10}K$ done in order to predict the temperature dependent isobar for growth of graphite-K compounds showing experimental intercalant uptake versus temperature difference between graphite and intercalant as shown page 145 in (Dresselhaus 1981). Other intercalate compounds C_nK are described by Dresselhaus, where e.g. n = 8, 10, 24, 36, 48 and 60. Our initial simulations indicated that the $C_{10}K$ compound was stable in nitrogen up to around 500°C but not in a gasification atmosphere, where e.g. K_2CO_3 was more stable. Also the intercalation compounds with potassium in nitrogen seem not stable above 500°C. Therefore the thermal properties and stability of O-K bonds or clusters will be the topic for the future work.

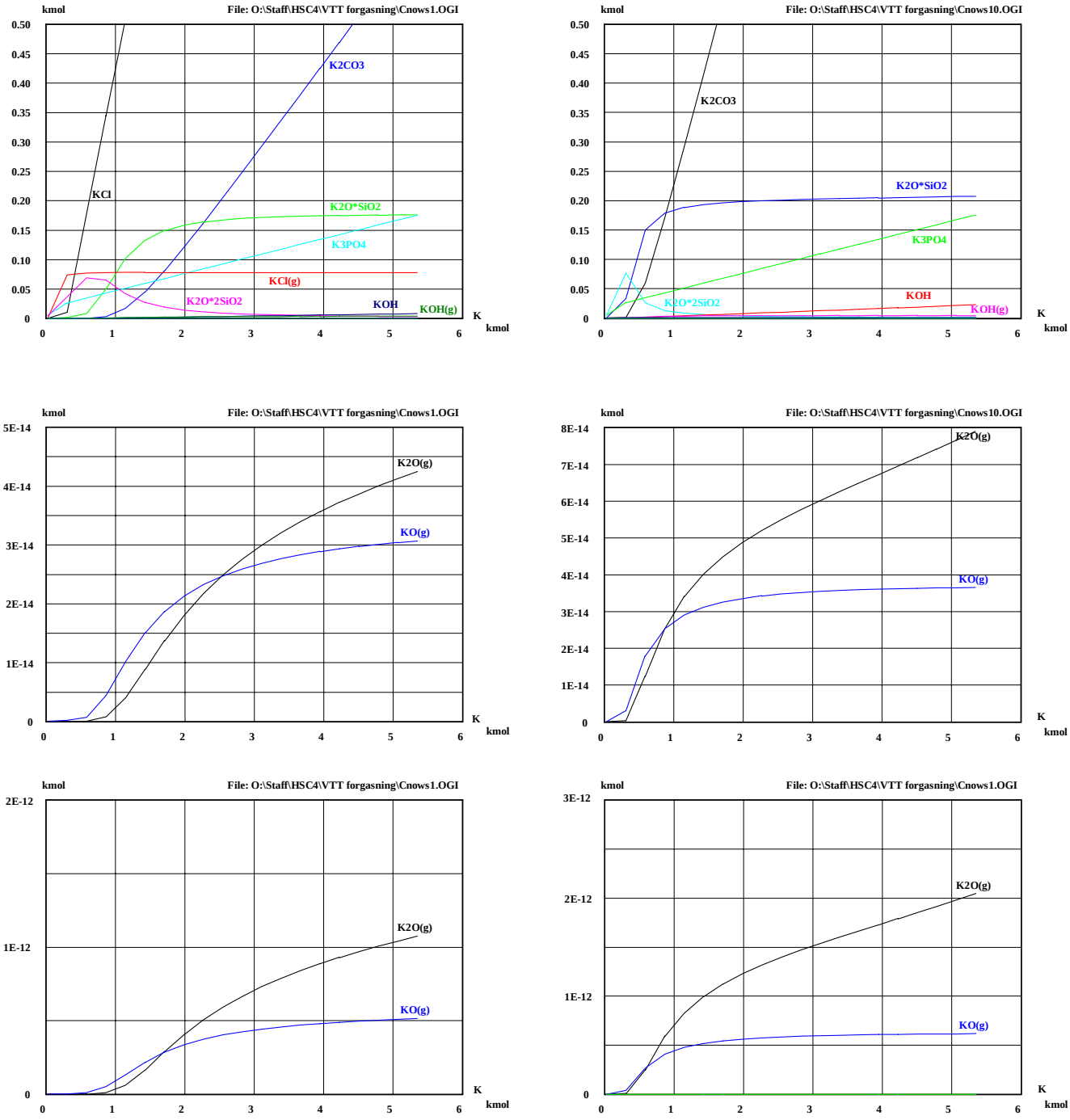

Figure 3.10.2. HSC predictions using input data from Table 5.1.1 made with soluble chloride as (left figures) and with no chloride added (right figures), Row 1 (800°C): main potassium components, Row 2 (800°C): KO(g) and $K_2O(g)$, Row 3 (850°C): KO(g) and $K_2O(g)$.

4. Experimental

ReaTech and VTT-Energy performed experiments on ten straws at VTT during summer and autumn 1998. These measurements were mainly conducted in order to investigate reactivity and agglomeration and sintering properties of a number of Danish straws. For the straw the geographical location, the quality of the field, and the amount and type of the fertilisers used for each straw were registered together with the amount N, P, K and S used [kg/Ha] added Also the weathering conditions varied. For each of the straws an elemental analysis were made. ReaTech following tested reactivity and agglomeration characteristics of synthetic carbon, ash and additive mixtures. Finally ReaTech and ET tested reactivity and agglomeration characteristics of one raw straw sample and the same straw mixed with various additives.

4.1. Instrumental

Thermal gravimetric analysis

A thermobalance (Moilanen, 1999) was used at VTT in order to study the reactivity and sintering properties of the Danish straws at 750 and 850°C. The fuel sample (particle size below 0.2 mm, sample amount 100-200 mg) was placed in the cylindrical sample holder having the wall made of wire mesh. In an isothermal test, after the corrections were completed (i.e. temperature, pressure, gas composition), the sample was lowered into the reactor with the winch system. During the measurement, the temperature and weight of the sample were monitored. The weight change recorded during the first 60 seconds period was due to several effects before the weight was stabilised (including buoyancy and pyrolysis), and this part of the weight-time curve was removed. The sintering degree of the ash residue after the reaction was inspected with a microscope. The reactivity is expressed in form of an instantaneous gasification reaction rate, %/min (i.e. mass change rate divided by residual ash-free mass), and the conversion (given as fuel conversion, % ash-free) is the reacted part of the whole biomass including pyrolysis. The ash residues from the thermobalance experiments were studied by microscopy using the SAI developed by [Moilanen, 1997], see section 3.7.

The macro-TGA located at ET, DTU consists of a reactor placed in an oven, see Appendix 3. The oven provides the energy for the gasification and preheats the steam/nitrogen before it enters the reactor. The reactor is suspended from a pipe through which the sample is connected to a balance. Inside the reactor about 5 g of pyrolysed char is placed in a basket hanging in the centre of the reactor with no direct contact to the reactor wall. The basket is cylindrical and has a length of 18 cm and an internal diameter of 3.5 cm. The sample is heated to 150-200°C to evaporate water. Following the sample is heated to 800°C or 850°C and kept isothermal until the char is completely devolatilised and the temperature is stable. A 100 % steam atmosphere is added and the gasification rate, the reactivity, R, and the time of complete char conversion at temperature T, $t_{b,T}$, is determined. After complete char conversion, the reactor is allowed to cool down. The ash is visually evaluated and the slagging and agglomeration index, SAI, and the corrosion index, CI, are determined. A number of ash samples were analysed using SEM-EDX and X-ray diffraction.

A "SDT 2960 simultaneous TGA-DTA Analyser" from TA-instruments was used at ReaTech for CO_2-CO-N_2 gasification tests and for the detection of ash-melting behaviour. The SDT was also utilised to test reactivity and agglomeration characteristics of synthetic carbon, ash and additive mixtures. The (P)TGA was used at ReaTech for H_2O-H_2-CO_2-CO reactivity measurements (Gøbel 1999) and (Bario et al. 1999) in a modified Du Pont thermogravimetric analyser (Rathmann and Stoholm 1995). The flow control is for both facilities performed using valves and gas mass flow controllers. The PTGA is shown in Figure 4.1.1. The gas lines have the set-up shown in Figure 4.1.2.

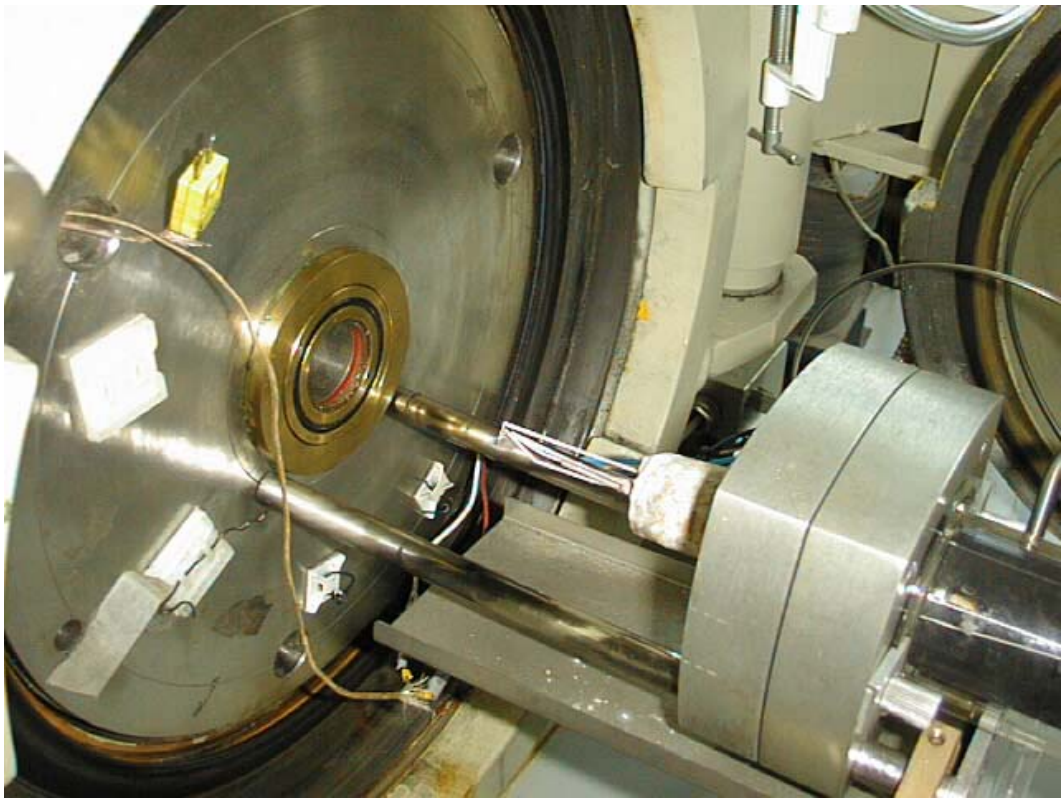

Figure 4.1.1. The ReaTech PTGA

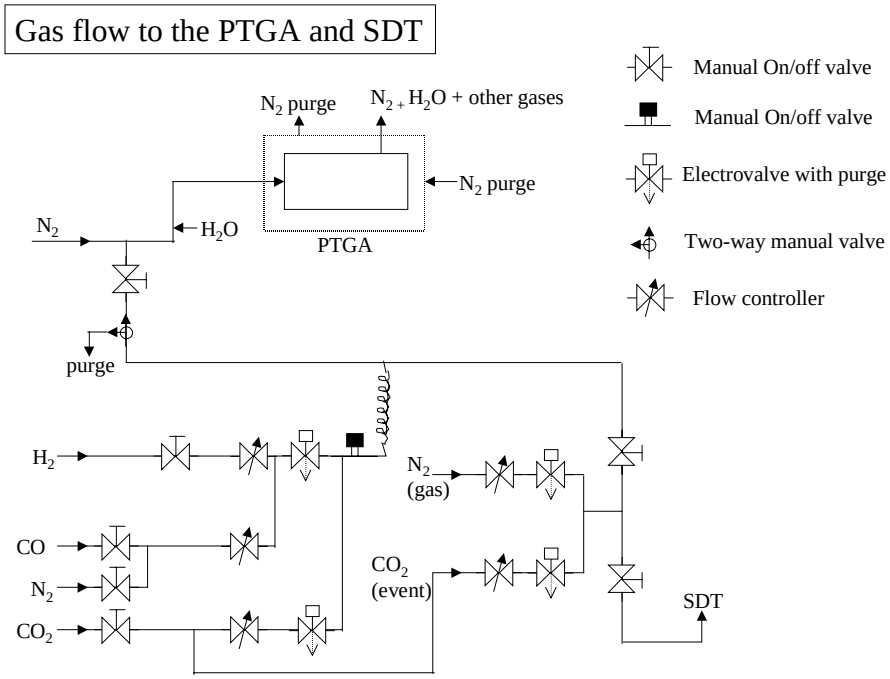

Figure 4.1.2. Set-up of gaslines for ReaTech's PTGA and SDT thermal analyser equipment.

Bench scale fluidised bed test

A bench-scale atmospheric fluidised bed test rig was used at VTT. The purpose of the tests was to estimate the gasification behaviour of ten Danish straws and to confirm laboratory findings concerning the ash sintering behaviour obtained using thermal gravimetric analysis (TGA). The char reactivity and mainly the ash sintering/deposition tendency were evaluated in the fluidised-bed reactor kept at 800°C in the bed and in the freeboard. The cyclone temperature is 750°C and the temperature of the ceramic filter is 570°C. Following one additional experiment at 770 or 830°C were performed, dependent of the success of the first run, hereby setting limits to the maximum gasification temperature. 420 g of dolomite bed material with a particle diameter range of 0.71-1.0 mm were fed to the reactor as one batch from the top of the reactor before the start of the experiment. Following 7-800 g/h straw is added for around 4 hours or until a pressure drop or temperature variation indicates bed sintering or blockage in the gas lines. No bed-ash is sampled until after the experiment. Fuel ash is thus accumulated during the whole test or until sintering behaviour is observed. The time until sintering t_{sint} together with the process parameters indicate the anti-sintering effects of the tested bed materials with respect to the specific fuel.

Product gases and tars are sampled and a mass balance is made. In the fluid bed molten agglomerates are collected from the wall after the shut down. The agglomerates consist in the case of straw mainly of K and Si that melts into molten silicates and fix to the wall. The amount of collected molten silicates indicates the straws ability to produce melts and thus it likely correlates to the tendency of agglomeration and sintering of the fuel in a typical circulating fluidised bed.

4.2 Samples

A number of samples were selected for experimental tests. Several straw samples from 1997, 1998 and one straw sample from 1995 are evaluated. The straw samples are obtained from different locations and field qualities in Denmark. For each straw the geographical location, the quality of the field, 'JB', and the amount and type of the fertilisers used for each straw were registered together with the amount of N, P, K and S used [kg/Ha], see Table 1. Ultimate and proximate analyses of the straws are shown in the following tables. Heavy metals were not measured, therefore mean values from the literature were used for modelling purposes, see Appendix 1.

	Straw	Year	Loc	Quality	Fertiliser	N	P	K	S
#				(JB)		Kg/Ha	kg/Ha	kg/Ha	kg/Ha
1	Wheat	1997	Sj	6-7	NPK + S	222	42	56	42
2	Wheat	1997	Jy	4	NPK+M	279	51	103	11
3	Wheat	1997	Jy	6	NPK+M	180	30	60	35
4	Wheat	1997	Jy	2-3	N+M	192	38	76	24
5	Barley (W)	1997	Sj	7-8	NS+Mink	200	63	11	20
6	Grass	1997	Sj	6-7	NPK + S	111	16	51	19
7	Barley (S)	1997	Sj	6	NPK + S	89	26	50	20
8	Barley98(S)	1998	Sj	6	NPK+TS	230	120	19	11
9	Wheat/rib-	1998	Sj	5	N+P+Mg+A	180	23	150	19
11	Wheat/rib+	1998	Sj	5	N+P+Mg+A	180	23	150	19

Table 4.2.1. Straw samples from different locations and field qualities in Denmark. The used amount of fertiliser is shown [kg/Ha]. Rib: 'Ribbe harvested'(+/-) straw, see text. S: summer, W: Winther, Mink: Mink manure used, (M): manure (pigs), TS: Town Sludge, A: Straw ash. Loc: Location of harvest, (Sj): Sjælland, (Jy): Jylland.

Straws from six wheat, three barley and one grass samples were tested and compared to results formerly made on a Danish wheat straw-95 (DW95) and additionally a Danish wheat straw from 1997 tested at VTT. Ribbe harvest is an old way of harvesting, where 80 % of the crop product with the best feeding value is harvested as 'rib-' and leaves the residual straw left at the field for later use as e.g. a fuel. The rain has washed out potassium and chloride from the matured straw. After the harvest the straw is standing upright and rapidly gets dry after rain. The 'ribbe' wheat was 'rib-' harvested after a rainy period, the matured straw 'rib +' is harvested after around 1 month and after additionally 60 mm rain. The other samples were characterised by dry seasons.

The samples were pulverised to a size below 0.25 mm for analysis in the thermobalance. Volatile matter and ash contents were analysed on a LECO TGA-500 and C, H and N contents on a LECO CHN-600 instrument. The sulphur contents were determined on a LECO Sulphur Determinator SC432. The compositions of the ashes (after ashing to 550°C) were analysed at the chemical Laboratory of VTT by an X-ray fluorescence spectroscopy method developed for ash analysis. The ultimate and ash analysis is reported for 11 Danish straws in Table 4.2.2 and 4.2.4 and for some additional biomass samples in Table 4.2.3.

The samples were heated in nitrogen to 750 and 850°C at VTT and at 800 and 850°C at DTU respectively and here gasified until no more mass-loss were detected. SAI_T, reported in Table 4.2.5, is the sintering tendency measured in terms of 'number of stars' obtained by gasifying the chars 'completely' at the temperature T. In some cases significant amount of unburned carbon, denoted '(u)' remained after the experiment.

Artificial samples

Artificial samples were made in order to make quantitative test of the effect of mixing water soluble salts (potassium carbonate and potassium phosphate), insoluble ash components and various additives in the presence of carbon on reactivity and agglomeration tendencies.

An almost salt- and ash-free carbon sample was prepared by pyrolyzing 200-gram wheat#2 straw in a nitrogen atmosphere at 850°C in a pyrolysis oven. The char was following washed in hydrofluoric acid, HF at GEUS and subsequently washed five times in distilled water. In this way an almost ash- and salt free carbon sample was produced.

Two grams of raw ash were produced at 500°C in air using wheat#2. Washed ash was produced by washing the raw ash three times, each time in 200 ml distilled water at 50°C. The elemental composition [mol%] of the raw ash and of the washed ash was estimated from using SEM-EDX see Figure 4.2.1. According to these measurements, the washing procedure removed about 98% Cl, 85% S, 80% K and 55% Na.

Sample	Water Wt. %	Ash Wt. % d.b.	Vol. m. Wt. % d.b.	F.C. Wt. % d.b.	HHV/LHV MJ/kg d.b.	C Wt.% d.b.	H Wt.% d.b.	N Wt.% d.b.	S Wt.% d.b.	O Wt.% d.b.
1 Wheat	9.7	5.4	76.5	18.1	18.53/17.27	46.9	5.8	0.8	0.18	40.92
2 Wheat	7.3	5.4	77.1	17.5	18.65/17.36	46.4	5.9	0.6	0.13	41.57
3 Wheat	7.7	5.3	76.2	18.5	18.40/17.13	46.9	5.8	0.7	0.13	41.17
4 Wheat	10.1	3.5	78.2	18.3	18.81/17.53	47.2	5.9	0.5	0.13	41.47
5 Barley (W)	12.5	5.7	76.2	18.1	18.40/17.16	46.4	5.7	0.7	0.13	41.37
6 Grass	12.9	5.2	75.9	18.9	18.17/16.89	46.7	5.9	1.0	0.15	41.05
7 Barley (S)	10.4	5.5	76.2	18.3	18.32/17.07	46.5	5.7	0.5	0.12	41.68
9 Wheat98/rib	8.5	15.5	68.0	16.5	16.90/15.76	42.1	5.2	1.2	0.14	35.86
11 Wheat/rib+	7.9	8.0	75.3	16.7	18.33/17.13	46.1	5.5	0.9	0.10	39.40
12 DW95	10.5	4.8	76.1	19.1	n.d.	47.5	5.9	0.7	n.d.	41.10
14 DW97	7.0	6.1	75.8	18.1	n.d.	46.5	5.7	1.4	0.12	40.10

Table 4.2.2. Proximate and ultimate analysis of ten Danish straws. Oxygen by difference.

Sample	Water Wt. %	Ash Wt.% d.b.	Vol. m. Wt. % d.b.	F.C. Wt. % d.b.	HHV/LHV MJ/kg d.b.	C Wt.% d.b.	H Wt.% d.b.	N Wt.% d.b.	S Wt.% d.b.	O Wt.% d.b.	Cl ppm-wt d.b.	Na ppm-wt d.b.	K ppm-wt d.b.
12 DW95	10.5	4.8	76.1	19.1	n.d.	47.5	5.9	0.7	n.d.	41.10	6120	140	16730
13 Willow	?	1.3	80.5	18.2	n.d.	49.4	6.0	0.5	-	42.8	126	-	-
14 Alfalfa	11.3	6.9	75.8	17.3	18.4/17.22	45.8	5.4	2.2	0.10	39.6	4000	890	14200

Table 4.2.3 Proximate and ultimate analysis and soluble K, Na and Cl (d.b.) in three samples.

	Si Wt. %	Al Wt. %	Fe Wt. %	Ca Wt. %	Mg Wt.%	K Wt.%	Na Wt.%	Ti Wt.%	S Wt.%	P Wt.%	Cl Wt.%	γ_K	$\gamma_{K,Na}$
1 Wheat	18	0.11	0.23	6.5	2.3	23	0.30	<0.02	2.5	2.0	10	5.31	5.03
2 Wheat	14	0.10	0.17	7.4	2.5	27	0.38	<0.02	2.4	1.7	11	3.06	2.92
3 Wheat	13	0.15	0.26	7.4	2.7	29	0.33	<0.02	2.1	1.6	12	2.63	2.53
4 Wheat	7.6	0.12	0.39	11	2.5	34	0.29	<0.02	3.0	0.77	12	1.07	1.04
5 Barley (W)	16	0.33	0.36	9.1	1.9	25	1.80	0.03	2.0	2.2	6.3	2.92	2.43
6 Grass	14	0.05	0.16	5.9	2.3	30	0.21	<0.02	2.0	2.5	11	2.65	2.59
7 Barley (S)	15	0.10	0.19	8.5	1.6	25	1.80	<0.02	1.9	1.5	13	4.76	3.53
9 Wheat98/rib	28	0.96	0.75	5.5	1.5	12	0.37	0.1	1.3	1.7	4.1	14.62	13.08
11 Wheat/rib+	33	0.16	0.23	5.8	2.0	7.5	0.38	0.02	1.1	2.0	0.42	20.36	17.81
12 DW95	16	0.16	0.14	6.0	1.3	25	0.40	0.01	1.3	1.7	6.0	2.74	2.63
14 DW97	14	0.42	0.91	7.6	3.4	23	1.11	0.04	2.2	4.7	4.2	3.13	2.72

Table 4.2.4. Elemental ash composition of eleven Danish straws (wt.% dry). The index, γ_K, is calculated as $\gamma_K=2(Si/28.09)/((K/39.10)-(Cl/35.45)-(P/30.97))$ and the index, $\gamma_{K,Na}$, is calculated as $\gamma_{K,Na}=2(Si/28.09)/((K/39.10)+(Na/22.99)-(Cl/35.45)-(P/30.97))$.

#	Straw	Ash d.b. (wt.%)	ReaTech γ_K	ReaTech $\gamma_{K,Na}$	ET $t_{b,850}$ (min)	ET $t_{b,800}$ (min)	VTT SAI_{750} 750°C	ET SAI_T 800°C	ET SAI_T 850°C	VTT SAI_T 850°C
1	**Wheat**	5.4	5.31	5.03	11	22	**(u)	*(*)	***	**(u)
2	**Wheat**	5.4	3.06	2.92	5	11	**	**	***	***
3	**Wheat**	5.3	2.63	2.53	7	12	**(*)	**	***	***
4	**Wheat**	3.5	1.07	1.04	4	7	*	*	**	*
5	**Barley (W)**	5.7	2.92	2.43	8	13	**(*)	**	***	***
6	**Grass**	5.2	2.65	2.59	9	16	**(u)	**	***	***
7	**Barley (S)**	5.5	4.76	3.53	10	22	**(u)	*(*)	***	***
8	**Barley98(S)**	n.d.	nd.	nd.	20	53	**nd.**	**0**	*	**nd.**
9	**Wheat/rib-**	15.5	14.62	13.08	18	40	**nd.**	**(0)**	**	*(*)
11	**Wheat/rib+**	8.0	20.36	17.81	31	70	**nd.**	**0**	**(0)**	**(0)**

Table 4.2.5. Theoretical agglomeration and sintering index, γ_K and $\gamma_{K,Na}$, Conversion times $t_{b,T}$ measured in the ET-macro TGA and the experimental sintering and agglomeration index, SAI_T, measured in the VTT-thermobalance. In case unburned carbon was present after the experiment the symbol: (u) is used.

For wheat#2 additionally SAI_{700}=0 (or 0.5*) was obtained from evaluating ash produced in the macro TGA, see Table 5.4.1(File 473).

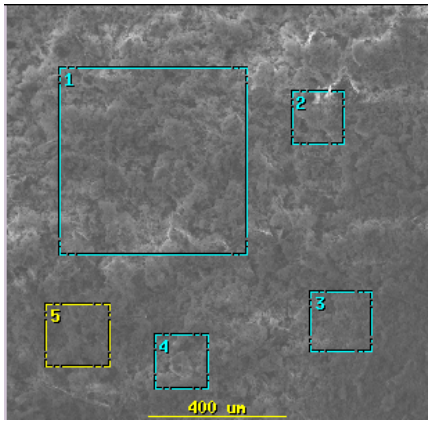

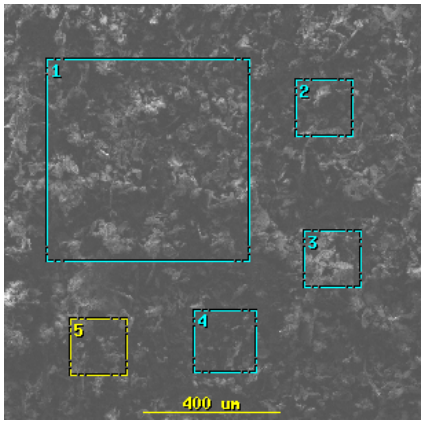

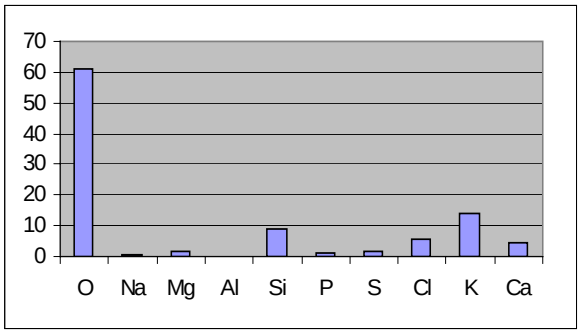

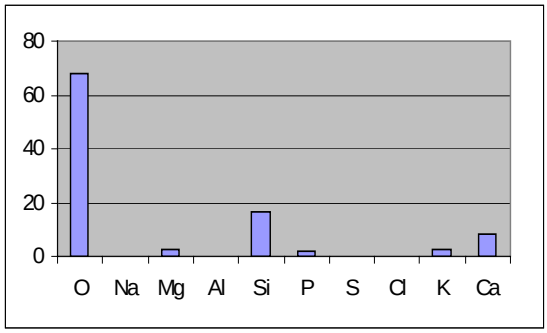

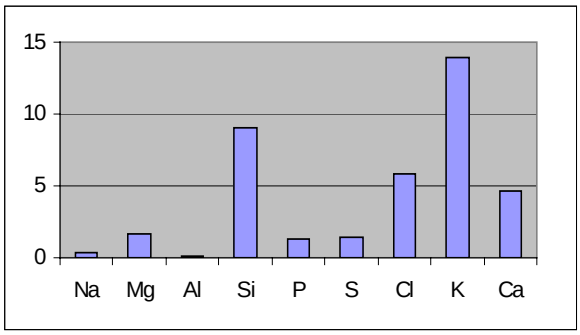

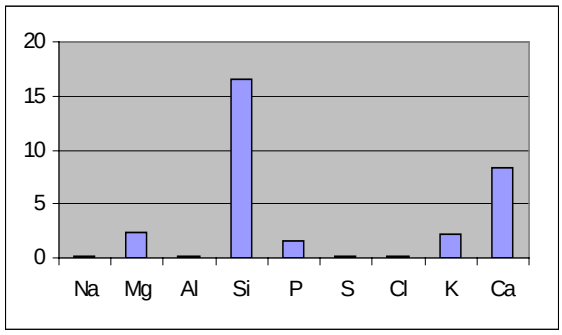

	O	Na	Mg	Al	Si	P	S	Cl	K	Ca	Ti	Cr	Mn	Fe	Ni	Cu	Zn
Sa	61.062	0.361	1.651	0.173	9.010	1.285	1.404	5.851	13.968	4.694	0.047	0.065	0.067	0.096	0.074	0.130	0.062
*		0.93	4.24	0.44	23.14	3.30	3.60	15.03	35.87	12.06	0.12	0.17	0.17	0.25	0.19	0.33	0.16
σ_{sa}	3.9	27.7	7.3	34.7	11.2	7.0	17.1	20.3	9.9	8.9	40.4	9.2	23.9	46.9	27.0	46.2	90.3
Saw	67.815	0.135	2.319	0.112	16.49	1.613	0.182	0.091	2.268	8.378	0.040	0.034	0.068	0.14	0.102	0.116	0.097
*		0.42	7.21	0.35	51.23	5.01	0.57	0.28	7.05	26.03	0.12	0.11	0.21	0.43	0.32	0.36	0.30
σ_{saw}	0.5	27.4	11.3	28.6	2.0	7.3	29.7	53.8	3.0	6.0	75.0	58.8	14.7	64.3	29.4	25.9	20.6

Figure 4.2.1 SEM figures [upper figures] and elemental composition [mol%] made using EDX of straw ash (Wheat#2), "SA" (left) produced at 500°C. Right the composition of the same ash "SAw", but washed three times in 50°C destilled water. Lower figures and: Elemental composition is oxygen free and normalised. The values are shown in the table as percent. Standard deviations, σ_{SA} and σ_{Saw} are given as %-of value.*

5. Results and Discussion

5.1 Testing different straws using thermal balance and macro-TGA

First different straws have been tested in order to see which fuel characteristics caused agglomeration and sintering and high and effected char reactivity. For the samples the char reactivity and SAI was determined and γ_K were estimated from the elemental analysis and the values were evaluated, compared and discussed.

The straws listed in Table 4.2.5 were gasified in the VTT-thermobalance at 750°C and 850°C. The reactivity profiles monitored are shown in Figure 5.1.1 to Figure 5.1.9, where also the SAI is shown for each of the samples. In Table 5.4.1, the time of conversion $t_{b,T}$(min) measured in the macro-TGA is shown together with the SAI and the γ_K and $\gamma_{K,Na}$ index.

The char sample with the significantly highest reactivity is wheat#4. Wheat#9 and wheat#11 have the significantly lowest reactivity, while the reactivity of the rest of the samples is very similar to each other. In the macro-TGA the reactivity of the straw samples were measured at 800°C and 850°C. Here the mass weighed reactivity (Henriksen 1996), $\underline{R_m}$ was calculated in the conversion range $0.2< X< 0.8$. After the straw was gasified the ash from the samples was visually evaluated in a microscope and the sintering and agglomeration index, SAI, was determined. $\underline{R_m}$ and SAI for the chars are shown in Table 4.2.5. It is first observed that SAI_T obtained at T = 850°C in the ET-macro-TGA and in the VTT-thermobalance are well correlated. Also the macro-TGA data obtained at 800°C are well correlated with the thermobalance data obtained at 750°C. For wheat#2, however a difference exist between the results at 750°C, see Table 4.2.5 and Table 5.4.1 File 473 with respect to the SAI indices. This indicates that the agglomeration tendency is very sensitive to small temperature and gasification condition variations. For the straw samples no. 1, 2, 3, 5, 6 and 7 we found that SAI_{850} = 3*. For these samples we have $2.63 \leq \gamma_K \leq 5.31$. These values are close to the SiO_2/K_2O ratio obtained for the problematic slag-phase obtained using the FACT programme at relevant temperature, see section 3.4. This is also the case for the wheat, DW95, where γ= 2.74. For wheat#4 in spite of a very high elemental potassium content a relatively low SAI value is observed, i.e. SAI_{850}=1*-2*, see Table 4.2.5. Wheat#4 is characterised by γ_K = 1.07. Such a SiO_2 to K_2O ratio likely produces relative high amounts of K_2O*SiO_2. K_2O*SiO_2 has a

melting point at 976°C. Also K_2CO_3 seems to be an important product. The ash samples from the Wheat#4 experiments contained relative large amounts of hydrated K_2CO_3 while no hydrated K_2CO_3 was observed in the wheat#2 ash (Jimmy Bak 1999).

Also with γ_K = 1.07 the potassium content is high, and relatively high K_2O(g), KO(g) and KOH(g) partial pressures may exist as is indicated in section 3.10. Therefore the concentration of potassium catalyst at the carbon surface and thus the reactivity is expected to be high as observed. For wheat#9(rib-) and wheat#11(rib+), i.e. the rainy season rib-harvested samples, γ_K = 14.62 and γ_K = 20.36 respectively. These very high values of γ_K obviously lead to lower agglomerating tendency (SAI_{850}=2* and 0.5* respectively) and a low reactivity. Low SAI_{850} and reactivity is also obtained for Barley98 (no elemental analysis was made). From the results shown in Table 4.2.5 we suggest that for γ_K<2 and for γ_K>20 the agglomeration tendency is low at 850°C.

For low γ_K, i.e. γ_K < 2, the reactivity is high since the catalyst is available for the carbon surface. For high γ_K the reactivity is low since the catalyst is bound to other inorganic species and the temperature must be significantly raised i.e. more than 100°C in order to get a high degree of conversion! Hereby other relevant melting temperatures are reached. For 2.5 < γ_K < 5.5 significant agglomeration is expected, but no simple correlation exist between γ_K and agglomeration and the reactivity (time of conversion). The true SiO_2/K_2O ratio in the melt depends on the precise elemental composition of the ash compounds, where e.g. also the reactive calcium content is important.

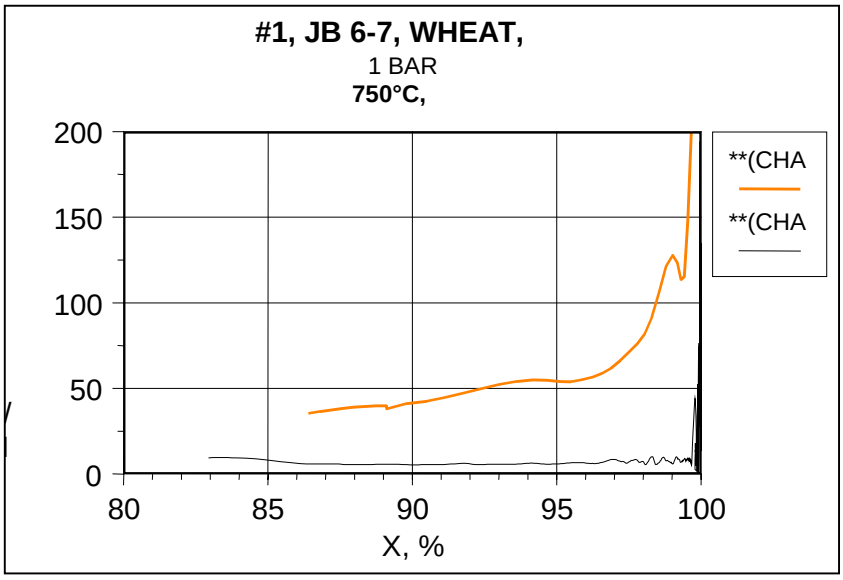

Figure 5.1.1. Reactivity measured at 750°C and 850°C for wheat#1.

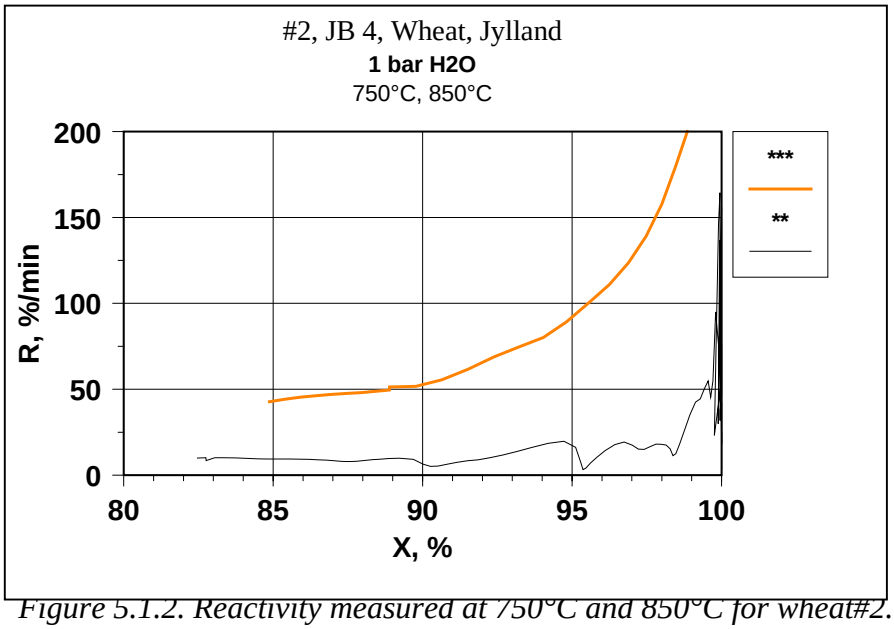

Figure 5.1.2. Reactivity measured at 750°C and 850°C for wheat#2.

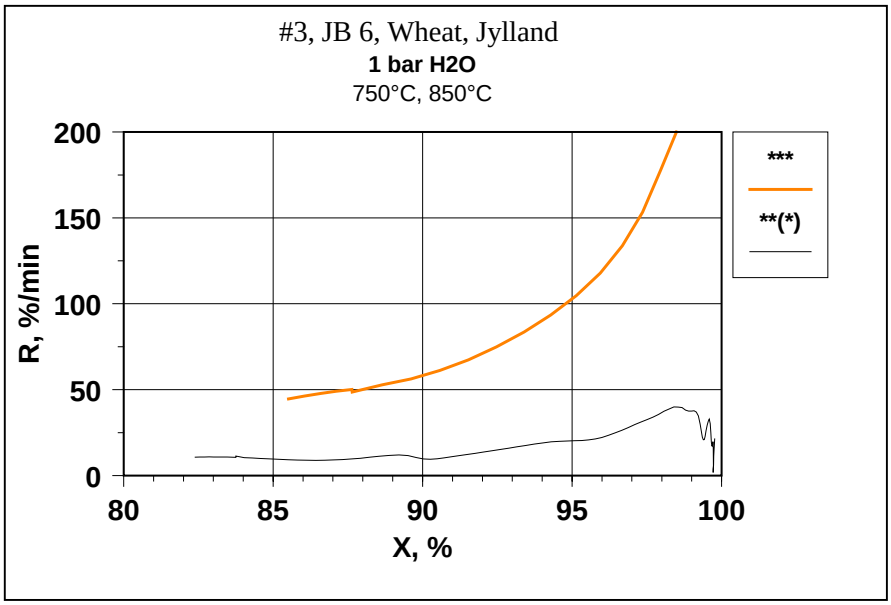

Figure 5.1.3. Reactivity measured at 750°C and 850°C for wheat#3.

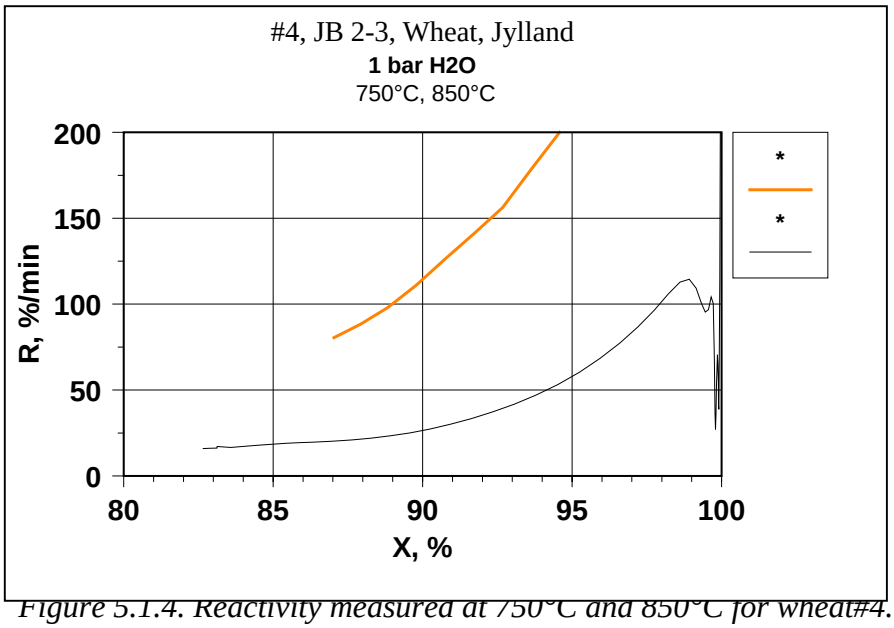

Figure 5.1.4. Reactivity measured at 750°C and 850°C for wheat#4.

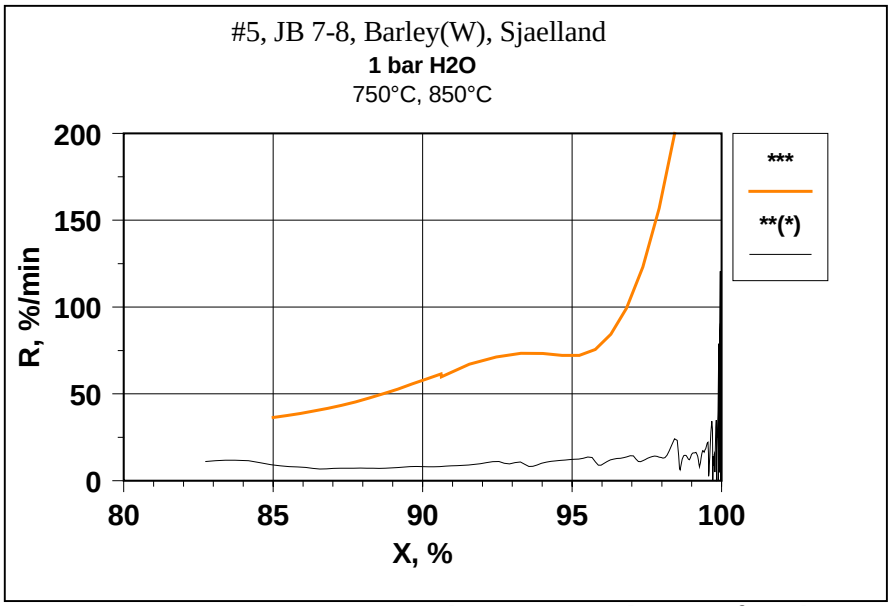

Figure 5.1.5. Reactivity measured at 750°C and 850°C for wheat#5

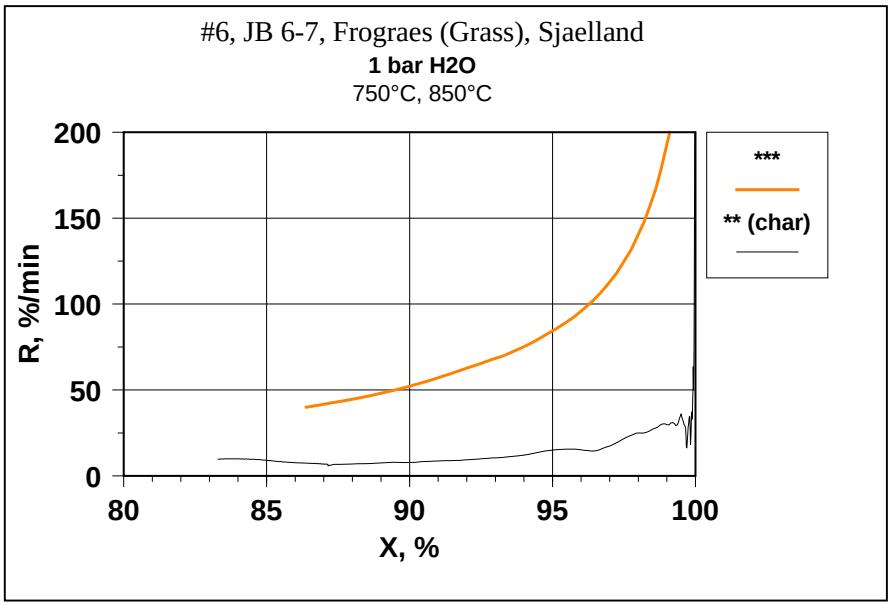

Figure 5.1.6. Reactivity measured at 750°C and 850°C for wheat#6

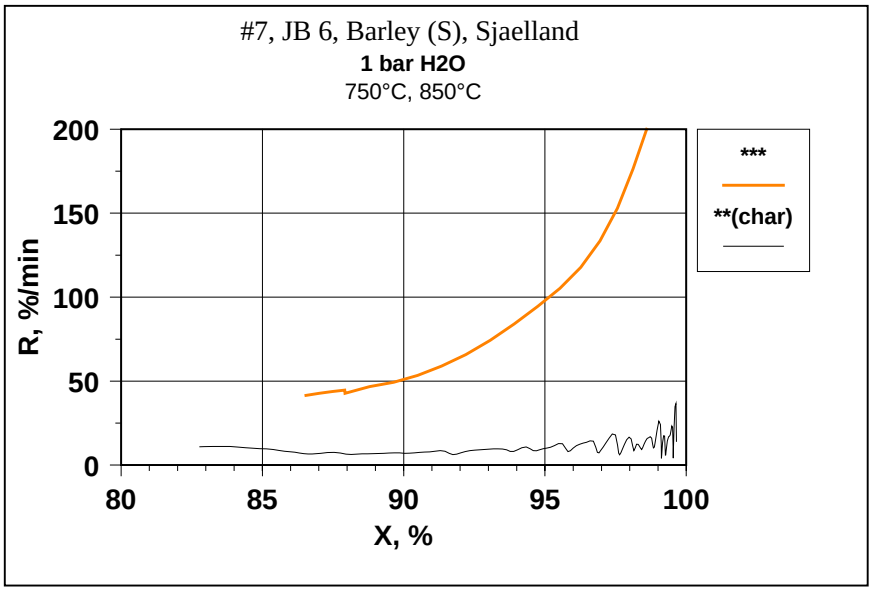

Figure 5.1.7. Reactivity measured at 750°C and 850°C for wheat#7

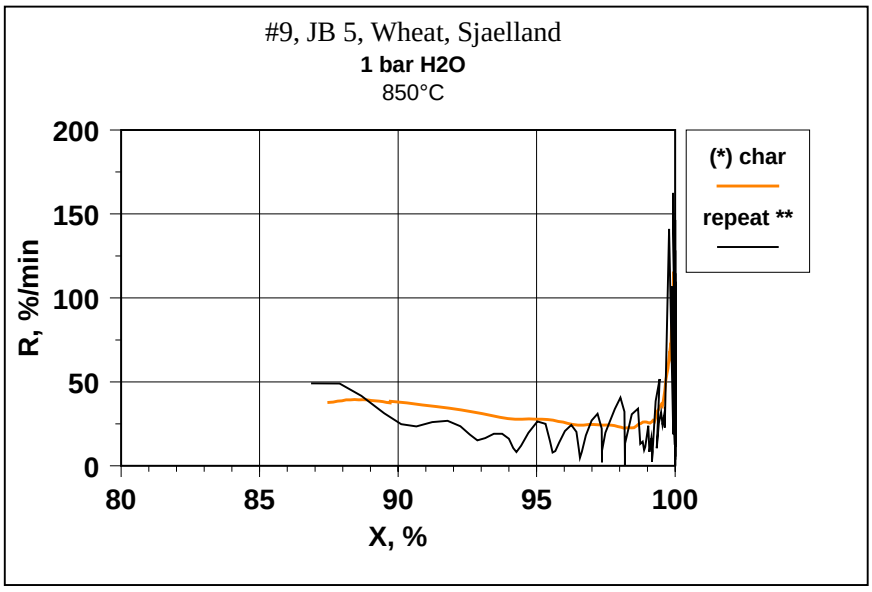

Figure 5.1.8. Reactivity measured 850°C for wheat#9

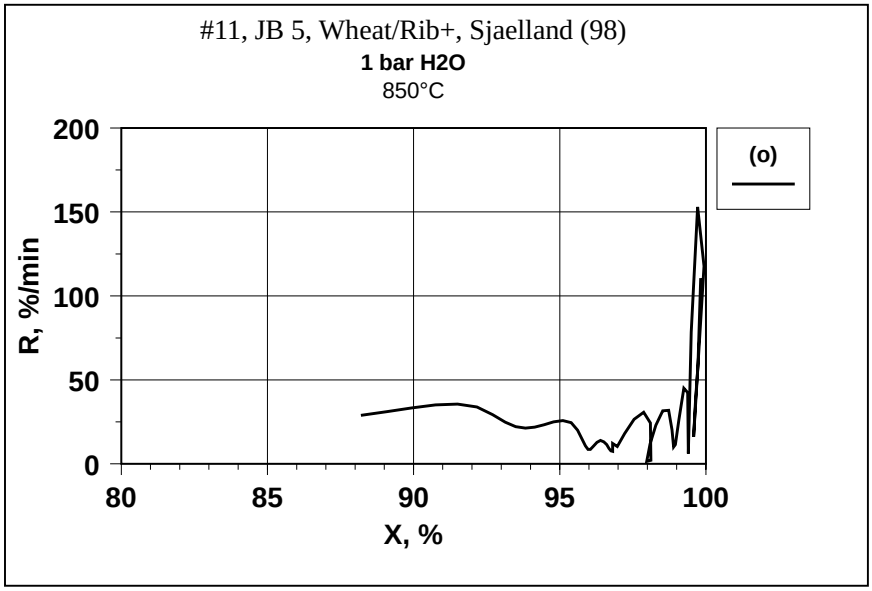

Figure 5.1.9. Reactivity measured at 850°C for wheat#11

5.2 Experiments and results from the bench-scale fluidised gasification rig

Gasification tests were carried out with the bench-scale fluidised-bed gasification test rig at VTT in a co-operation with senior scientists Esa Kurkela and Jaana Laatikainen-Luntama who were responsible for the operation of the gasifier and Antero Moilanen, who was responsible for the ash agglomeration and deposit analyses (Moilanen 1999). The wheat#4 and the barley#7 straws were crushed to below 2 mm particle size and pelletised into small pellets in order to increase the bulk density and to remove long fibres and thus facilitate feeding the sample to the test facility using a screw feeder. The pellets were crushed to below 1mm sieve size and used in the bench-scale tests. Also a Danish wheat straw (DS-97) was tested. The chemical composition of the used feedstock fraction (0.55-0.92 mm) is shown in Table 5.2.1. With respect to the inorganic elemental composition DS-97 is close to DS-95 with respect to the content of silicium and potassium and thus the value of γ_K. From this point of view DS-95 and DS-97 may be expected to behave alike during gasification.

	Wheat #4	Barley #7	DS-97 (W#1)
Moisture, wt.%	7.5	9.1	7.0
Proximate analyses, wt.% (dry basis)			
Volatile matter	75.9	76.4	75.8
Fixed Carbon	19.8	18.9	18.1
Ash	4.3	4.7	6.1
Ultimate analyses, wt.% (d.b.)			
C	47.9	47.0	46.5
H	5.7	5.7	5.7
N	0.5	0.4	1.4
O (as difference)	41.5	42.1	40.1
S	0.13	0.12	0.12
Ash	4.3	4.7	6.1

Table 5.2.1. Fuel analysis for the straw samples tested at the VTT-AFB.

The reactor is operated at atmospheric pressure and electrical heating elements were used to compensate heat losses. The feedstock was fed from a live-bottom hopper into the fluidised-bed by screw feeders. The fuel feeding point was located close to the air distributor. A mixture of air and steam was used as the fluidising gas, which was fed into the reactor through a multiorifice plate distributor. In addition, small amounts of purging nitrogen were introduced to the feeding screw and through the bed material remove pipe located in the centre of the air distributor. Myanit dolomite was used as the bed material in all experiments. Particle size of the bed material was 0.71-1.00 mm, and the superficial velocity was selected so that good fluidisation was maintained.

tained.

The test procedure is briefly described in the following. Before the test run the facility was cleaned from earlier deposits and preheated in a nitrogen atmosphere to the target operation temperature. Then, the flow rates of fluidisation gases and purging nitrogen were set to the calculated target values and the fuel feed was started. Measurements were started about an hour after the start-up when the operation conditions had become stable. At all steady-state operation periods the necessary measurements for material balances were done (analysis of gas, tar and cyclone dust sample).

After about 4 hours operation the test run was finished by stopping the fuel feed and by switching the gasification agent to nitrogen. The electric heating elements were put off and the facility was slowly cooled down to the room temperature. In the following day, the reactor was opened, the bed material was removed and the reactor was inspected for the ash deposits. After the inspection, the deposits were photographed, removed, weighed and studied further microscopically. Based on the results from the fuel, cyclone and filter dust, gas and tar analyses, the material balances were calculated.

The first **experiment 98/1** was carried out with straws from **wheat#4** at about 800°C. The test run was successful and no signs of ash-related problems were met during the operation; the bed temperature was constant and no signs of pressure drop fluctuations were seen. The bed material after the test contained only small agglomerates and the freeboard and the gas outlet pipe was clean. The second **experiment 98/2** was carried out with wheat#4 at 830°C. The results were similar to the results for experiment 98/1, i.e. the bed material after the test contained only small agglomerates and the freeboard and the gas outlet pipe was clean.

Experiment 98/3 was carried out with **Barley#7** at 800°C. After one hour the pressure started to raise and for that reason the experiment was finished already after 93 minutes. The removed bed-material was quite clean, as was the freeboard and gas outlet pipe. The blockage that caused the increasing reactor pressure was found in the gas line after the cyclone. This straw could not be tested at another temperature any more because barley#7 could not be easily pelletised and thus not enough samples were available for more experiments.

Experiment 98/4 was carried out with wheat–97 **(DS-97)** at 800°C. No signs of ash-related problems were met during the operation. However, after the test there were large agglomerates in the bed, but the freeboard and gas outlet pipe were clean. Because the temperature of 800°C caused large agglomerates, **experiment 98/5** was carried out at 770°C. This time no agglomerates were observed in the bedmaterial and the freeboard and gas outlet pipe were clean.

The conclusion from the experiments is that wheat#4, when using a dolomite-bed, gave no serious agglomeration problems up to 830°C in accordance with the thermobalance and macro-TGA results. This is also expected from the γ_K-value, since γ_K=1.07

As expected from the knowledge of the γ_K-value, DS-97 caused some problems at 800°C. At 770°C DS-97 caused only a few agglomerates but at this temperature the char conversion will be slower. Barley#7 only showed a few agglomerates in the bed, but a relatively high amount of deposits were sampled after only 93 minutes experiment, see Table 5.2.2. The γ_K value is γ_K=4.76 and $\gamma_{K,Na}$=3.53 and thus a high agglomeration or deposition tendency is expected. The high deposit formation to bed agglomerate formation ratio of the agglomerates indicates that the barley#7 melt-ash fraction has a lower viscosity than the DS-97 wheat ash and we therefore suggest that this straw present a large potential risk for deposit formation, while DW97 rather causes bed agglomeration. These conclusions are made from a very few results and should therefore be tested further.

Experiment	**98/1**		**98/2**		**98/3**	
Feedstock	Wh#4, JB 2-3		Wh#4 JB 2-3		B#7 JB6	
Particle size, mm	0.55-0.92		0.55-0.92		0.55-0.92	
Bed material	Dolomite		Dolomite		Dolomite	
Particle size, mm	0.71-1.00		0.71-1.00		0.71-1.00	
T(bed, average), °C	800		830		800	
T(freeboard, average), °C	805		830		805	
U(bed), m/s	0.80		0.80		0.80	
U(freeboard), m/s	0.30		0.30		0.30	
Air ratio[1)]	≈ 0.30		≈ 0.30		≈ 0.30	
Tars, g/m^3 n	5.5		5.7		4.6	
Gas analysis, vol.%	Dry	Wet	Dry	Wet	Dry	Wet
CO	8.78	6.18	7.69	5.37	4.48	2.89
CO_2	19.3	13.6	19.2	13.4	20.4	13.2
H_2	19.4	13.7	18.6	13.0	15.2	9.83
CH_4	2.68	1.89	2.81	1.96	1.99	1.29
C_2H_y	1.00	0.76	0.94	0.66	0.73	0.47
C_3-C_5H_y	<0.10	<0.10	<0.10	<0.10	<0.10	<0.10
Gasification agents, mg/s						
primary air	352		335		352	
purge N_2	42		42		42	
steam	150		150		150	
Steam in fluidising gas, vol.%	41		42		41	
mg freeboard deposits/ g fed feedstock	0.7		1.0		5.8	
Total amount of						
fed feedstock, g	3655		3155		1200	
used bed material, g	420		420		420	
Total test time, min	240		240		93[2)]	
Initiation sign of bed sintering, min	-		-		-	
Bed sinters after the test:	Only small agglomerates with the same size as bed particles		Only small agglomerates with the same size as bed particles		Only small agglomerates with the same size as bed particles	
SAI	*		*		*	

Table 5.2.2. Results from AFB test runs of Danish straws.

1) Target air ratio was 0.30
2) Test run was finished because the pressure of the reactor was increasing. There was obviously forming a blockage after the cyclone.

Experiment	**98/4**		**98/5**	
Feedstock	DS-97		DS-97	
Particle size, mm	0.55-0.92		0.55-0.92	
Bed material	Dolomite		Dolomite	
Particle size, mm	0.71-1.00		0.71-1.00	
T(bed, average), °C	800		770	
T(freeboard, average), °C	805		770	
U(bed), m/s	0.80		0.80	
U(freeboard), m/s	0.30		0.30	
Air ratio[1)]	≈ 0.30		≈ 0.30	
Tars, g/m^3 n	7.5		9.4	
Gas analysis, vol%	Dry	Wet	Dry	Wet
CO	6.86	4.83	5.16	3.41
CO_2	20.20	14.20	20.4	13.5
H_2	18.60	13.10	14.5	9.61
CH_4	2.52	1.77	2.38	1.57
C_2H_y	1.10	0.77	1.09	0.72
C_3-C_5H_y	<0.10	<0.10	0.13	<0.10
Gasification agents, mg/s				
primary air	352		369	
purge N_2	42		42	
steam	150		150	
Steam in fluidising gas, vol%	41		40	
mg freeboard deposits/ g fed feedstock	1.3		<0.5	
Total amount of				
fed feedstock, g	3565		3380	
used bed material, g	420		420	
Total test time, min	252		240	
Initiation sign of bed sintering, min	252		-	
Bed sinters after test	Very large Agglomerates		Larger char agglomerates and small molten ash particles (only few small agglomerates)	
SAI	***		(*)	

Table 5.2.3. Results from AFB test runs of Danish straws.
Target air ratio was 0.30.

5.3 Reactivity and sintering measurements

Testing synthetic samples

The trends observed for the reactivity and agglomeration tendency seems to be fairly general for the natural straws tested and a function of the inorganic composition of the straw. The are only few major inorganic elements in the straw and Henriksen (1996) established credibility that the catalytic properties as well as the sintering tendency of the inorganic components in the straw are roughly invariant to washing the sample and re-mixing. Therefore synthetic artificial samples was used for the following test. Carbon and synthetic ash produced as described in Chapter 4.2 were mixed with selected additives and catalysts in order to test and control the char reactivity as well as the agglomeration tendency of the inorganic mixtures. The purpose is to quantitatively optimise the type and amount of additives that should be added during straw gasification.

ReaTech in a co-operation with (Maria Barrio 1999a), NTNU, have tested the effect of two potassium salts, K_2CO_3 and K_3PO_4. The purpose of the experiments was to test how the addition of these salts affected the reactivity at 750°C (catalysis effect) in CO_2. The reactivity measurements in a 100 % CO_2 atmosphere, were first made using samples prepared by varying the K/C ratio in a sample composed of HF washed carbon and K_2CO_3 (dry mixed) see Figure 5.3.1. On a weight basis the K_2CO_3/washed ash ratio is 0, 0.2 and 0.3. This gives on a molar basis: K/C = 0, 0.035 and 0.052 respectively. The reactivity, $R_{½}$, measured at 50 % char conversion, increases significantly as a function of the K_2CO_3/Char ratio: $R_{½}(K/C=0)=0.003$, $R_{½}(K/C=0.035)=0.058$ and $R_{½}(K/C=0.052)=0.106$. The reactivity increases at least up to a K_2CO_3 loading of 30 wt.%. Such high values are also reported by (Mimst and Pabst 1987), where saturation was obtained for a Pittsburgh#8 coal for a mole ratio K/C of around 0.1. Next it was tested which effect an added amount of washed ash, see Figure 5.3.2, had on the reactivity. The samples with K_2CO_3/Char mass ratio of 0.2 were chosen, and washed ash was added with Ash/K_2CO_3 weight ratios of 0, 1.57 and 3.16 resulting in $R_{½}$= 0.058, 0.023 and 0.012 respectively, see figure 5.3.2. Thus the reactivity significantly decrease as the washed-ash fraction increases.

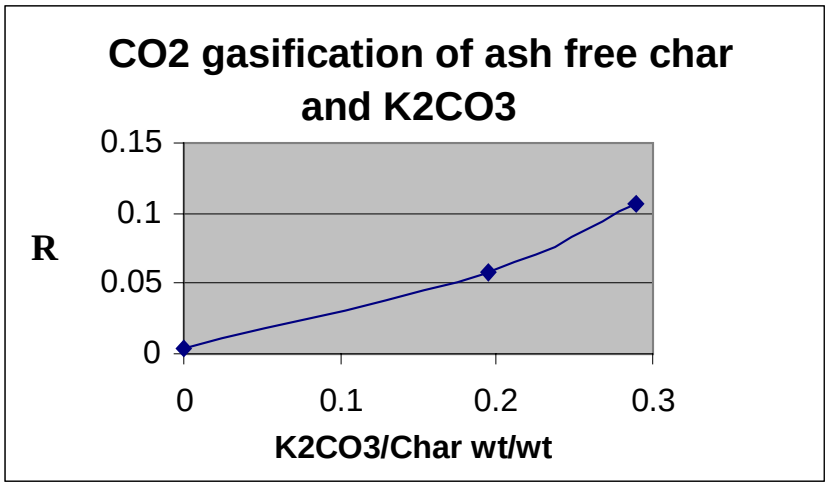

Figure 5.3.1. Straw char reactivity $R_{½}$[g/g min^{-1}], measured at X=0.5 for some K_2CO_3/Char weight ratios in 100% CO_2 atmosphere at 750°C.

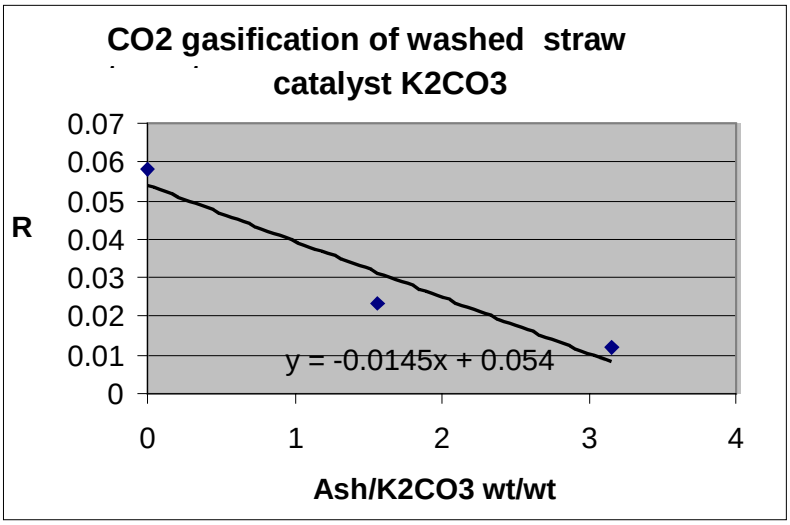

Figure 5.3.2. Straw char reactivity $R_{½}$[g/g min^{-1}], measured at X = 0.5 for some Ash/K_2CO_3 weight ratios in 100 % CO_2 atmosphere and 750°C.

The conclusion from the carbon-K_2CO_3-washed ash experiments is that K_2CO_3 is a good gasification catalyst, but that the catalytic effect of K_2CO_3 decreases when it is combined with inherent straw ash already at 750°C. The quenching effect on reactivity of inherent elemental Si and Ca on the reactivity are also supported by the measurements at VTT where SAI_{750}=2*-2.5* for all tested samples with $4.76>\gamma_K>2.63$.

The reactivity measurements were next made using samples prepared by varying the potassium: carbon ratio in a sample composed of HF washed carbon and K_3PO_4. In Figure 5.3.3, $R_{½}$ is shown

for the weight ratio: K_3PO_4/char = 0.26-0.3. No significant change in reactivity is detected when adding washed ash up to an ash/K_3PO_4 ratio of 1.5, this indicate that K_3PO_4 is relatively stable. The reactivity in figure 5.3.3 is 0.029 compared to 0.003 for the HF washed carbon and thus K_3PO_4 has a catalytic effect.

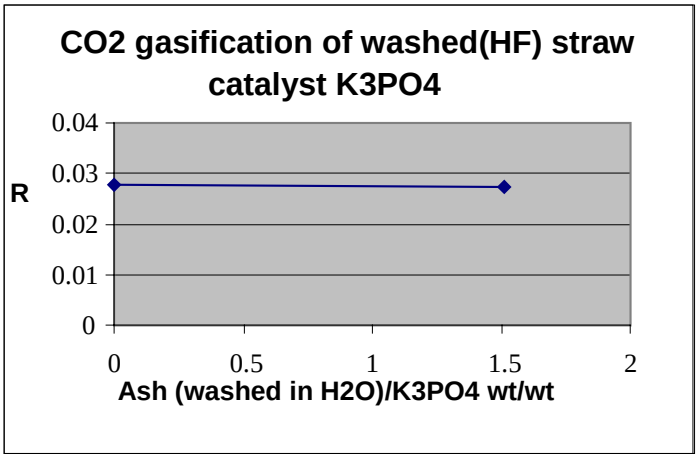

Figure 5.3.3. Straw char reactivity $R_{½}$[g/g min^{-1}], measured at X=0.5 for two ash:K_3PO_4 ratios. The temperature is 750°C and the atmosphere is 100% CO_2.

From these experiments it is indicated that K_3PO_4 may be preferred to K_2CO_3 as a catalyst during gasification of straw, since K_2CO_3 is very reactive to straw ash already at 750°C. It is however of interest to see, what happens when the temperature is increased to 900-1000°C.

ReaTech has tested a variation of samples, composed of various amounts of catalyst, washed ash (see Figure 4.2.1), HF-washed carbon and additive. The samples were ramped in the SDT equipment by 10°C/min to 900°C in nitrogen. Representative DTA curves for the various samples are shown in Figure 5.3.4. ΔT representing the difference between the ramped sample temperature and the ramped reference temperature is shown versus temperature. The amount of ash used was approximately 5 mg and the amount of additive was in the range of 1-5 mg or in the range of µl, when liquid additives were used. Without the addition of additives, the gasified raw-ash + carbon sample sintered into a melt.

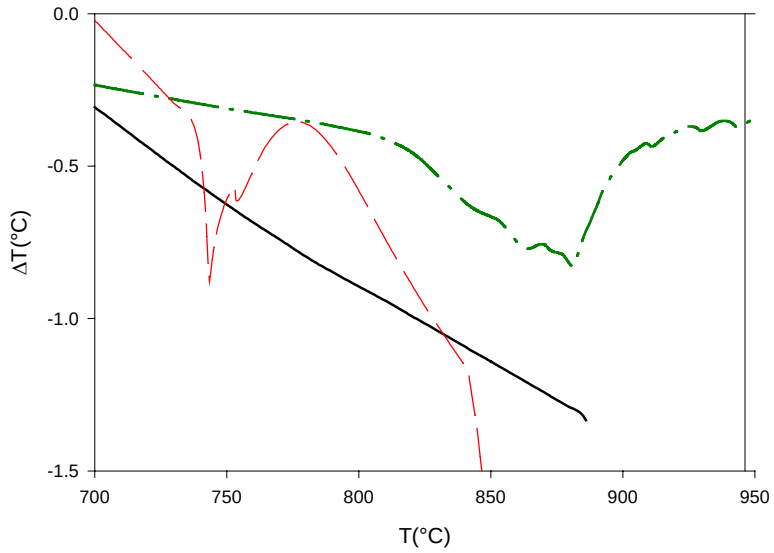

Figure 5.3.4. DTA curves for various samples. ΔT is shown versus temperature. The individual lines are representative for the following input samples: (1) Solid line (no melt formation): raw ash+antiagglomeration additive or washed ash and washed ash + K_3PO_4. (2) Slash (melt formation): K_2CO_3 + washed ash. (3) Slash dot (melt formation): K_2CO_3+SiO_2 (quartz).

The endothermic temperature peaks, line (2) and (3) in Figure 5.3.4, shows that washed ash and quartz significantly reacts with K_2CO_3 above 810-815°C (K_2CO_3 melting temp. 901°C). The quartz–K_2CO_3 reaction is not significant until above 800°C. Since eutectic melts are expected already from 750°C this suggests that the shown quartz – K_2CO_3 reaction is slow below 800°C. For the sample (2) including washed ash and K_2CO_3, a significant endothermic peak is already observed in the range 740-770°C. This suggests that some melting already can take place at these low temperatures. This is in accordance with expectations since eutectica exist in this temperature range in the $K_2O*4SiO_2$ – $CaO*SiO_2$ system, see Figure 391 and 395 in phase diagrams for ceramist (Levin et. al. 1964).

No detectable endothermic peaks (1) were observed when K_3PO_4 where heated together with washed ash to 900°C. This was also the case when some specific additives, were used in combination with raw ash. One of the specific additives is the well-known kaolinite in the form of "pibeler". With the use of sufficient amounts of additives no detectable agglomeration, sintering or melting took place, and the residual ash was soft and dry. A number of other additives were also tested. These additives should according to results obtained from equilibrium calculations

(HSC) prevent agglomeration effectively. This was, however, not the case in the SDT experiments made at ReaTech. These additives and the raw ash were after being heated to 900°C located as two separated phases and the ash phase was melted into one or more sintered or liquid drops. From these results it was concluded that under the tested conditions in order to be an effective anti-agglomerating agent, the additive had to be very reactive. The other additives tested may however be effective as bed materials.

ReaTech and ET following tested the most effective additives in the macro TGA. Straw char was here mixed with the additives, e.g. kaolinite, in various ways (dry or by impregnation) and the sample was gasified at temperatures up to 1000°C, see Chapter 5.4. The purpose was to provide rules for the optimum quantitative addition of controlled amounts of additive to char and raw straw samples.

5.4 Macro-TGA Measurements

At the Department of Energy Engineering, DTU, the mass weighed reactivity, $R_{0.25<X<0.75}$, and the time of conversion, the sintering tendency index (SAI) and the corrosion tendency index (CI) were determined for Wheat#2. This was done for a number of conditions. The straw samples were initially pyrolysed at 600°C and the produced chars were mixed with different additives or washed. Following the samples were gasified in a 100% preheated steam (Henriksen 1996), see Table 5.4.1. For selected samples important products was identified by X-ray diffraction.

File	T (°C)	R [min^{-1}]	Addition	Time [min]	SAI	CI
456	850	45	-	8	3	1
457	850	14	1X A^i	25	1-2	3
461	850	5.7	2X A^i	76	0	3
462	850	13	1.2 g powder	46	0	
469	800	26	-	8-12	2	
470	850	61	-	4-8	3	
471	900	92	-	4	3	
472	900	30	1 g powder	9-17	3	
473	750	9.4	-	25-33	1	
474	850	32	1 g pibeler	11-20	0	
475	900	18	1.5 A^i	15-20	0	3
476	700	3.6	-	82	0	
477	850	7.4	1.5 A^i	43	0	3
478	850	16	- & washed	18-36	1	
479	950	37	1.5 A^i	7	0	3
480	900	40	1 g pibeler	8	0	
481	950	68.4	1 g pibeler	5	2	
482	950	48	2 g pibeler	5-8	0	
483	950	52.2	1 g $pibeler^i$	7	0	
484	850	16.1	1 g $pibeler^i$	30	0	
485	900	21.4	1 g $powder^i$	15	0	
486	950	47	1 g $powder^i$	7	0	0
487	1000		1.5 A^i		0	3

*Table 5.4.1. The reactivity $R_{0.25<X<0.75}$, the burnout time, for Wheat#2, the sintering tendency (SAI) and the corrosion tendency (CI) for the ashes measured for a 5 gram wheat#2 char and with various amounts of additive. The char contains about 1 g of ash. For a few samples major components measured using X-ray diffraction are shown. Corrosion is evaluated visually for the sample holders made by the steel type : 253 MA and Wst 14841. *Fe_3O_4, i.e. $Fe(II)Fe(III)_2O_4$, magnetite was found using X-ray diffraction when CI>0. i: impregnated.*

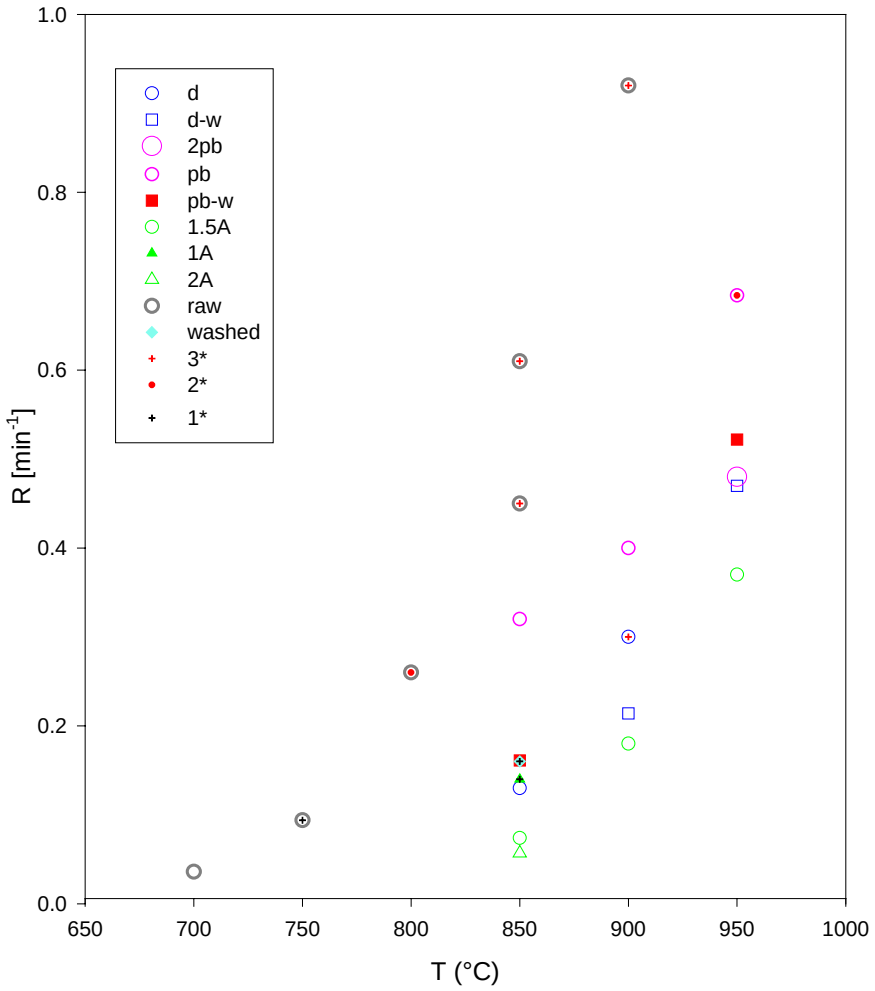

Figure 5.4.1. Reactivity and sintering index for Wheat#2 measured as a function of temperature and additive addition. Symbols: d: dry powder, d-w: impregnated powder, pb: pibeler(kaolin), pb-w: impregnated pibeler, A: Additive, raw: raw straw ash, washed: washed straw. 1, 2*, 3*: sintering tendency in terms of one, two or three 'stars'. nA: amount of additive is 0.2nm$_{ash}$, where m$_{ash}$ is the mass of the ash in the sample.*

For the raw straw the char reactivity and the value of SAI increases with temperature as expected. Introducing kaolinite (pb) clearly decreases reactivity but also the SAI value. This is also the case with the other additives ('A' and powder). However with the additives used the reactivity for low SAI values can be increased beyond the reactivity of raw or washed straw (observe that SAI$_{850}$=1* for washed straw). Also observe that impregnation of additive is the most effective preparation technique for prevention of agglomeration. The results in Figure 5.4.1, are also presented in Figure 5.4.2-5.4.4.

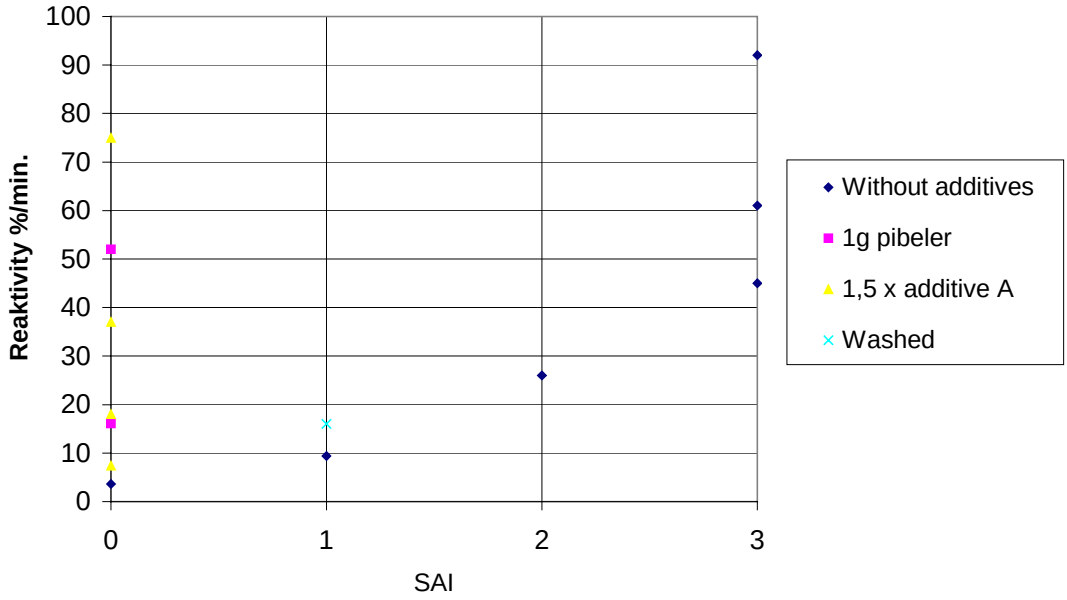

Figure 5.4.2. The reactivity versus the sintering index value, SAI, for raw samples (without additives), washed samples or additive-impregnated samples.

In Figure 5.4.2 the reactivity is shown as a function of the SAI value. It is illustrated seen that for the char from the raw straw, the SAI is increasing as a function of the reactivity, thus if SAI<1* is required for the gasification condition to be optimal, a relatively low maximum reactivity is obtainable. Also observe that SAI=1 for the washed straw sample. For all additive-impregnated samples tested SAI=0 (yellow and red dots), thus the utilisation of additives provides the possibility of obtaining a higher fuel reactivity. The higher reactivity is obtained by increasing the temperature.

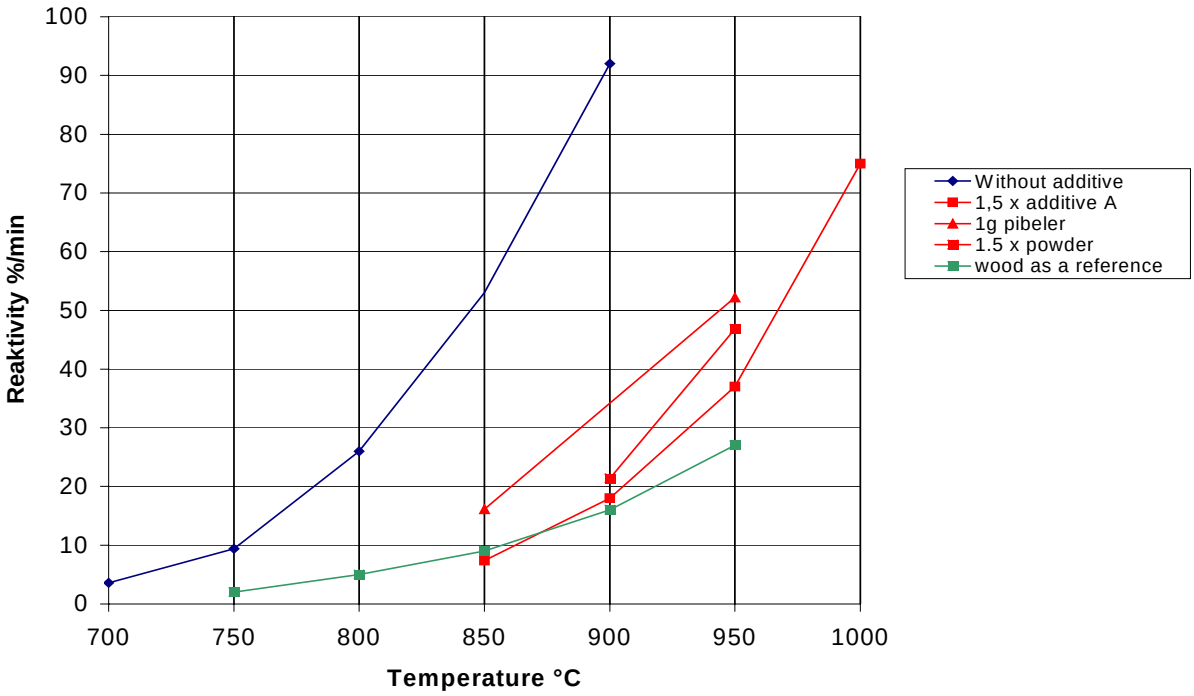

Figure 5.4.3. Mass-weighted reactivity as a function of the reactor temperature is shown for different samples. The red points indicate that the sample have a sintering index SAI which is 0.

In Figure 5.4.3 the reactivity is shown as a function of temperature. The used additives reduce the reactivity at a specific temperature. It is also shown, recalling that SAI=0 for the additive-impregnated samples, that for a specific additive a high reactivity can be obtained by increasing the temperature. Furthermore the reactivity of the additive-impregnated samples here tested only differs slightly from each other's and their reactivity is higher than those measured for a reference wood char.

Figure 5.4.4. The sintering index, SAI_{850}, is plotted versus the amount of added 'A'.

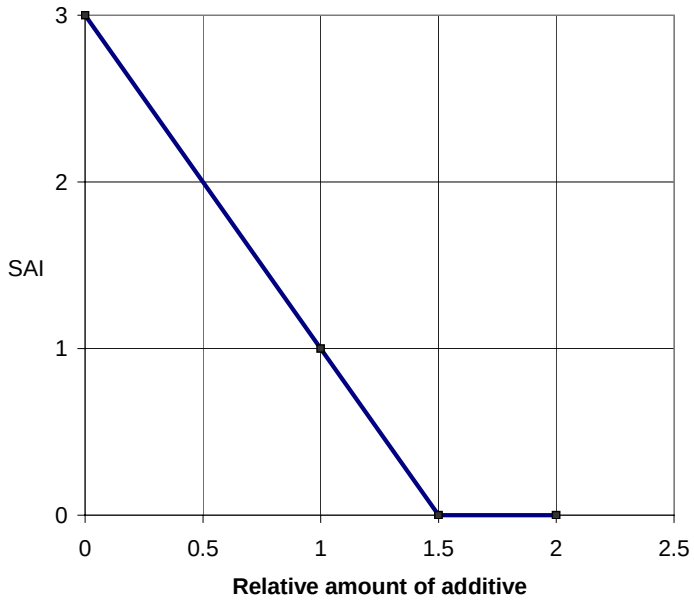

In Figure 5.4.4 it is seen that the SAI is a function of the amount of additive 'A' used. SAI decreases as expected with increasing amount of the additive 'A'.

In Appendix 1 it is shown how the quantitative effects of adding kaolinite to straw can be estimated using an equilibrium calculation procedure. An experimental evaluation of the effect of adding kaolinite to straw ash is made in Chapter 5.5.

5.5 Melting Analysis of ash using High-Temperature Light Microscopy

A Wheat#95 ash sample was prepared at 500°C at VTT by Moilanen. Using the same technique a number of different ashes were prepared from the straws 1 to 7. The idea was to observe whether these ash samples behaved differently during heatup in the high-temperature light-microscope equipment (HTLM) developed at dk-TEKNIK (Hjuler 1997). Since the straws behaved almost identical with respect to sintering in the VTT-thermobalance it was decided to cancel these measurements. Instead it was decided to test a raw straw ash sample and following a number of straw ash + kaolinite samples. The amount of kaolinite was varied according to the calculations made with HSC Chemistry, see Table 5.5.1.

Sørensen L.H. and K. Hjuler (1999) made the analysis using the HTLM equipment at dk-TEKNIK. About 0.1 mg ash sample is placed on a sapphire disk that is located in the sample holder on the heating stage. During the test made here, a second sapphire disk was used as a cover in order to prevent or delay evaporation of gases from the sample; i.e. the sample is "sandwiched". Additionally one glass cover is mounted on the heating stage that thus becomes gas tight and is operated in a controlled atmosphere (nitrogen saturated with water at room temperature). The microscope is focused on a random part of the ash, the magnification is set at typically 100-120 X, and the light conditions are optimised. The digital camera and the heating stage are operated from a personal computer. The temperature is ramped at 10°C/min from an initial temperature of 550°C and up to 1100°C. The ash sample is photographed initially and then every fifth second [Hjuler 1997]. Calibrations were made using LiF. The experiments were followed in-situ in the microscope and any observed variation was written down. The picture was recorded in-situ by a digital camera. Additionally a videotape was produced, so that the events could be observed later and discussed. In the following the samples are commented and the “melt fraction” = ‘mf’ curve are shown. The mf curves are obtained as the fraction of the ash layer that becomes transparent during the heating procedure. This curve should however be supported by careful visual inspection of the ash behaviour, since much more information is obtained this way and since the ‘mf’ curve has to be interpreted in order to give full information. The mf curves and the experiments performed are described in Figure 5.5.1 to Figure 5.5.4.

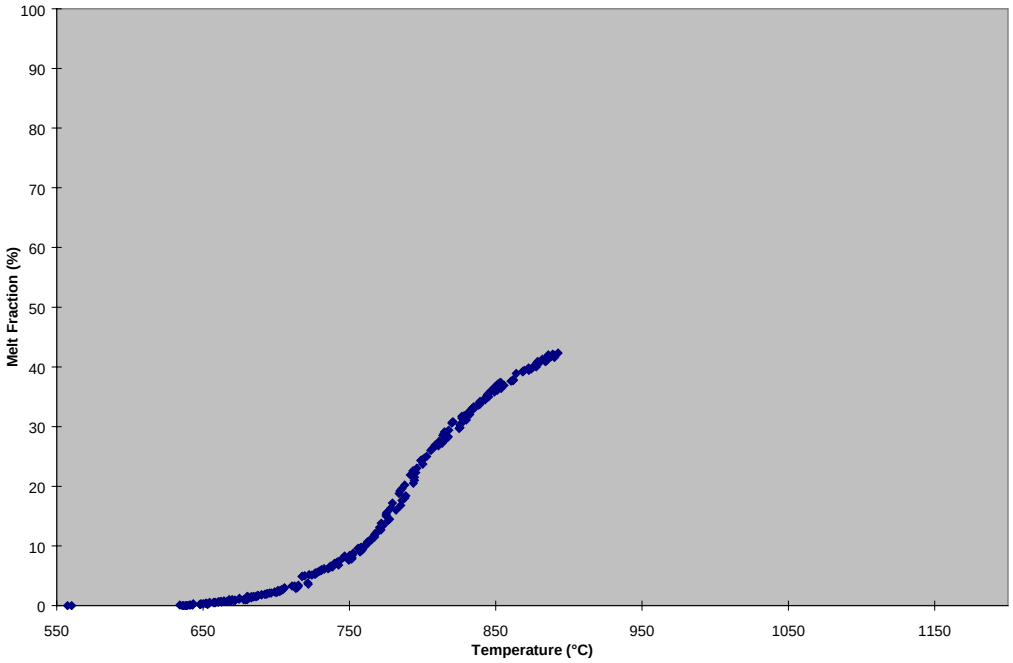

Figure 5.5.1. Danish wheat straw 1995. The formations of a few KCl drops or crystals are formed at the upper glass at about 650 ℃ and significant formations of crystals are observed at 705 ℃. Significant voids in the bulk ash are observed at 780 ℃. At 805 ℃ the small crystals are melting and all drops have visually disappeared at 815 ℃. At 820-825°C some central bulk melting takes place and at 840-850°C large homogeneous melted parts has been formed. At 900 ℃ most material has melted.

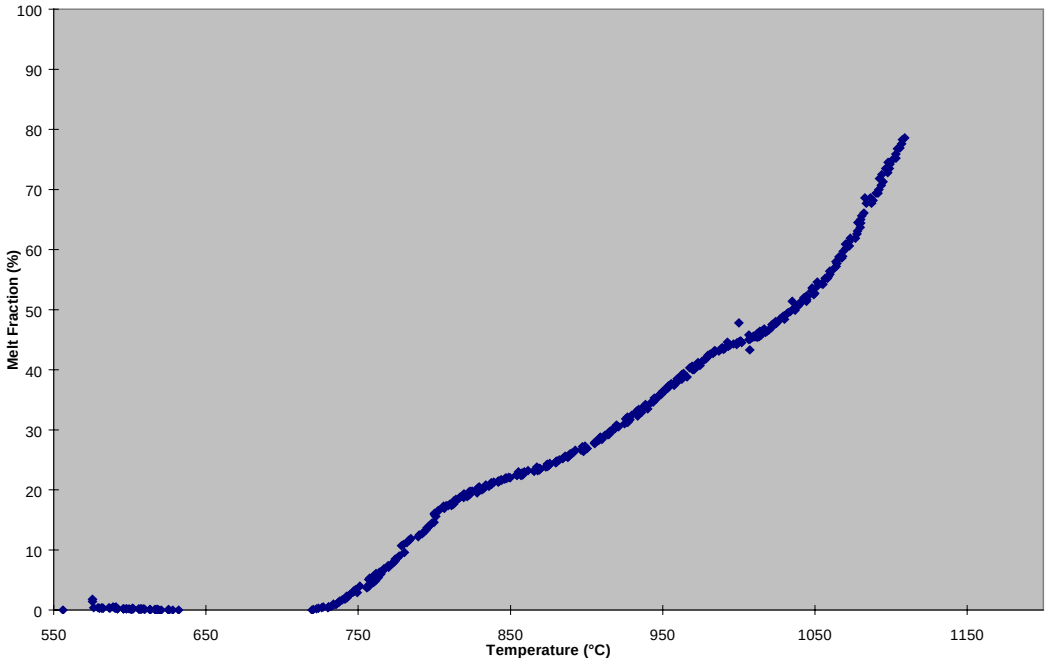

Figure 5.5.2. 2 wt.% Kaolinite added to Danish wheat straw DW95. The formation of a few KCl drops or crystals are formed at the upper glass at about 650 ℃ crystals and significant formation of crystals is observed at 730 ℃. Voids in the bulk ash are produced from 780 ℃ and assumed due to the evolution of gaseous species. At 805 ℃ the small KCl crystals are melting and all KCl crystals have disappeared at 810 ℃. At 820-825°C some melting takes place but at 830 ℃ the sample is getting dry again until 920 ℃ where a few drops evolve centrally in the sample. At 965 ℃ a significant amount of new (potassium silicate-) drops evolves and settle at the upper sapphire disk. At 1015°C melting takes place in the bulk and the drops at the upper disk melts and evaporates – the experiment is stopped while a few drops remain. The melted drops at the upper disk consist of potassium, silicium and oxygen.

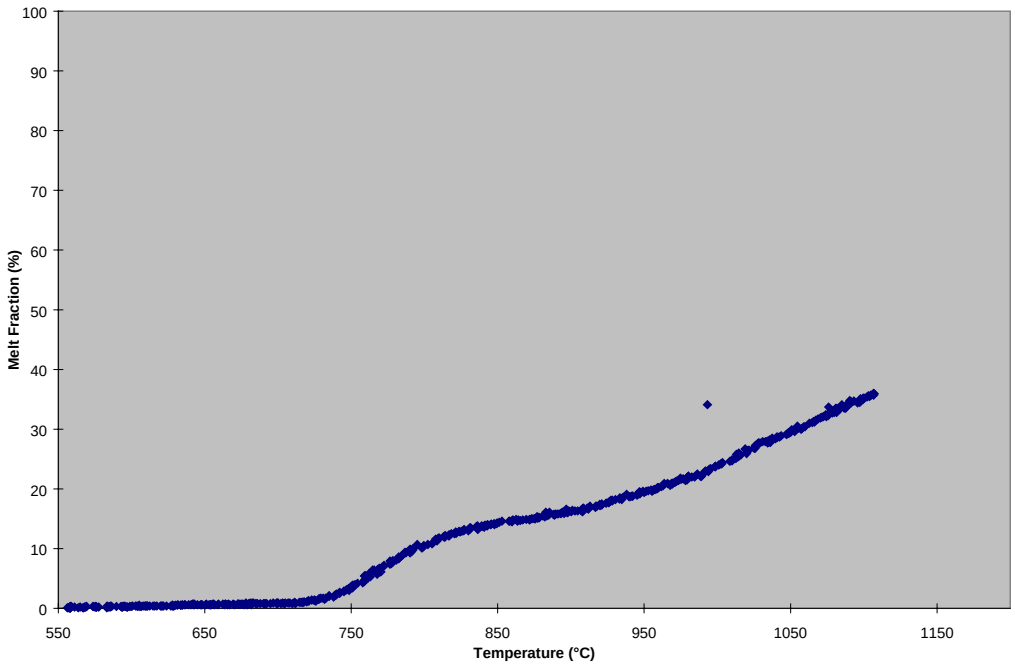

Figure 5.5.3: 4 wt.% kaolinite added to Danish wheat straw 1995. The formations of a few KCl crystals are formed at the upper glass at about 650 ℃ a few more crystals are observed at 705-750 ℃. At 750 ℃ almost all KCl crystals have disappeared. Voids in the bulk ash are produced at 770 ℃ and at 780°C some few voids are produced – these voids are assumed to be due to the evolution of gaseous species. At 805 ℃ a slight melting takes place but at 830 ℃ the sample is getting dry again until 1030 ℃. When the temperature is increased to 1100 ℃ a few drops evolves centrally in the sample. The sample gives probably SAI = 0-1 stars. Only a very small amount of new drops evolves and settles at the upper sapphire disk above 1000 ℃.

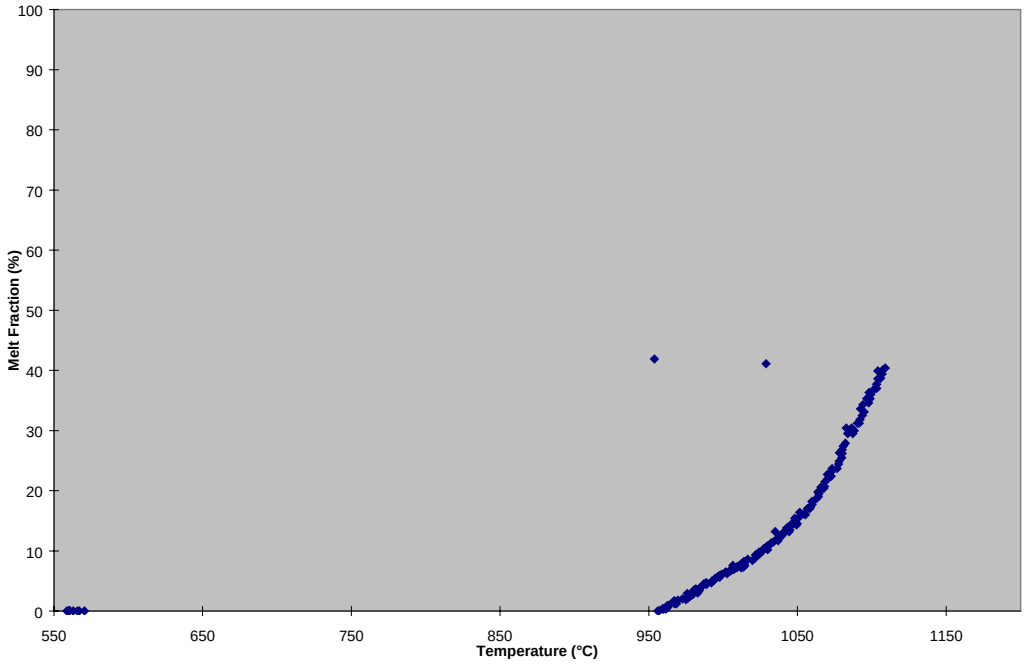

Figure 5.5.4: 15 wt.% kaolinite added to Danish wheat straw 1995. About nothing visually happens until around 1080 ℃, where a few drops evolve in the bulk.

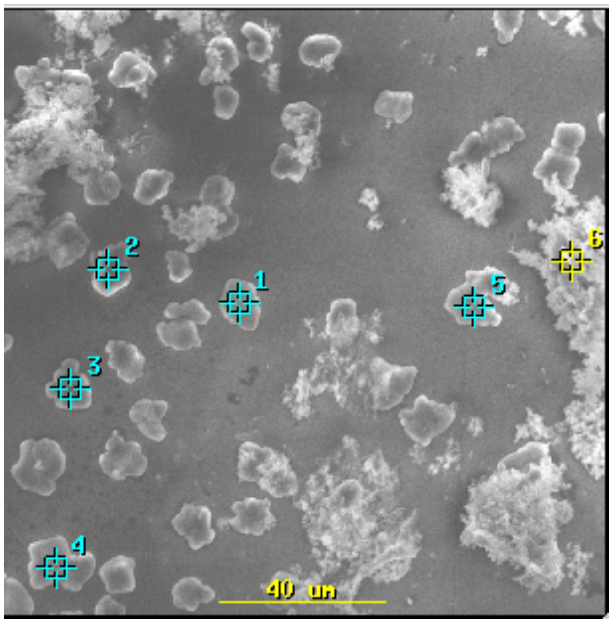

Figure 5.5.5. Crystalline KCl drops settled at the upper glass during the high-temperature light microscope experiments when testing the raw-straw sample.

From Figure 5.5.1 to Figure 5.5.3, it is seen, that in general KCl(g) is evolving from the sample at about 650°C and even more up to around 750°C and settling at the upper glass, see Figure 5.5.5. This is in accord with the predictions from using the HSC-Chemistry equilibrium program, see Figure 2-4 in Appendix 1. With increasing kaolinite addition the amount of KCl crystals at the upper glass is decreasing and has almost diminished at a kaolinite/K molar ratio of 2/1. The observation of melt formation at higher temperatures is summarised in Table 5.5.1. It is seen that the start temperature of melts formation (the onset temperature) and in particular the temperature of significant melt formation is increased with the kaolinite/K ratio. If the onset temperature determines the necessary amount of kaolinite addition, more than 4 wt.% kaolinite should be added together with the straw in order to prevent agglomeration during the gasification process. If instead the temperature of significant melt-formation (as we suggest) is determining the melt-formation, 2 wt.% kaolinite is sufficient, if the kaolinite effectively contacts the sample ash components.

Kaolinite/K molar ratios	Kaolinite wt.% of dry fuel	Temperature of start melt formation (onset temperature)	Temperature of significant melt formation
0	0	805°C	820-850°C
0.25	1.98	820-825°C	920°C
0.5	3.96	830°C	1030°C
1	7.93	-	-
2	15.9	1080°C	>1080°C

Table 5.5.1. Summary of melt-formation data observed during high-temperature light microscope (HTLM) experiments when testing the raw-straw sample.

The results above are however made with the assumption that kaolinite readily reacts with the sample ash. The validity of this assumption depends (as with other additives) on the contact that can be established between the kaolinite and parts of the straw ash that includes potassium and silicium. This contact depends on the process and the quality of the kaolinite, its particle size distribution and the addition technique. The kaolinite results reported in chapter 5.5 are obtained using a high-quality finely pulverised kaolinite (“Pibeler”) and the best results were obtained by impregnation of the samples with the additives.

The experiment where the raw straw was tested, see Figure 5.5.1, was first run without a second sapphire disk as a cover in order to prevent or delay evaporation of gases from the sample; i.e. the sample was not "sandwiched". In this case significant melting took place at around 920-950°C. From this result we conclude, that for comparison with the melts formation in a gasifier more realistic results are obtained using a cover and thereby changing the mass balance around the sample (salts are retained on the cover for a period). We also conclude that the gaseous and liquid salt-melts play a significant role during the melt formation.

6. Summary

From the experiments performed on a variety of Danish straws it is observed that no great difference between the reactivity and the agglomeration and sintering properties of the straws were observed due to the type and amount of fertiliser used. The Danish straws #1, #2, #3, #5, #6 and #7 differed slightly in ash content. Still all these samples caused a sintering and agglomeration index of SAI=3* at 850°C. The Wheat#4 straw was special in the sense that it contained much less Si than the others and despite a high potassium content a low SAI_T (SAI_{850}=1) was obtained for this straw. Wheat#4 was grown on a relatively poor quality field with high sand content that may be the cause of the relatively low content of Si in that fuel, while the amount of fertiliser addition did not differ particularly from normal. The char gasification reactivity and the index, SAI_T, are greatly effected by weathering. Since potassium being the most abundant active catalytic element in the straw is washed out by rain together with chloride while silicium remains in the straw, the value of the γ index or the SiO_2/K_2O ratio is high for two ribbe-harvested straws. For both these straws and in particular for the matured straw this results in a low SAI-value and a low reactivity. Raising the temperature increases the reactivity R but since the washed straw still contains a non-vanishing amount of potassium, an acceptable reactivity is not obtained until high temperature melting phases again show up. SAI_{850}=1 for washed straw, see Table 5.4.1 sample file 478 and Figure 5.4.1, (Henriksen 1996) experimentally demonstrated this already in 1996.

Equilibrium calculations were performed using the FACT program to simulate a fluid bed gasifier. We found in Chapter 3.5 for wheat DW95 that a slag-phase was likely obtained in a CFB-gasifier. At T= 740°C and even lower, this phase consisted of SiO_2 and K_2O in a mole-ratio of around SiO_2/K_2O= 3.3 at 740°C and SiO_2/K_2O= 2.8 at 900°C. This phase accounted for around 80 mole % of the silicium added with the straw. $MgO*CaO*Si_2O_4$(s) and $K_2O*2SiO_2$ accounted for almost the rest of the straw-ash silicium. Also major parts of potassium, not bound as KCl, was accounted for by these components. From HSC calculations and from experiments we have observed that potassium to some extent is also bound as a phosphate. The phosphates however, when available in small amounts, seem not to contribute much to the melting phases. Therefore we introduce the theoretical sintering and agglomeration index, $\gamma_K \equiv SiO_2/K_2O \approx 2(Si/28.09)/((K/39.10)-(Cl/35.45)-a(P/30.97))$ and incorporating also sodium, $\gamma_{K,Na} \equiv SiO_2/K_2O \approx 2(Si/28.09)/((K/39.10)-(Cl/35.45)-a(P/30.97))$, where Si, K, Na, Cl and P is

measured as weight % in the fuel ash, the coefficient 'a' may vary but has been chosen in the present work as a=1. It was found for the straw DW95 that the γ_K value was a good approximation to the slag-SiO_2/K_2O ratio for an 800-1000°C hot 100 MW gasifier as calculated using the FACT program. Therefore the somewhat simplified γ_K is used as an index for agglomeration and sintering and since the formation of the slag phase reduces the amount of volatile potassium, e.g. KO(g), γ_K also roughly correlates with the conversion time and inversely to the reactivity of the fuel. Here, however, it will be more valuable to utilise an actual measured or calculated KO(g) or K_2O(g), since they depend of the mass balance and the precise ash composition as well as of γ_K. The KO(g) partial pressure depends as it is discussed in chapter 3.10 on the temperature, the gas composition, the ash composition and state and also the amount of carbon available in the gasification reactor. The relation between KO(g) and the catalyst loading on the active sites at the carbon surface is complicated. Therefore we suggest developing a model, that includes the determination of the number of active sites at the carbon surface, where catalysts can possible settle. The estimation of Gibbs free energy for the catalyst located at such sites is therefore a topic of future work. Following this information should be included in the FACT and HSC databases.

Experimentally we have found that the addition of K_2CO_3 and K_3PO_4 to a carbon increases the reactivity until a maximum reactivity is achieved. When adding salt-free washed ash to samples catalysed by salts like K_2CO_3, the catalysing effect is reduced. This seems not to be the case if the catalyst is K_3PO_4. Samples were heated to 900°C in chapter 5.3. It was observed that washed ash mixed with K_2CO_3 gave an endothermic peak above 740°C and in particular above 780°C. Also a melted phase was observed after the heating of the sample. In the case where some specific additives were used the behaviour characteristic for raw-ash melting was removed. It was shown in Appendix 1 that the amount of additive necessary for preventing serious ash melting could be estimated for the well-known additive "kaolinite". In Chapter 5.5 it was demonstrated from adding kaolinite in controlled amounts to straw and straw ash, that kaolinite is an efficient anti-agglomeration additive. It has also been shown that fair predictions are made using the HSC Chemistry equilibrium program and that the high-temperature light microscope technique developed by Klaus Hjuler (1997) is valuable as a tool for ash investigations. HSC Chemistry was used (together with a ReaTech's user database) to predict the necessary amounts of additive, and HSC gave a fair prediction of the experiments at dK-Teknik. The program FACT have been used for prediction of melt behaviour for an alkali-containing fuel. Besides gasification of straw, also

waste may be a topic for future work.

The makro-TGA technique as utilised by (Henriksen 1996) was successfully used to test the effect of using various types and amount of additives in steam gasification. Besides providing measures for the reactivity and the ash agglomeration, sintering and corrosion tendency of biomass fuels, the ash residues from the makro-TGA are abundant, so that ash fractions can following be analysed in detail – e.g. by microscopic techniques. The macro-TGA technique was used for the characterisation of various straw ashes and for the quantitative test of one anti-agglomeration additive. It was shown that the success of using a specific amount of additive was dependent of the addition technique. Impregnation were in general more efficient than addition of the additive as a powder. Finally the experimental technique here was also used as an indicative corrosion test.

7. Conclusion

This work focus on the connection between char reactivity, ash, agglomeration and sintering and the gas composition in the turbid environment in a circulating fluidised bed gasification process, where biomass, i.e. straw, wood or peat and waste are gasified. The model approach intends to combine equilibrium calculation programming of complex multicomponent-multiphase systems with the concept of catalytic effects in fuel reactivity. Both the experimental and the theoretical work showed that the reactivity of char is dependent on the silicium as well as the potassium content and the form of the potassium compound. This was established from the use of synthetic ash and carbon together with catalytic potassium compounds. We have introduced the (theoretical) sintering and agglomeration bed-mole-ratio index, $\gamma_K = SiO_2/K_2O$. We find that as γ_K decreases, the char reactivity increases. We suggest that a fuel has high agglomeration tendency if $2<\gamma_K<15$ and very high agglomeration tendency if $3<\gamma_K<5$. Reactivity measured in H_2O and CO_2 atmospheres on a series of straw chars had a significant inverse correlation with γ_K. γ_K may be estimated analytically from the elemental analysis of the straw ash, but better information is obtained from the results of equilibrium calculations. It has also been found that a number of additives if properly added are effective for the prevention of agglomeration and sintering of straw ash. The quantification of the necessary and sufficient amounts of catalysts and additives are supported by the modelling approach and index developed by the authors in the present work.

Preliminary literature studies on gas cleaning show that dolomite as well as nickel catalyst can be used to crack tar from a fluidised bed gasifier. Nickel has a higher catalytic activity than dolomite, but for a tar concentration larger than 2 g/m^3 nickel becomes deactivated and is therefore poor as an initial tar cracker. Dolomite is not deactivated at high tar concentrations but it is elutriated in a fluid bed and therefore dolomite must be continuously renewed with the input feed.

Dolomite may also be used in an external fixed bed. The actual cracking solution depends on the application of the raw gas (boiler, GT, engine) and the demand to the gas quality; and the other gas cleaning equipment (cyclones, filters etc.). With respect to addition of calcium based catalysts as a char catalyst and a tar cracker we conclude that the activity of calcium depends on the method by which it is added to the fuel.

References

Aronson S., Salzano F.J., Bellafiore D. [1968]. J. Chem. Phys., **49**, 434

Albrect J., Deutsch S., Kurkela E., Simell P., Sjöström K., [1998]. "Provisional protocol for the sampling and analysis of tar and particulates in the gas from large scale biomass gasifiers". Prepared by a working group of the biomass gasification task of the IEA Bioenergy Agreement. (Draft version, June).

Aristoff E., Rieve R.W. & Shalit H., [1981]. "Low temperature tar". In: Elliot, M.A. (ed.). Chemistry of coal utilization. New York, Wiley, p. 983-1002.

Bak J.[1999], Risø National Laboratory, Denmark (personal communication).

Barin I. [1995]. Thermochemical Data of Pure Substances. 3rd ed., Weinheim, Germany.

Barrio M., Gøbel B., Risnes H., Sørensen L.H. [1999]. "Steam gasification of birch and beech char. Chemical kinetics". In: Proceedings of the Nordic Seminar on Single Particle Conversion, Trondheim, October 21, 1999.

Barrio M. [1999a]. Visit at ReaTech, Roskilde February-March 1999.

Bale C.W., Pelton A.D. [1974], "Mathematical Representation of Thermodynamic Properties in Binary Systems and Solution of Gibbs-Duhem Equation", Metall. Trans., **5**, 2323-2337.

Bale C.W., Pelton A.D. [1990], "The Unified Interaction Parameter Formalism – Thermodynamic Consistency and Applications", Metall. Trans. A, **21**, 1997-2002.

Bale, C.W., Pelton, A.D. [1999]. "FACT-Win - Users Manual". CRCT, Ecole Polytechnique de Montréal, Québec, Canada.

Blander M., Pelton A.D. [1984]. "Analysis and Predictions of the Thermodynamic Properties of Multicomponent Silicates". In: Proceedings of the 2nd International Symposium on Molten Slags and Fluxes, Lake Tahoe, Nevada. TMS-AIME, Warrendale, PA, p. 294-304.

Blander M., Pelton A.D. [1987]. "Thermodynamic Analysis of Binary Liquid Slags and Prediction of Ternary Slag Properties by Modified Quasichemical Equations", Geochim. Cosmochim. Acta, **51**, 85-95.

Blander M., Pelton A.D. [1997]. Biomass Bioenergy, **12**, 295-298

Cerfontain M.B., Moulijn J.A. [1983]. Fuel, **62**, 256-258

Chen S.G., Yang R.T. [1997]. Energy Fuels, **11**, 421-427

Corella J., Orío A., Toledo J.-M. [1999]. Energy Fuels, **13**, 702-709.

Dresselhaus M.S., Dresselhaus G. [1981]. Adv. Phys., 30, 139-326

Elliott, D.C. [1986] "Comparative analysis of gasification/pyrolysis condensates". Pacific NorthWest Laboratory, Richland, Washington.

Elliott S.R. [1998]. The physics and chemistry of solids, Wiley, Chichester.

Franklin h.D., Peters W.A., Cariello F., Howard J.B. [1981]. Ind. Eng. Chem. Process Des. Dev., **20**, 670-674

Hillert M. [1980]. CALPHAD, **4**, 1.

Fjellerup, J. [1989]. "Optimale Procesbetingelser for en Dolomitkrakker til Krakning af Tjære fra Forgasning af Biomasse". Optimal processing conditions for a dolomite cracker for cracking of tar from gasification of biomass fuels (in Danish). Risø National Laboratory, Roskilde.

Gøbel B. [2000]. Modellering af koksbed. Ph.D. thesis, DTU, Lyngby, Denmark. To be published.

Hallgren A.L., Oskarsson J. [1998]. In: Biomass for Energy and Industry – 10th European Conference and Technology Exhibition.
Hallgren A. [1994]. In: Proceedings of the 29th Intersociety Energy Conversion Engineering Conference, Aug. 1994, Monterey, CA, vol. 4, p. 1566-1571.
Hallgren A. [1996]. Theoretical and engineering aspects of the gasification of biomass. Dissertation thesis. LUTKD-I-TKKT-96-1037. Lund University, Department of Chemical Engineering II, p.102-107.
Hansen L.A. [1997]. Melting and Sintering of Ashes. Ph.D thesis, DTU, Department of Chemical Engineering, Lyngby, Denmark.
*Kracek F.C. [1932]. J. Phys. Chem., **36**, 2529*
Henriksen U. [1997]. In: Termisk forgasning af biomasse. Teknikdag, Apr. 1998. Ed. by J. Noes. Institut for Energiteknik, DTU, Lyngby, Denmark, p. 29-46.
Henriksen U., Jacobsen M.P., Lyngbech T., Hansen M.W. [1996]. Relationship between Gasification Reactivity of Straw Char and Water Soluble Compounds present in these materials. Presented in Conference: Developments in Thermochemical biomass Conversion, Banf, Canada 20-24. May.
Hjuler K. [1999]. In: Impact of Mineral Impurities in Solid Fuel Combustion. Proceedings of an Engineering Foundation Conference on Mineral Matter in Fuels, November 2-7, 1997, Kona, Hawaii. Eds. R. P. Gupta, T.F. Wall and L. Baxter. New York, Kluwer Academic. .
Ivarsson E., Nilsson C. [1988]. Smaelttemperaturen hos halmaskor med respektive utan tillsats medel. Smelting temperatures of straw ashes with and without additives (in Swedish). STEV-FBT-88-24. Swedish University of Agricultural Sciences, Dept. of Farm Buildings, Lund, Sweden.
Kiørboe L., Lilleng I. [1990]. Slaggedannelse i fyringsanlæg: Litteraturundersøgelse. Slagging in boiler furnaces: Literature survey (in Danish). dk-Teknik, Copenhagen.
Knacke O., Kubaschewski, Hesselmann K. [1991]. Thermochemical Properties of Inorganic Substances. 2nd ed., Berlin, Springer, vol. 1-2.
Kurkela E. [1996]. "Formation and removal of biomass-derived contaminants in fluidized-bed gasification processes". VTT-PUB-287. VTT, Technical Research centre of Finland, Espoo.
Kurkela E., Ståhlberg P. [1992]. Fuel Process. Technol., **31**, 1-21
Larsen K.-A.H., Nielsen H.K. [2000]. Reaktiviteten for Hvedehalm. Project report, IMFUFA, Roskilde University, Denmark (in Danish).
Leboda R., Skubiszewska-Zieba J., Grzegorczyk, W. [1998]. Carbon, **36**, 417-425
Levin E.M., Robbins C.R., McMurdie H.F. [1964, 1985]. Phase Diagrams for Ceramists. Vol. 1. National Bureau of Standards, The American Ceramic Society, Columbus, U.S.A.
Marchner H. [1995]. Mineral Nutrition of Higher Plants. 2.ed., Academic Press, London.
*McKee D.W. (1983). Fuel **62**, 170-175*
Meier R., Weeda M., Kapteijn F., Moulijn J.A. (1991). Carbon, **29**, 929
Mimst C.A., Pabst J.K. [1981]. Proceedings of the International Conference on Coal Science, Düsseldorf. Verlag Glückauf, Essen, p. 730.
Mimst C.A., Pabst J.K. [1987]. J. Catal., **107**, 209-220
McNeil D. [1981]. "High temperature coal tar". In: Elliot, M.A. (ed.). Chemistry of coal utilization, New York, Wiley, p. 1003-1083.

Moilanen, Antero; Kurkela, Esa [1999]. Prevention of Ash-related Problems in Fluidized-Bed Gasification of Biomass Residues, carried out in 1997-1999.
Final Report for Progas project No. 21, VTT Energy, Espoo 25 June 1999. 25. pp +App
Moilanen, A., Kurkela, E., Laatikainen-Luntama, J. [1999], Ash behaviour in biomass fluidised-bed gasification. In: Impact of Mineral Impurities in Solid Fuel Combustion. Proceedings of an Engineering Foundation Conference on Mineral Matter in Fuels, November 2-7, 1997, Kona, Hawaii. Eds. R. P. Gupta, T.F. Wall and L. Baxter. New York, Kluwer Academic, pp. 555-567.
Morita, Y. [1978]. J. Jpn. Pet. Inst. **21**, 2
Ohtsuka Y., Yamausichi A., Zhuang Q. [1996]. Am.Chem.Soc. **41**, 221-225.
Olivares A., Aznar M.P., Caballero M.A., Gil J., Francés E., Corella J. [1997]. Ind. Eng. Chem. Res. **36**, 5220-5226.
Norby P. [1999], University of Oslo, Norway (personal communication).
Pelton A.D., Bale C.W. [1986]. Metall. Trans. A **17**, 1057-1063.
Pelton A.D., Bale C.W. [1986]. Metall. Trans. A **17**, 1211-1215.
Pelton A.D. [1986]. Computer Modeling of Molten Salts and Slags for Phase Diagram Calculations. In: Computer Modeling of Phase Diagrams. Proceedings of a symposium, Toronto, Canada, October 13-17, 1985. Ed. L.H. Bennett. Warrendale, Metallurgical Society, pp. 19-48.
Pelton A.D. [1988]. CALPHAD J. **12**, 127-142.
Pelton A.D. [1991]. Thermodynamics and Phase Diagrams of Materials. In: Materials Science and Technology, vol. 5. Ed. R.W. Cahn, P. Haasen, E.J. Kramer. Weinheim, VCH, chapt. 1, pp. 1-76.
Posselt D. [1999 & 2000]. Roskilde University: Department of Physics. Private communication.
Rathman O. and Stoholm P. [1995]. The pressurised thermogravimetric analyser at Department of Combustion Research, Risø: Technical description of the instrument. Risø-R-823(EN).Risø National Laboratory, Roskilde, Denmark.
Roine A. [1999]. HSC Chemistry® for Windows. Chemical Reaction and Equilibrium Software with extensive Thermochemical Database, Version 3.0.
Roine, A.[1999]. "Outokumpu HSC Chemistry® for Windows. Chemical Reaction and Equilibrium Software with extensive Thermochemical Database". Version 4.0.
Simell P.A., Bredenberg J.B. [1990]. Fuel **69**, 1219-1225.
Simell P., Kurkela E., Ståhlberg P. [1992]. In: Advances in thermochemical biomass conversion. London, Blackie Academic, vol. 1.
Simell P.A.[1997]. Catalytic hot gas cleaning of gasification gas. Dissertation for the degree of Doctor of Technology. Helsinki University of Technology.
Skrifvars B.-J., Sfiris G., Backman R., Widegren-Dafgård K., Hupa M. [1997]. Ash behaviour in a CFB boiler during ombustion of salix. Energy Fuels **11**, 843-848.
Skrifvars B.-J. [1994]. Sintering tendency of fuel ashes in combustion and gasification conditions. Doctoral Thesis, Åbo Akademi University, Åbo/Turku, Finland.
Sørensen L.H, Stoltze P. [1998-1999]. Private communication.
Sørensen L.H., Kurkela E. [1998]. Private communication at VTT Energy, Helsinki, Finland
Sørensen L.H., Henriksen U., Risnes H., Poulsen K.T., Hansen L.K., Olsen A., Rathman O., [1997]. Straw – H2O gasification kinetics: determination and discussion. Nordic Seminar on Thermochemical Conversion of Solid Fuels. Chalmers University of Technology, Göteborg, Sweden, 3 December 1997.

Stoltze P. [1999]. Ålborg University Esbjerg, Department of Chemical Engineering. Private communication.
Steenari B.-M., Lindquist O. [1998]. Biomass Bioenergy **14**, 67-76
Zevenhoven-Onderwater M., Skrifvars B.-J., Backman R., Hupa M. [1999]. In: Nordic Workshop on Ash Chemistry, Properties and Behaviour, June 3-4, Gothenburg, Sweden.
Yuh S.J., Wolf E.E. [1983]. Fuel **62**, 252-255
Yang R.T. [1984]. In: Chemistry and physics of carbon. Ed. by P.A. Thrower. New York, Marcel Dekker.
Yokoyama S., Miyahara K., Tanaka k., Tashiro J., Takukuwa T. [1980]. Nippon Kagaku Kaishi **6**, 974

Appendix 1

Kaolinite as an Additive in Fluidbed Gasification of Straw

Jan Fjellerup[1], Lasse Holst Sørensen[1], Antero Moilanen[2], Esa Kurkela[2]

[1]ReaTech, [2]VTT-Energy

Abstract

Theoretical studies of kaolinite addition in connection with fluidbed gasification of straw have been performed using the equilibrium code HSC. Equilibrium constants have been calculated for 10 reactions between kaolinite and potassium components (pure components). Equilibrium calculations show that the kaolinite + potassium compound to potassium aluminium silicate compound reactions are thermodynamically favourable above 650°C. A mass balance for VTT's circulating fluidised bed gasifier has been set-up and an input file to HSC has been constructed. Equilibrium calculations have been performed in the temperature range of 200 to 1000°C using a kaolinite to K molar ratio of 0, 0.25, 0.5, 1 and 2. The potassium components have been plotted for each calculation and the amount of KCl(g), K_2Cl_2(g), $K_2O*2SiO_2$ and K_3PO_4 are plotted versus the kaolin to K molar ratio.

Contents

1 Introduction

Simulations of gasification of straw at fluidbed temperature and simulations of subsequent gas-cleaning have been carried out at ReaTech. This work is related to the development of atmospheric gasification of biomass. In Denmark there is an increasing interest in the utilisation of biomass for power production and in CO_2 reduction and a number of projects within the area of biomass utilisation have been started. In Denmark the major biomass resource is straw. The high alkali and chlorine content in straw posses a lot of problems at gasification, among these are sintring and corrosion problems due to the high amount of potassium and chlorine. The aim of this work is to find out whether these problems can be avoided or reduced by the addition of kaolinite, which can react with potassium components. Equilibrium calculations have been performed using the HSC equilibrium code (1). HSC includes a database with more than 11000 components. It has been necessary to check a great number of component data, and a "ReaTech" database with 145 components has been made and added to the HSC database.

2 Kaolinite reactions

Kaolinite, $Al_2Si_2O_5(OH)_4$, can react with KCl, K_2Cl_2, K_2CO_3, K_2SO_4 and KOH. KCl can be both solid/liquid and gaseous (indices (g)). According to (2) K_2Cl_2 is a gas. KOH can be both gaseous and solid/liquid.

With KCl we get: $Al_2Si_2O_5(OH)_4 + 2\ KCl(g) \rightarrow 2\ KAlSiO_4 + H_2O(g) + 2\ HCl(g)$ (1)

$Al_2Si_2O_5(OH)_4 + 2\ KCl(g) + 2SiO_2 \rightarrow 2\ KAlSi_2O_6 + H_2O(g) + 2\ HCl(g)$ (2)

With K_2Cl_2 we get: $Al_2Si_2O_5(OH)_4 + K_2Cl_2(g) \rightarrow 2\ KAlSiO_4 + H_2O(g) + 2\ HCl(g)$ (3)

$Al_2Si_2O_5(OH)_4 + K_2Cl_2(g) + 2SiO_2 \rightarrow 2\ KAlSi_2O_6 + H_2O(g) + 2\ HCl(g)$ (4)

With K_2CO_3 we get: $Al_2Si_2O_5(OH)_4 + K_2CO_3 \rightarrow 2\ KAlSiO_4 + 2\ H_2O(g) + CO_2(g)$ (5)

$Al_2Si_2O_5(OH)_4 + K_2CO_3 + 2\ SiO_2 \rightarrow 2\ KAlSi_2O_6 + 2\ H_2O(g) + CO_2(g)$ (6)

With K_2SO_4 we get: $Al_2Si_2O_5(OH)_4 + K_2SO_4 \rightarrow 2\ KAlSiO_4 + 2\ H_2O(g) + SO_3(g)$ (7)

$Al_2Si_2O_5(OH)_4 + K_2SO_4 + 2\ SiO_2 \rightarrow 2\ KAlSi_2O_6 + 2\ H_2O(g) + SO_3(g)$ (8)

With KOH we get: $Al_2Si_2O_5(OH)_4 + 2\ KOH(g) \rightarrow 2\ KAlSiO_4 + 3\ H_2O(g)$ (9)

$Al_2Si_2O_5(OH)_4 + 2\ KOH \rightarrow 2\ KAlSiO_4 + 3\ H_2O(g)$ (10)

The equilibrium constant for the ten reactions are calculated:

$$K1 = p_{H2O} p_{HCl}^2 / p_{KCl}^2 \quad [bar] \tag{11}$$

$$K2 = p_{H2O} p_{HCl}^2 / p_{KCl}^2 \quad [bar] \tag{12}$$

$$K3 = p_{H2O} p_{HCl}^2 / p_{K_2Cl_2} \quad [bar^2] \tag{13}$$

$$K4 = p_{H2O} p_{HCl}^2 / p_{K_2Cl_2} \quad [bar^2] \tag{14}$$

$$K5 = p_{H2O}^2 P_{CO2} \quad [bar^3] \tag{15}$$

$$K6 = p_{H2O}^2 p_{CO2} \quad [bar^3] \tag{16}$$

$$K7 = p_{H2O}^2 p_{SO3} \quad [bar^3] \tag{17}$$

$$K8 = p_{H2O}^2 p_{SO3} \quad [bar^3] \tag{18}$$

$$K9 = p_{H2O}^3 / p_{KOH}^2 \quad [bar] \tag{19}$$

$$K10 = p_{H2O}^3 \quad [bar^3] \tag{20}$$

The equilibrium constant for the ten reactions is calculated using HSC, and Log K is plotted versus temperature in fig.1. Log K is calculated using Gibbs free energy for the reaction (1).

$$K = \exp(-\Delta G / RT) \tag{21}$$

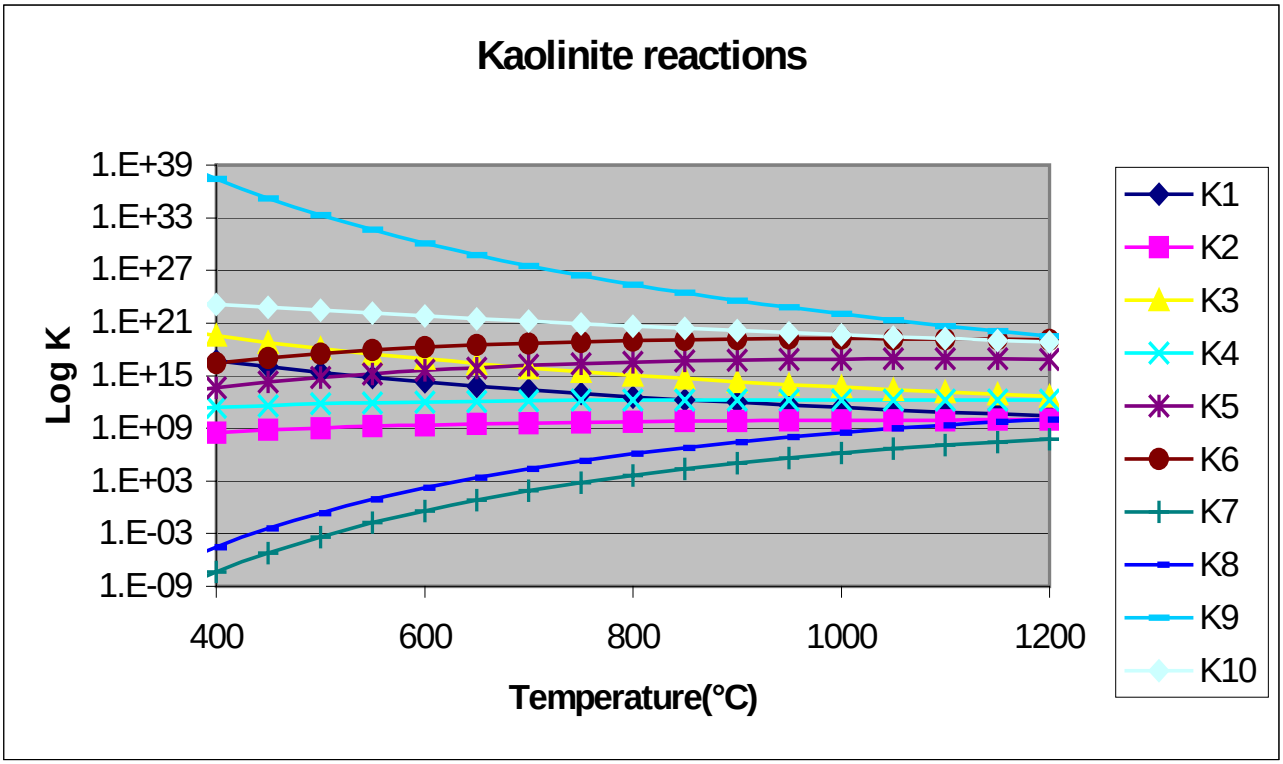

Figure 1. Equilibrium constant for kaolinite reactions with potassium components.

For temperatures above 650°C, the equilibrium constant for all reactions is above 1, which means that all reactions are thermodynamically favourable above 650°C ($\Delta G < 0$). In reaction 1, 3 and 9, kaolinite reacts with gaseous components; in the other reactions, kaolinite is in equilibrium with one or more solid species. The reaction pathways most likely include solid-gas reaction pathways.

To evaluate the effect of kaolinite as a getter for K-components in a multicomponent system, HSC calculations have been performed using different kaolinite to K ratios for gasification of straw. Wheat straw from 1995 has been used as a fuel in all calculations. Figure 2 shows the distribution of K-components with no addition of kaolinite.

3 Kaolinite additive in gasification

3.1 Mass balances for VTT's circulating fluidised bed gasifier (3).

Table 1. Mass balances for gasification of straw (1995) in a fluidized bed gasifier.

Gasifier 95	Straw 95, ds		dry feed fuel	Normalised
Moisture (%)	12		sample	to
Ash %, d.r.	4.8		kmol/kg dry	186.99
Daf feed	Mw	Straw	[kmol /kg,d.r]	[kmol]
C	12.011	47.5	3.95E-02	**3.95E+01**
H	1.0079	5.9	5.85E-02	**5.85E+01**
N	14.007	0.7	5.00E-04	**5.00E-01**
S	32.06	0.1	3.12E-05	**3.12E-02**
O	15.999	41	2.56E-02	**2.56E+01**
Major elem.d.r. (SUM)		**95.2**	1.24E-01	1.24E+02
Ash composition, %				
Si	28.086	16.00	2.73E-04	**2.73E-01**
Al	26.982	0.16	2.82E-06	**2.82E-03**
Fe	55.847	0.14	1.20E-06	**1.20E-03**
Ca	40.08	6.00	7.19E-05	**7.19E-02**
Mg	24.305	1.30	2.57E-05	**2.57E-02**
K	39.098	25.00	3.07E-04	**3.07E-01**
Na	22.99	0.40	8.36E-06	**8.36E-03**
Ti	47.867	0.01	1.20E-07	**1.20E-04**
S	32.06	1.28	1.92E-05	**1.92E-02**
P	30.974	1.70	2.64E-05	**2.64E-02**
C, carbonate	12.011	0.00	0.00E+00	**0.00E+00**
O, oxygen in ash	15.999	31.06	9.32E-04	**9.32E-01**
Ash-form.(dry ash%),SUM		**83.07**	1.67E-03	1.67E+00
Trace components, ppm.(dry fuel) SUM				
Cu	63.546	46	7.24E-07	**7.24E-04**
Zn	65.38	110	1.68E-06	**1.68E-03**
Pb	207.2	86	4.15E-07	**4.15E-04**
Cd	112.41	0.02	1.78E-10	**1.78E-07**
Hg	200.59	0.01	4.99E-11	**4.99E-08**
Cl	35.456	5970	1.68E-04	**1.68E-01**
Trace el,ppm.(dry fuel)SUM		6212	1.71E-04	1.71E-01
Steam+air				
Steam (added)	18.015	0.05	2.78E-03	**2.78E+00**
Moisture (Fuel)	18.015	0.1364	7.57E-03	**7.57E+00**
Moisture(Air)	18.015	0.009	4.99E-04	**4.99E-01**
Moisture, kg (SUM)		0.1953	1.08E-02	1.08E+01
N2+CO2+O2, purge+air				
SUM N2	28.014	1.1032	3.94E-02	**3.94E+01**
Purge N2	28.014	0	0.00E+00	**0.00E+00**
N2 (air)	28.014	1.1032	3.94E-02	**3.94E+01**
CO2 (air)	44.108	0.0007	1.50E-05	**1.50E-02**
O2 (air)	31.998	0.3351	1.05E-02	**1.05E+01**
Air, kg (SUM)		1.439	4.99E-02	4.99E+01
Bed material+additive, kg (SUM)				
Al2O3	101.96	0	0.00E+00	**0.00E+00**
TiO2	79.898	0	0.00E+00	**0.00E+00**
CaCO3	100.09	0	0.00E+00	**0.00E+00**
MgCO3	84.313	0	0.00E+00	**0.00E+00**
CaMg(CO3)2	184.4	0	0.00E+00	**0.00E+00**
SiO2	28.086	0	0.00E+00	**0.00E+00**
Al2Si2O5(OH)4	258.16	0.05	1.94E-04	**1.94E-01**
Bed material, kg (SUM)		0.05	1.94E-04	1.9368E-01
Total & normalisation			**1.8699E-01**	**186.99**

Gasif. temp [C]	850
Comb. Temp [C]	850
feed [kg/h]	**23376.62**
dry feed [kg/h]	**20571.43**
steam [kg/h]	**1028.57**
air [kg/h]	**29602.28**
kg dry air/kg dry feed	**1.439**
steam/dry feed	**0.05**
Bed material feed	**1028.57**
Bed mat. F./dry feed	0.050
Purge N2	**0**
Purge N2/kg dry feed	0.0000
Ash (kg/h)	**987.43**
HHV, [MJ/kg]	
LHV, [MJ/kg]	17.5
Air, 15°C and 60% humidity	
Humidity	0.6

Air, dry	**mole %**	**Mw**
N2 (%)	78.97	**28.014**
CO2(%)	0.03	**44.108**
H2O(%)	0	**18.0148**
O2(%)	21	**31.998**
Air, dry	**Weight%**	
N2 (%)	76.667	
CO2(%)	0.046	
H2O(%)	0.000	
O2(%)	23.287	
Sum	100.000	
H2O vol.%, with dry a	1	18.0148
H2O wt% with dry air	0.624	

bedmaterial/ash

0.05 in gasifier, 0.2-0.4 in FB and PDU

bed materials:	kg/kg dryfuel	efficiency
Al2O3	0	0
TiO2	0	0
CaCO3	0	0
MgCO3	0	0
CaMg(CO3)2	0	0
SiO2	0	0
Al2Si2O5(OH)4	**0.05**	1
Sum bed (kg/kg dF):	**0.05**	

O(daf fuel) + O(ash)	**26.559**
C(daf.)+C(carbonat	**39.547**

0.05 kg kaolin/kg fuel

Estimated trace elements concentrations[ppm] for calculations (4). Wheat data used.

Trace elements	Wood	Salix	Wheat	Rape	Barley	Peat	Coal
Cu	1.8 (0.5-6)	3.8±2.4	46±13	62±15	29±18	10±12	13 (7-50)
Zn	22 (0-40)	66±19	110±40	110±40	120±60	10±16	27 (4-180)
Pb	3.6 (0.5-13)	1.5±0.6	86±20	45±17	58±36	2.5±5	13 (2-70)
Cd	0.2 (0.1-0.4)	1.3±0.7	0.02±0.01	0.050±0.07	0.02±0.02	0.2±0.2	0.3 (0.03-0.8)
Hg	0.02 (0.01-0.02)	-	0.01	0.01±0.006	0.01	0.05±0.1	0.1 (0.02-1.6)

3.2 Effect of kaolinite on potassium components in gasification

The effect of kaolinite on potassium components in gasification of straw (table 1) is tested using kaolinite/K molar ratios from 0 to 2; the input data is listed in table 2.

Table 2. Kaolinite input data to HSC.

Kaolinite/K molar ratios	Kaolinite wt.% of dry fuel	Figure no.
0	0	2
0.25	1.98	3
0.5	3.96	4
1	7.93	5
2	15.9	6

HSC calculations have been performed using table 2 data and the potassium components is shown in the temperature range of 200 to 1000°C.

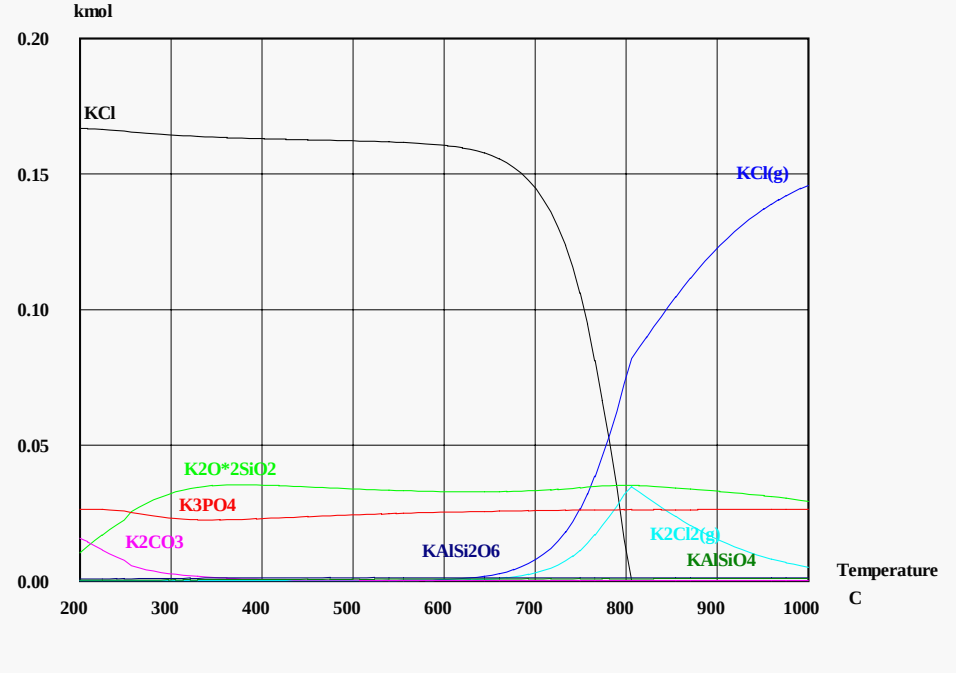

Figure 2. Gasification of straw, 5 wt.% steam. K-components as a function of temperature. No addition of kaolinite.

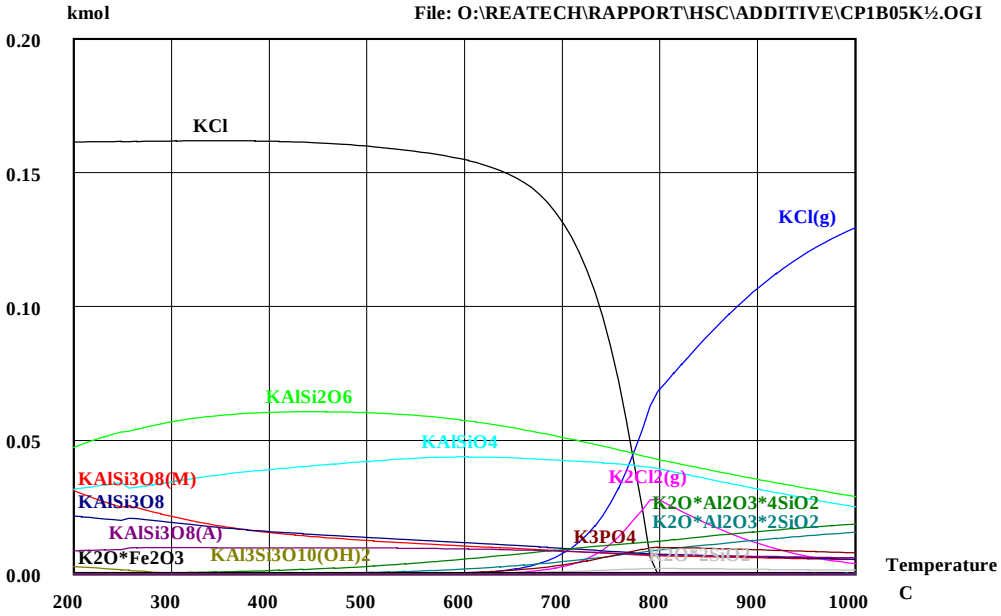

Figure 3. Gasification of straw, 5 wt.% steam. K-components as a function of temperature. Kaolinite/K molar ratio 0.25, this corresponds to 1.98 wt.% kaolinite on a dry fuel basis

The concentration of K_3PO_4, K_2CO_3 and $K_2O*2SiO_2$ are 3.5E-3, 9.39E-4 and 4.6E-7 respectively.

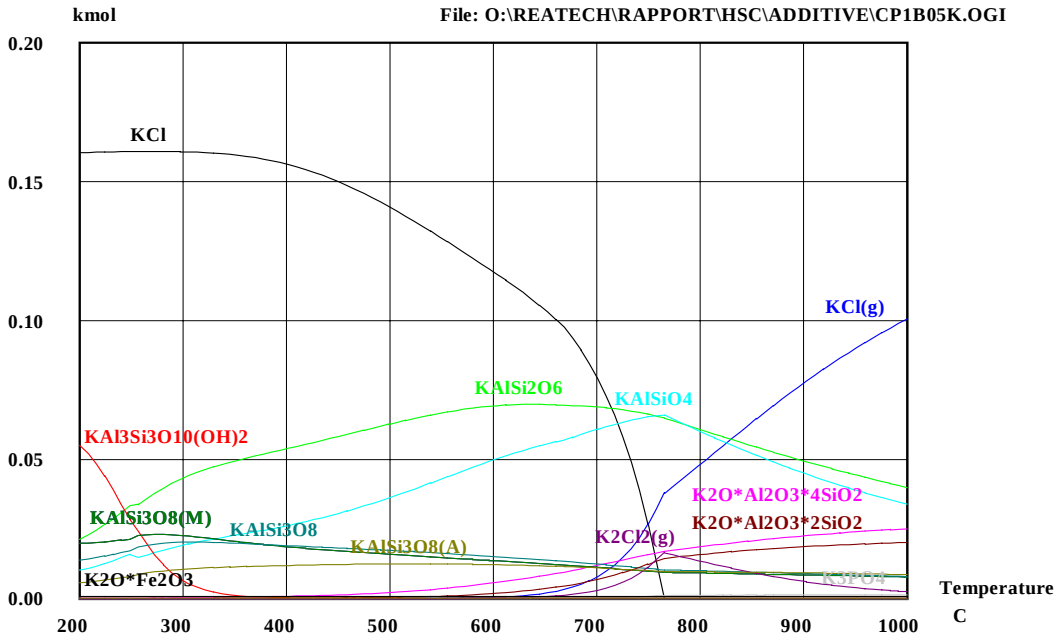

Figure 4. Gasification of straw, 5 wt.% steam. K-components as a function of temperature. Kaolinite/K molar ratio 0.5. This corresponds to 3.96 wt.% kaolinite on a dry fuel basis.

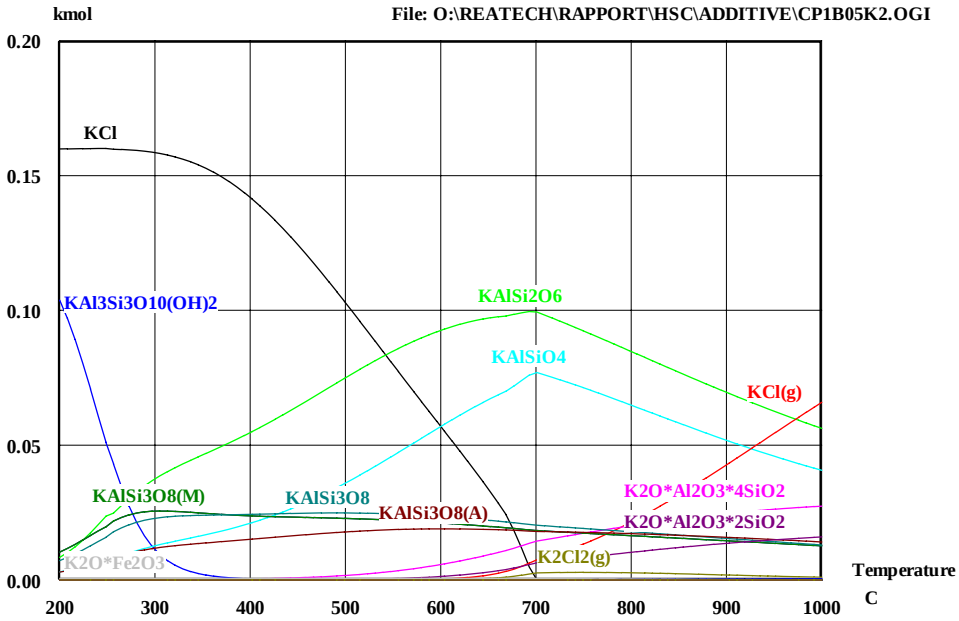

Figure 5. Gasification of straw, 5 wt.% steam. K-components as a function of temperature. Kaolinite/K molar ratio 1, corresponding to 7.93 wt.% kaolinite on a dry fuel basis.

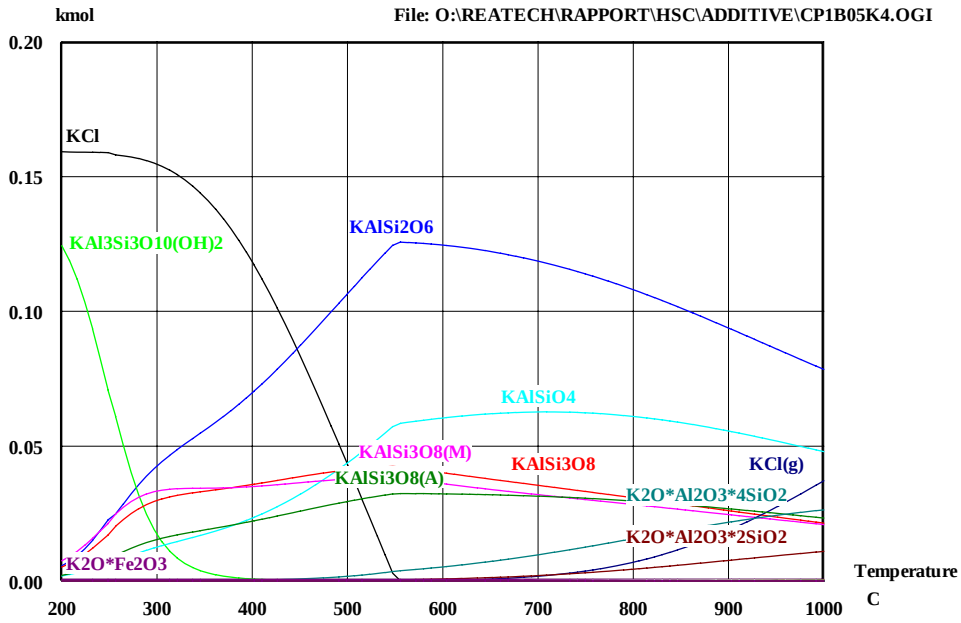

Figure 6. Gasification of straw, 5 wt.% steam. K-components as a function of temperature. Kaolinite/K molar ratio 2, corresponding to 15.9 wt.% kaolinite on a dry fuel basis.

From the equilibrium calculations it is seen, that already addition of 3.5 wt.% kaolinite depletes potassium components such as $K_2O*2SiO_2$, K_3PO_4 and K_2CO_3 and parts of KCl. To convert almost all KCl to $K_xAl_ySi_ZO_q$ and HCl requires addition of more than 15 wt.% kaolinite from an equilibrium point of view.
The total effect of kaolinite addition on KCl(g), K_2Cl_2(g), $K_2O*2SiO_2$ and K_3PO_4 is summarised in figure 7.

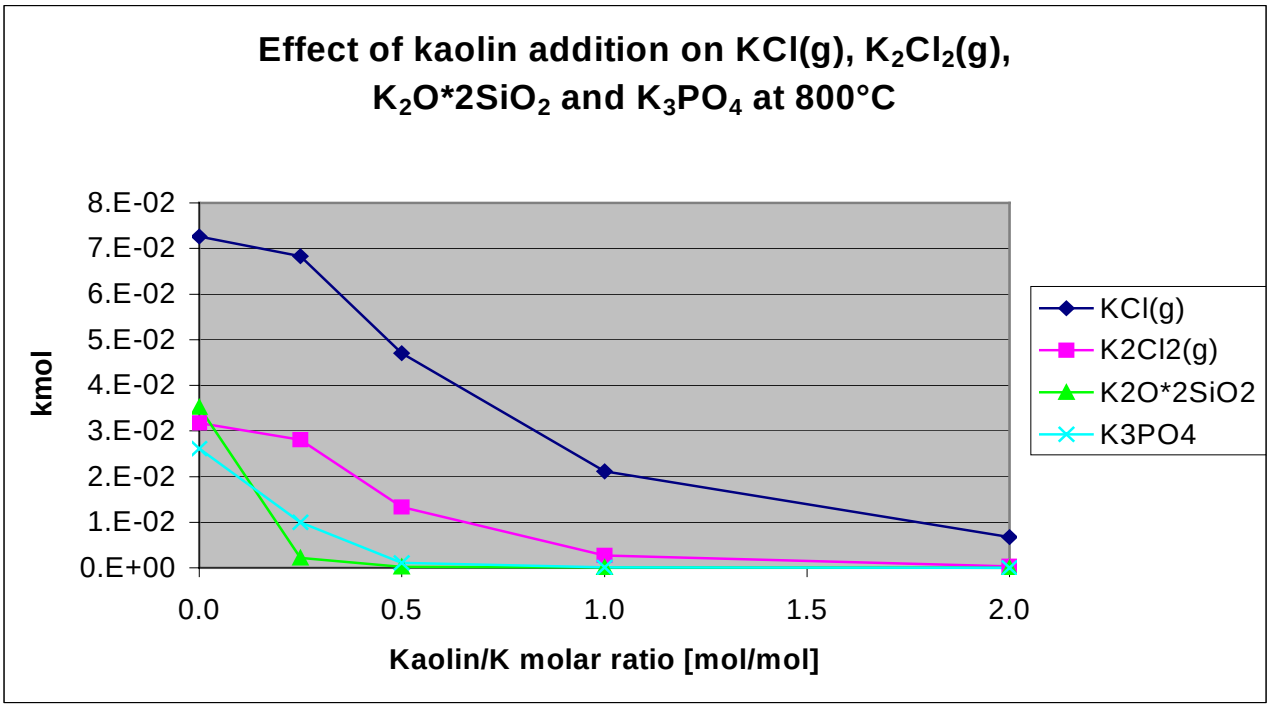

Figure 7. Gasification of straw, 5 wt.% steam. Effect of kaolinite addition on KCl(g), K_2Cl_2(g), $K_2O*2SiO_2$ and K_3PO_4 at 800°C, as a function of kaolinite to K molar ratio.

4. Conclusion

As can be seen, kaolinite reduces the concentration of K_2Cl_2(g) in the range of 0 to 2 molar ratio of kaolinite to K. Kaolinite reduces the concentration of KCl(g) from 7.3E-2 to 2.1E-2 and 6.8 E-3 kmol respectively, when the kaolinite/K molar ratio is increased from 0 to 1 and 2. At a kaolinite to K molar ratio of 0.25, the concentration of K_3PO_4 and $K_2O*2SiO_2$ is quite small.

5. References

1. HSC Chemistry for Windows. Chemical Reaction and Equilibrium Software with extensive Thermodynamical Database.
2. Thermochemical Data of Pure Substance. Ihsan Barin, 1995.
3. Pressurised fluidised-bed gasification experiments with biomass, peat and coal at VTT in 1991-94. Part 3. Gasification of Danish wheat straw and coal. Esa Kurkula, Jaana Laatikainen-Luntama, Pekka Ståhlberg, Antero Moilanen. VTT Energy, 1996.
4. CHEMICAL ELEMENTAL CHARACTERISTICS OF BIOMASS FUELS. Anders Nordin, 1994. Biomass and Bioenergy, Vol. 6, pp. 339-347.

Appendix 2 Cracking of Tar from Fluid Bed Gasifiers

Content

A literature survey has been performed to investigate tar cracking from fluidised bed gasification of biomass.

Cracking of tar from fluid bed gasifiers

Tars produced from a gasifier can block downstream filters, gas coolers and other downstream equipment. To avoid this it is necessary to clean the gas for tars. This gas cleaning can be accomplished using catalytic gas cleaning or wet gas cleaning. Wet gas cleaning using solvents demands that the gas is cooled to near ambient temperature using gas coolers. Furthermore, wet gas cleaning demands a complicated waste solvent treatment system. For this reason it is an advantage to use catalytic gas cleaning which can operate close to the gasifier temperature (800-900°C). Cracking of tars may be performed either in-situ in the fluid bed gasifier or the cracking may be performed in a separate reactor downstream of the fluid bed gasifier using tar cracking catalyst.

Tars are heavy hydrocarbon components, which can be defined using the pyrolysis temperature, the molecular weight or the boiling point of the collected tar samples. Low temperature tar is formed at temperatures below 650°C, and is mainly composed of components that are primary decomposition products of the fuel structure (Aristoff, 1981). Some of the low temperature tars, e.g. phenol and cresol, are water-soluble, contrary to the high temperature tars (Elliott, 1986). High temperature tars are composed of mono- and polyaromatic oxygen-free compounds formed mainly in the secondary reactions of the primary pyrolysis products of the fuel (McNeil, 1981). In gasification processes, low temperature tar is formed in updraft gasifiers and high temperature tars in fluidised-bed, downdraft and entrained bed gasifiers (Simell 1997). Tars from updraft gasifiers have a large content of phenolic and aliphatic components, which are more easy to crack catalytic than tars from fluid bed gasifiers, which have a large content of aromatic components (Simell 1997). Using the molecular weight, the tar fraction can according to (Simell 1998) is defined as components with a molecular mass equal to or heavier than 78 g/mol. This corresponds to the molecular mass of benzene. Albrecht et al. (Albrecht 1998) has coordinated and developed a detailed tar sampling and tar characterisation procedure as part of an IEA project.

Thermal cracking

Part of tars will be cracked in situ in the fluid bed as the temperature is increased. Figure 2.1 shows the tar concentration in g/m_n^3 as a function of the freeboard temperature for different feedstock's (Simell et. al. 1992). In this Figure, tar means hydrocarbons with a molecular weight equal to or heavier than benzene. As can be seen the biomass type influences the amount of tar produced, the sequence of the amount of tar for the different fuels is wood (sawdust) > peat > brown coal. The tar concentration in saw dust gasification is nearly 10 times higher than in brown coal gasification. The freeboard temperature and biomass type also influences the tar composition as can be seen in Figure 2.2 (Simell et al. 1992). The tar concentrations can also be reported as yields of the dry ash free matter of the feedstock. The total yields of tars for gasification at 900°C was 3-4 wt.% for wood, 0.7-1.2 wt.% for peat and below 0.5 wt.% for brown coal gasification. Figure 2.2 shows the effect of gasification temperature on tar composition. Benzene is the major tar component, and accounts for 60-98 wt. % of the total tar. The second most abundant tar component is naphthalene. The differences in tar results with the different fuels may be caused be the pyrolysis process (thermal breakdown of solid material) in the fluid bed. Another explanation is related to the mineral matter of the fuel (Simell 1990). The brown coal contains some dispersed calcium, which may catalyse tar decomposition, while the mineral matter content of wood (sawdust) was very low. The activity of calcium depends on the method by which it is added to the fuel. The finely dispersed natural calcium in brown coal and the calcium salts impregnated by solution techniques seem to be very effective cracking catalysts (Kurkela 1992).

Data for the tar production from fluid bed gasification of straw is scarce, however (Kurkela, 1996) reports that for fluid bed gasification of straw with a freeboard temperature of 800°C, more than 4 wt.% of the dry ash-free straw was released as benzene and tars (heavier than benzene). When the gasification temperature was raised to 860°C the major part of the tar components was decomposed, leaving the more stable components. The high temperature tar produced from gasification of straw had a similar composition to the tar produced from gasification of wood (Kurkela, 1996).

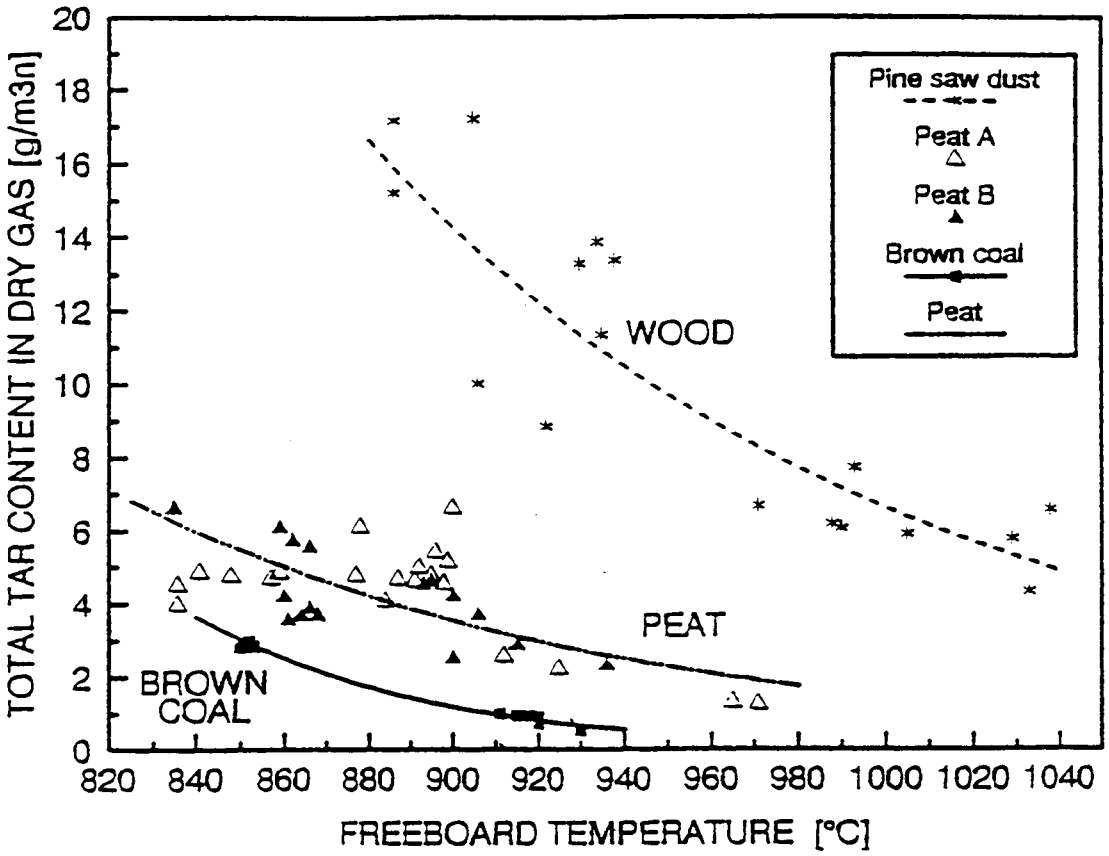

Figure 2.1. The measured tar concentrations for different feedstocks as a function of gasification temperature (operating pressure 5-8 bar).

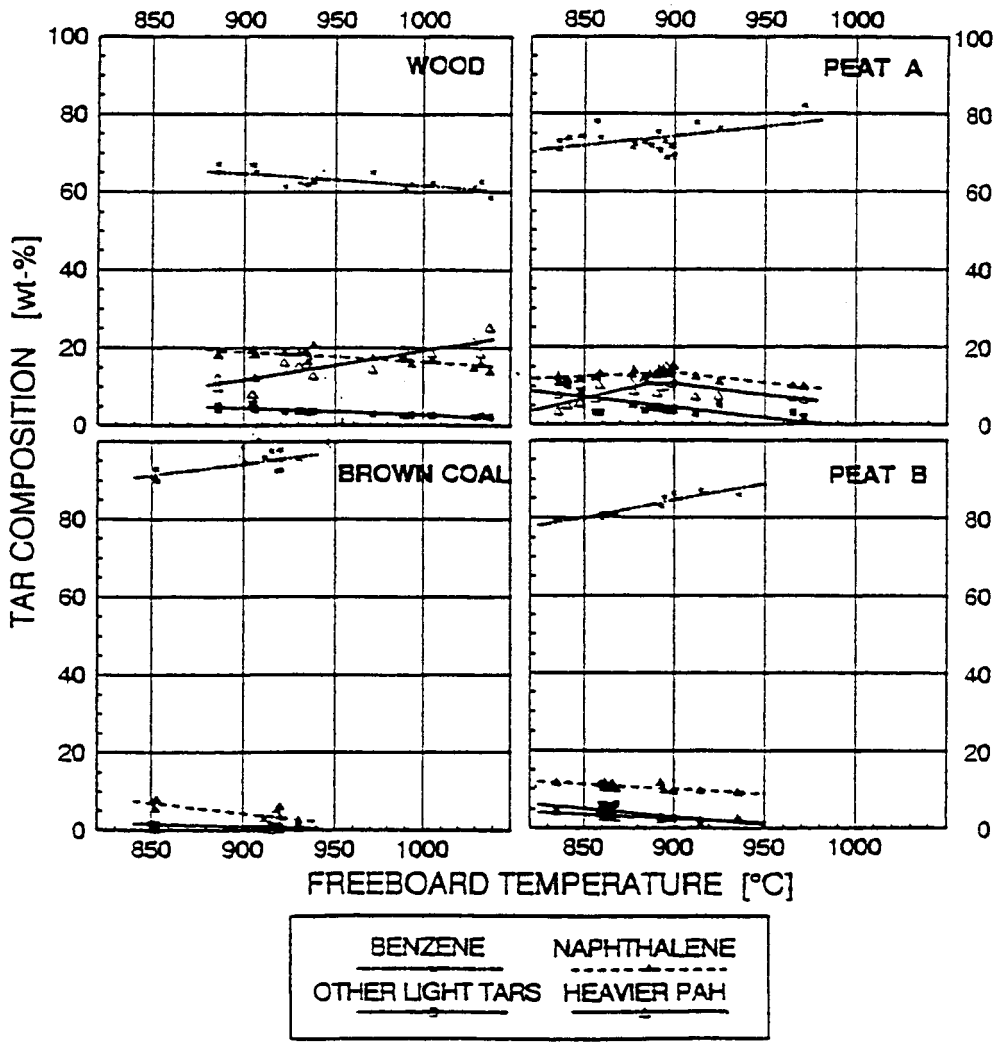

Figure 2.2. The effect of freeboard temperature on tar composition with different feedstocks.

Tar cracking catalyst

Catalysts, which can be used for tar cracking, are commercial nickel catalysts (Ni on Al_2O_3), dolomite, activated alumina, MgO and CaO. (Simell 1990) described the tar cracking capability as: commercial nickel catalyst > dolomite > activated alumina catalyst, with nickel catalyst as the most effective. The surface area of the catalyst can not explain the difference in tar cracking capability between the different catalyst. (Corella, 1997) reports that under the same experimental conditions, commercial nickel-based catalyst are 8-10 times more active than calcined dolomite, but they are also more expensive and can also become deactivated. Deactivation of nickel catalyst in biomass gasification can be due to, i.e. dust, coke and sulphur. Coke can be formed in tar cracking reactions, but it can simultaneously be removed from the catalyst surface by steam and CO_2 gasification. If the rate of coke formation is higher than the simultaneous coke removal by gasification, a coke build-up occurs with a subsequent deactivation of the catalyst. (Navares 1997) reports that when the tar content is 2 g tar/m^3_n or higher, tar will be deposited at the catalyst surface. So to use nickel based catalyst for gas cleaning, it is necessary that the raw gas have a low tar content. Deactivation of calcined dolomite catalyst has not been reported.

The tar concentration from fluid bed gasifiers varies with fuel type and temperature, see fig. 2.1, from VTT. However due to differences in tar analysis procedure it can be difficult to compare tar cracking results from different organisations. Tar cracking can be performed either in situ in the fluid bed gasifier or in an external reactor. The majority of work with tar cracking has been performed using an external tar-cracking reactor.

In situ tar cracking in fluid bed gasifiers

Calcium-based bed material such as dolomite are effective as tar cracking catalyst, (Olivares, 1997), have added calcined dolomite to a fluid bed gasifier, gasifying pine chips. Dolomite will be calcined according to the following reaction:

$$CaCO_3*MgCO_3 \rightarrow CaO*MgO + 2\ CO_2(g) \qquad (1)$$

The equilibrium constant of reaction 1 is larger than 1 for temperatures above 610°C. Calcined dolomite, CaO*MgO, have a higher catalytic activity than uncalcined dolomite for tar cracking. The higher surface area of the calcined dolomite, 5-20 (typical 10) m^2/g, compared to uncalcined dolomite 0.6-1 m^2/g (Fjellerup, 1989), may cause this. Deposited surface carbon is suggested to be an important intermediate in hydrocarbon steam reforming on dolomite (Morita,1978).

(Olivares, 1997) have performed gasification experiments in an atmospheric bubbling fluid bed gasifier which gasifies 10 kg/h of pine chips using steam/O_2 mixtures. Olivares reports that the tar content in the raw gas is reduced from 12 to 2-3 g tar/m^3_n (Figure. 2.3) when the dolomite content in the bed is increased from 0 to 50 wt.% (the remainder is sand). Olivares recommends that the dolomite content in the bed be kept at an amount of 10 wt. % of the bed.

Dolomite catalyse both the tar cracking and the shift reaction. Olivares reports that the net effect of dolomite addition on the gas quality from the gasifier is the following. The H_2 content is increased from 28 to 43 vol.% (dry), the CO content is decreased from 45 to 27 vol.% (dry) and the amount of methane and C_2 hydrocarbons is decreased when the dolomite content in the bed is increased from 0 to 50 wt.%. However (Olivares,1997) reports that in their experiments, the dolomite becomes eroded and is eluted out of the bed. To keep a stationary amount of dolomite in-bed during their experiments, it was necessary to feed an amount of 2-3 wt. % of dolomite with the biomass.

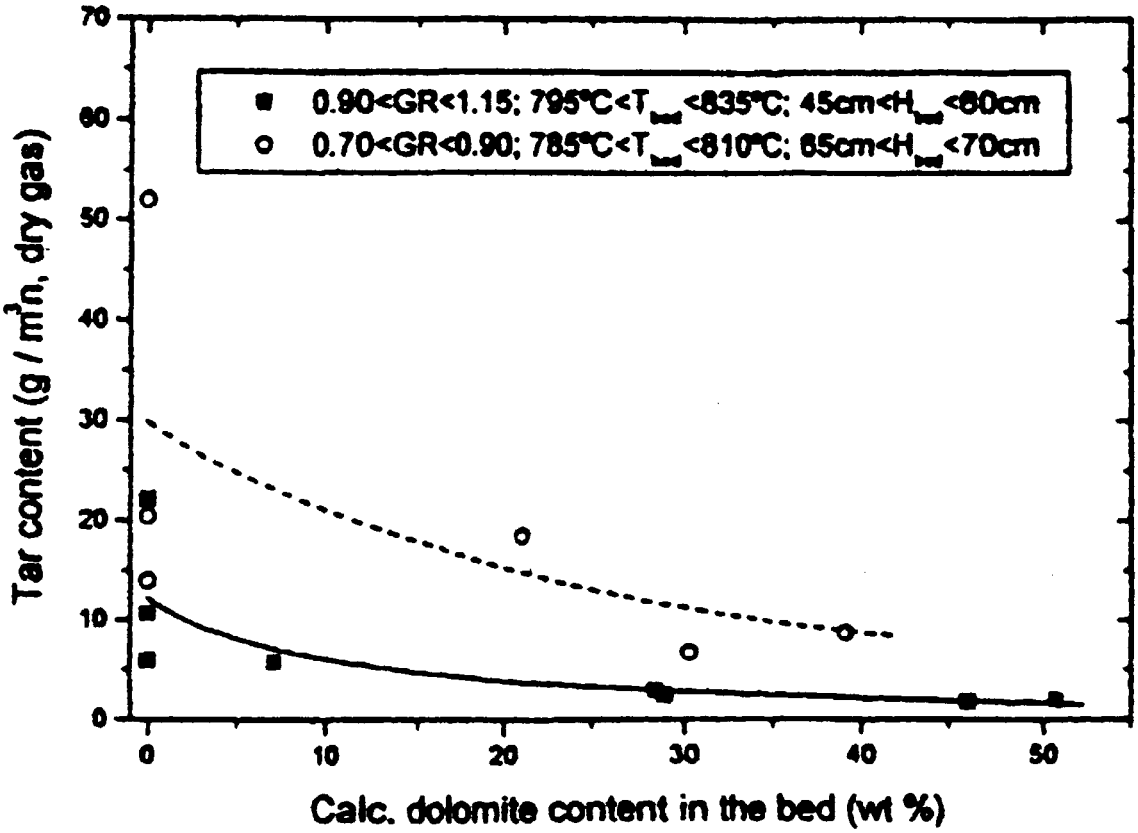

Figure 2.3. Tar content in the gas at the exit of the gasifier vs time-averaged content of calcined dolomite in the bed.

Tar cracking using an external reactor

The tar cracking in an external reactor can be performed using either a fixed bed reactor or a secondary fluid bed reactor. (Orío,1997) has performed experiments with tar cracking in an external reactor using different dolomite types. Orío reports that it is necessary to use a fixed bed reactor contrary to a fluid bed reactor, to avoid that the dolomite becomes eroded.

Using a secondary fixed bed reactor, (Simell 1997) has determined first order rate constants for different catalyst, SiC, dolomite (Finnish and Swedish), ankerite (iron dolomite) and nickel catalyst (A0 and B). Simell finds that the rate constant for tar cracking from updraft gasification is larger than the rate constant for tar cracking from fluid bed gasification under similar conditions. This is caused by the thermal decomposition of the unstable updraft gasifier tar, which occurs simultaneously with the catalytic reactions. Simell and his co-workers at VTT (Simell 1990, Simell et. al. 1993) have operated fixed-bed nickel catalysts with product gases derived from both updraft and fluidised-bed gasifiers. Complete (>99 %) tar decomposition has been determined for both gasifier gases when the catalyst was operated at 900^{o}C. VTT has also carried out a 500-hour-long extended time test [Simell et. al., 1993] with operated a nickel monolith catalyst. In these tests the catalyst was operated at 0.5 MPa pressure and an average temperature of 905°C. The gas was derived from bubbling fluidised-bed gasification of wood and peat and it's inlet concentration of tars varied in the range 1-7 g/m$^{3}_{n}$ (sum of compounds heavier than benzene). No signs of deactivation by soot formation or sulphur poisoning were found and the tar catalysing activity remained constant (100%) during the 500 hour tests. However the temperature of 905°C is higher than the usual operating temperatures of a fluid bed gasifier.

(Corella, 1999) has tested a number of steam cracking nickel catalyst from BASF, ICI, Topsoe and United Catalyst in a fixed bed reactor located downstream of an atmospheric fluid bed gasifier. The gasifier was feed with small pine wood chips and the gasifier bed was silica sand without dolomite. After the gasifier there is a hot (500-550°C) ceramic candle filter and a guard bed with calcined dolomite, which cracks the tar content to about 1 g/m$^{3}_{n}$. The fixed bed reactor is located after the guard bed. They have used two types of steam reforming catalyst, one type for light hydrocarbons and one type for heavier hydrocarbons. The last group of catalyst is the most active, with a tar conversion of about 98 %. Due to the size of the reactor (internal diameter of 60 mm), there is a large temperature difference between the centre and the wall and between the inlet and the exit of about 5-20°C. The original size of

the catalyst are big rings of about 15 mm external diameter, and this causes a low catalyst effectiveness due to internal mass transfer resistance, low heat transfer rates, and large temperature gradient. This has caused Corella to crush the catalyst particles to a size of 1.6-2.6 mm, but even so he reports that internal diffusion controls the cracking process. Due to the above mentioned experimental uncertainties it is problematic to derive kinetic parameters, but nevertheless Corella obtains conversion rates of about 98 %, and the difference in activity between the tested catalyst is less than 10 %.

Conclusion

This study shows that both dolomite and nickel catalyst can be used to crack tar from a fluidised bed gasifier. Nickel has a higher catalytic activity than dolomite, but the nickel catalyst must be operated at conditions where carbon (soot) formation and sulphur poisoning are avoided. According to (Simell 1997) temperatures of over 900°C are required at 20 bar pressure to avoid catalyst deactivation by H_2S or carbon deposition. According to (Simell 1997) and (Kurkela[1]) for typical atmospheric-pressure fluidised-bed gasification applications this means that temperatures of the order of 850°C or more is necessary, this temperature is above the hitherto usual operating temperature of a fluid bed gasifier using straw.

Calcined dolomite does not become deactivated by tar deposition, and for this reason dolomite can be used in the bed where the tar concentration is high. It has however been reported in the literature that when dolomite is used in-bed, it becomes elutriated and is blown out of the bed. This means that it is necessary to add dolomite with the input feed to avoid this. Furthermore the activity of calcium depends on the method by which it is added to the fuel. The finely dispersed natural calcium in brown coal and the calcium salts impregnated by solution techniques seem to be very effective cracking catalysts [Kurkela 1992]. Another solution is to have dolomite in an external fixed bed. The actual cracking solution depends on the application of the raw gas (boiler, GT, engine) and their demand to gas quality; and the other gas cleaning equipment's (cyclones, filters etc.).

1. Kurkela, E., VTT, Finland, personal communication based on confidential VTT research.

Appendix 3 The macro-TGA reactor

At ET, DTU a macro-TGA reactor has been constructed and was used during about 10 years.

The reactor is constructed as a cylinder. The diameter is 125 mm and the height is 140 mm. The total reactor is hanged in a balance. The reactor is surrounded by an oven, which gives a constant temperature with a maximum of 1000^{o}C. The gasification agent is preheated to the reactor temperature.

The macro-TGA reactor can test samples from 1 to 20 grams, which is 100-200 times more than used in traditional TGA equipment. Therefore the macro-TGA reactor makes it possible to produce ash samples that are sufficiently large for further analysis to be made.

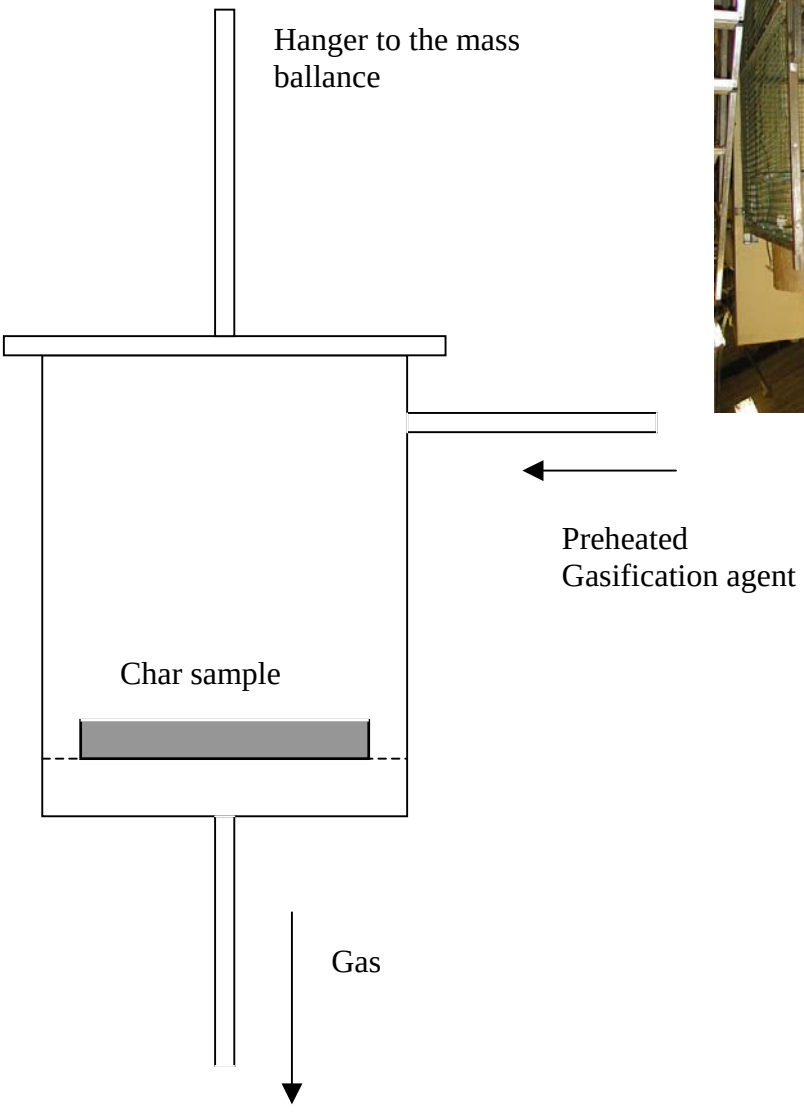

Figure XX1. The macro-TGA reactor with the char sample.

ReaTech
ISBN 87-988105-0-2